Revista Română de Inginerie Civilă

Indexată în bazele de date internationale (BDI)

ProQuest, IET INSPEC, EBSCO, GOOGLE SCHOLAR, CROSSREF, TDNET, DIMENSIONS, DRJI, J-GATE, INDEX COPERNICUS, ULRICH'S, JOURNALSEEK, RESEARCH GATE, SEMANTIC SCHOLAR, ERIHPLUS, WORLDCAT

Volumul 16 (2025), Numărul 2

MATRIX ROM
3 Politehnicii Street, Bucharest, Romania
Tel. +4021.4113617, +40733882137
e-mail: office@matrixrom.ro
www.matrixrom.ro

EDITORIAL BOARD

Romanian Journal of Civil Engineering is founded, published and funded by publishing house MATRIX ROM
Executive Director: mat. Iancu ILIE

Online edition ISSN 2559-7485

Print edition ISSN 2068-3987; ISSN-L 2068-3987

Manufacture of artificial aggregate using alkaline solution

Fabricarea agregatelor artificiale folosind soluție alcalină

Maahira M[1], Neethu K Pradeep[2], Jeshva P R[3], Dr.M.Siva[4]

[1,2,3]UG Students, Department of Civil Engineering, Easwari Engineering College (Autonomous), Chennai, Tamil Nadu, India
[4]Assistant professor, Department of Civil Engineering, Easwari Engineering College (Autonomous), Chennai, Tamil Nadu, India
e-mail: *siva.manogaran@gmail.com*

DOI: 10.37789/rjce.2025.16.2.1

ABSTRACT
The construction industry's continuous quest for sustainable practices has led to the exploration of alternative construction materials that minimizeenvironmental impact while maintaining structural integrity. Aggregate constitutes the major part of any concrete construction. Conventional aggregates are obtained directly from nature. The major problem associated with conventional aggregates is the depletion of resources. The project work describes the utilization of industrial slag which is dumped as landfill. Slag, a by-productof various industrial processes, have emerged as promising candidates for use as construction aggregates in concrete. This study explores the feasibility of replacing traditional coarseaggregates with slag. This project aims to investigate the performance and feasibility of incorporating different types of slags, including Copper Slag (CS), and Steel Slag (GGBS), as raw material and alkaline solution as binding material in the manufacture of coarse aggregate. Through laboratory testing, mechanical properties analysis, and environmental assessments, the study seeks to provide valuable insights into the development of eco-friendly and high-performance coarse aggregate for the production of concrete. The results of the manufactured aggregate shows that the properties tested are nearer to the aggregate properties suggested by Indian standards (IS 456- 2000, IS 383, and IS 9103-1999). The study also focuses on the effect of curing temperature to enhance the properties of the manufactured aggregates in the Phase-II of the project.

Keywords: Conventional Aggregate, Copper slag, Ground granulated blast furnace slag (GGBS), Geopolymer, Pelletization

1. INTRODUCTION

The construction industry's continuous quest for sustainable practices has led to the exploration of alternative construction materials that minimize environmental impact while maintaining structuralintegrity. Aggregate constitutes the major part of any

The article was received on 08.02.2025, accepted on 21.05.2025 and published on 22.05.2025

concrete construction. They include fine aggregates which passes through IS 4.75mm sieve,coarse aggregates which retain on IS 4.75mm sieveand ‘all in aggregates ’which constitutes all of the major fractions. Conventional aggregates are obtained directly from nature. The major problem associated with conventional aggregates is the depletion of resources. The harm caused to the environment is tremendous. So, the requirement of proper substitution for conventional aggregate is a matter of immediate importance. Slags, a byproduct of various industrial processes, have emerged as promising candidates for use as construction aggregates in concrete. The utilizationof industrial byproducts as raw materials for coarseaggregates aligns with the principles of the circular economy, turning waste into a valuable resource. This approach not only reduces the environmental impact of aggregate production but also minimizesthe need for extensive quarrying, therebyconserving natural resources and mitigating habitatdisruption. This introduction sets the stage for an exploration of the various industrial byproducts, production processes, engineering properties, and environmental implications associated with the innovative endeavor to create sustainable coarse aggregates. This study explores the feasibility of replacing traditional coarse aggregates with slag. This project aims to investigate the performance and feasibility of incorporating different types of slags, including Copper Slag (CS), and Steel Slag (GGBS), as raw materials in the manufacture of coarse aggregate. This progressive initiative seeks to address environmental concerns associated with traditional aggregate extraction while simultaneously offering a valuable solution for managing industrial waste.

2. OBJECTIVE

- To Prepare Light Weight Aggregate Using alkaline solution as binding material
- To vary the molarity and curing temperature from 50°C to 70°C and studying the properties as per Indian standards
- To study the mechanical properties of concretemanufactured using artificial aggregate
- To study the durability properties (Sulphateattack) of concrete manufactured usingartificial aggregate

3. SCOPE

- The scope of this project involves reducing theenvironmental impact due to traditional aggregate extraction.
- The scope involves creating awareness and fostering market acceptance of sustainable coarse aggregates.
- The scope extends to fostering innovation and collaboration across industries.
- Researchers, engineers, and stakeholders collaborate to optimize production processes, develop new technologies, and share best practices, contributing to the continuous improvement of sustainable aggregate production.

 The project considers the market feasibility of sustainable coarse aggregates. This involves evaluating the economic viability, cost- effectiveness, and market acceptance of these alternative materials. Stakeholder engagement and communication strategies are essential components to promote awareness and acceptance within the construction industry.

4. SIGNIFICANCE

 Waste management: Utilization of the industrial slag which are dumped as landfill

 Lower carbon emission: Method of production of aggregate reduces greenhousegas emission

 Sustainability: Substitution of natural aggregate with LWA manufactured from wastematerials to reduce the dependency on nonrenewable resource usage.

 Cost effectiveness: The project considers the market feasibility of sustainable coarse aggregates. This involves evaluating the economic viability, cost-effectiveness, andmarket acceptance of these alternative materials.

5. METHODOLOGY

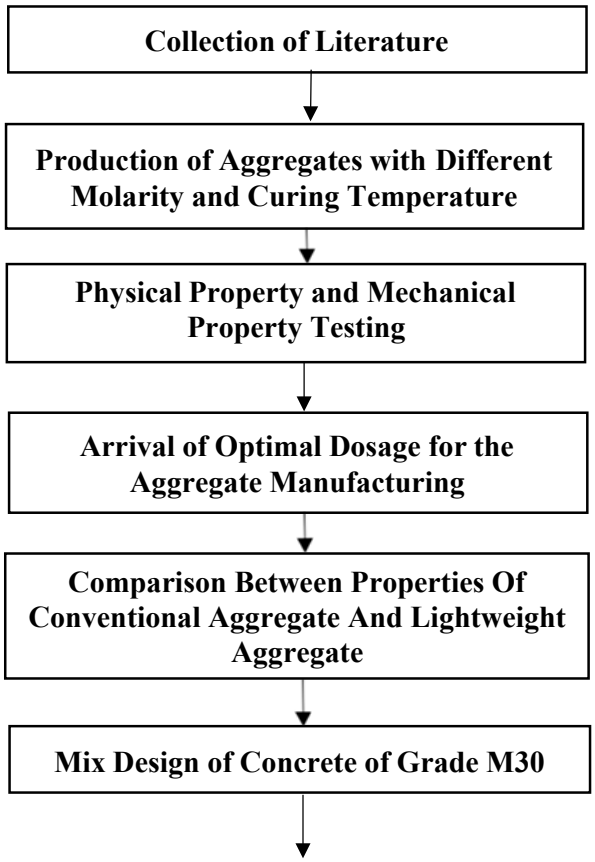

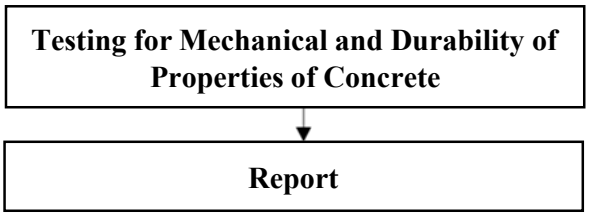

6. MATERIALS

6.1 SLAG

6.1.1 Copper Slag

Copper slag is a byproduct of the copper smelting process, composed mainly of iron, silica, and otherminerals. It can be recycled to recover valuable metals like copper and iron, and is often used as a partial replacement for sand in concrete or as agranular material in road construction due to its density and strength. While it offers economic and environmental benefits by reducing waste and promoting recycling, proper management is essential to mitigate potential risks associated withheavy metal leaching. Its abrasive nature also makes it suitable for sandblasting applications.

COMPONENT	PERCENTAGE (%)
SiO2	35 to 45
Fe	30 to 40
CaO	8 to 16
Al_2O_3	5 to 15
MgO	1 to 6
S	1 to 5
Cu	less than 1

Advantages And Applications

Copper slag is a valuable resource in construction, reducing waste and environmental impact. It enhances concrete and asphalt's strength and durability, making it ideal for sandblasting and surface preparation. It's also used in land

reclamation, glass manufacturing, soil stabilization, and cement production, contributing to sustainability and resource efficiency.

6.1.2 Ground Granulated Blast Furnace Slag (GGBS)

Ground Granulated Blast Furnace Slag (GGBS) is a byproduct of the iron and steel manufacturing process, created by rapidly cooling molten slag from a blast furnace. This results in a glassy, granulated material that is then finely ground into a powder. GGBS offers numerous benefits, including high resistance to chemical attack, low permeability, and enhanced durability, making it anexcellent alternative to traditional Portland cement in concrete mixes. By partially replacing cement with GGBS, construction projects can significantly reduce their carbon footprint, as GGBS production generally emits fewer greenhouse gases. It is widely used in various applications, including ready-mix concrete and precast products, particularly in environments requiring increased durability, such as marine structures. Overall, GGBS promotes sustainability in construction while improving the performance of concrete.

COMPONENT	PERCENTAGE (%)
SiO2	35 to 45
CaO	35 to 45
Al_2O_3	10 to 15
MgO	5 to 15

Application and Advantages

The use of GGBS not only provides a sustainable approach to managing industrial by-products but also contributes to the advancement of environmentally friendly construction materials with high performance. GGBS demonstrates pozzolanic properties, allowing it to react withcalcium hydroxide in the presence of water to create additional cementitious compounds.

Incorporating GGBS into concrete reduces the reliance on energy-intensive Portland cement production, thereby contributing to a decrease in carbon dioxide emissions associated with cement manufacturing. Additionally, the utilization of GGBS offers an environmentally friendly solutionfor handling blast furnace slag, transforming an industrial by-product into a valuable construction material. This reduces the problem of pollution caused by dumping slag in landfills. GGBS is a versatile and sustainable material with valuable properties that enhance the performance of concrete and other construction materials. Its adoption contributes to both environmentalsustainability and efficient use of industrial byproducts in the construction industry.

6.2 ALKALINE SOLUTIONS

6.2.1 Sodium Hydroxide Solution

Sodium hydroxide (NaOH) solution is a colorless, odorless, and highly alkaline liquid that is more dense than water. A colorless liquid that is more dense than water. A strong base that feels slippery and has a high pH. Used in many products, including soaps, drain cleaners, and cement mixes.Can cause severe burns to the skin and serious tissue damage if it gets into the eyes or is inhaled. Should be stored in a cool, dry, well-ventilated location separate from organic and oxidizing materials, acids, and metal powders.

6.2.2 Sodium Silicate Solution

Sodium silicate solution, also known as water glass, is a colorless, transparent, and non- flammable aqueous solution of sodium silicate.

Composition

Sodium silicate is a chemical compound with the formula NaSiO, and its chemical formula varies depending on the ratio of sodium oxide (Na2O) and silicon dioxide (SiO2).

Uses

Used in adhesives for bonding paper, glass, porcelain, leather, textiles, and stoneware. Used in refractory cements and construction. Used in food and beverage processing. Injected into the soil to stabilize it and increase its strength and stiffness. Sodium silicate solution is a strong irritant to skin,eyes, and mucous membranes. It may be toxic by ingestion. When handling sodium silicate solution, you should wear protective gloves, clothing, eye protection, face protection, and hearing protection.Store sodium silicate solution locked up at +15°C to +25°C.

7. TRIAL MIX DESIGN

- 3 coarse aggregate mixes were made with different Molarities were prepared.

S.No	MIX	MOLARITY	ALKALINE\ ASH RATIO
1	MIX 1	8 M	2.5 : 1
2	MIX 2	10M	2.5 : 1
3	MIX 3	12 M	2.5 : 1

7.4 PREPARATION OF COARSEAGGREGATE

- Pelletization is a process that turns material fines into pellets or granules to make themeasier to handle.
- It's used in many industries to process materials that are difficult to handle, such as powders and fines. In the context of aggregates, pelletization is used to create artificial lightweight aggregates.
- GGBS and Copper Slag serves as primary materials with copper slag adding density and GGBS contributing to the binding properties
- For the production of coarse aggregate initiallythese materials dry mixed in the pelletizer machine for 5 to 10 minutes.
- The speed and angle of the pelletizer can be changed accordingly.
- In that dry mix geopolymer solution (NaoH + Na2sio3) is added in the pelletizer gradually while the pelletizer is still rotating for the formation of pellets.
- The production of our lightweight aggregate is carried out in a disc pelletizer.
- These aggregates are produced in a disc type pelletizer machine which has 100mm depth and 500mm diameter with speed and angle variation from 1 to 65rpm and 0-90° respectively.
- After 45 to 55 minutes the formed pellets are carefully collected and spreaded in a sheet at room temperature 25° C and left to dry for 12 hours.
- These aggregates are then heated / immersed inwater.
- Then all the physical and mechanical tests are carried out for the prepared aggregates.

8. TESTING OF AGGREGATES

8.1 FLAKINESS INDEX TEST

- The Flakiness index test was conducted andthe following observations were noted.

S.NO	MIX	FLAKINESS INDEX
1	MIX 1	17.5
2	MIX 2	17.4
3	MIX 3	16.5
4	CONVENTIONAL AGGREGATE	18.1

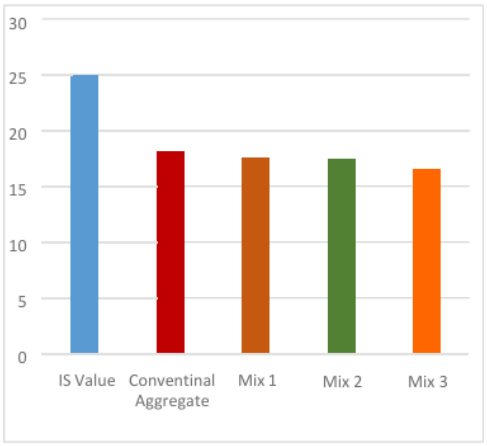

8.2 ELONGATION INDEX TEST

 The Elongation Index test was conducted andthe following observations were noted.

S.NO	MIX	ELONGATION INDEX
1	MIX 1	25.8
2	MIX 2	20.4
3	MIX 3	20.9
4	CONVENTIONAL AGGREGATE	21.81

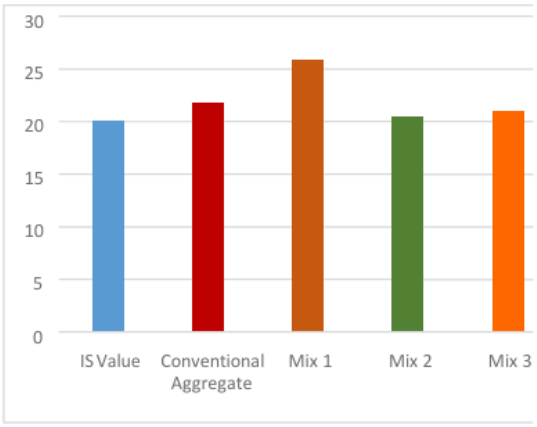

8.3 SPECIFIC GRAVITY TEST

 The Specific Gravity test was conducted and the following observations were noted.

S.NO	MIX	SPECIFIC GRAVITY
1	MIX 1	2.26
2	MIX 2	2.51
3	MIX 3	1.73
4	CONVENTIONAL AGGREGATE	2.8

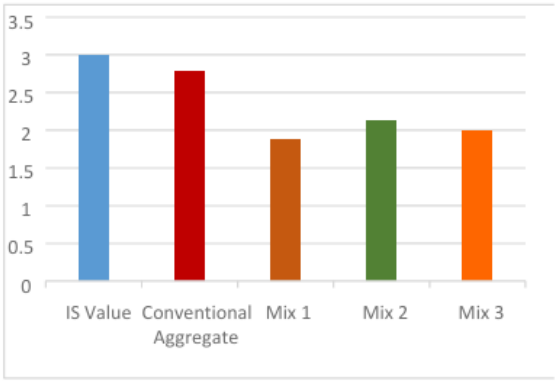

8.4 WATER ABSORPTION TEST

 The test was conducted and the following observations were noted.

S.NO	MIX	WATER ABSORPTION
1	MIX 1(8M mix)	9.1
2	MIX 2(10M mix)	8.8
3	MIX 3(12M mix)	8.4
4	CONVENTIONAL AGGREGATE	5.58

This makes them suitable for high-strength lightweight concrete applications, particularly where weight reduction is critical without compromising strength (e.g., high-rise buildings or long-span bridges). However, lightweight aggregates may not always have the same load- bearing capacity as conventional aggregates in specific structural contexts.

8.5 CRUSHING TEST

S.NO	MIX	CRUSHING VALUE
1	MIX 1(8M mix)	**14.2**
2	MIX 2(10M mix)	**19**
3	MIX 3(12M mix)	**18.46**

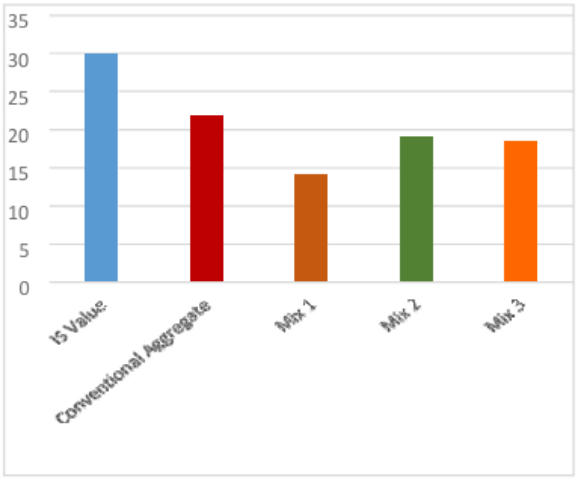

The crushing value is an important property of aggregates, representing their resistance to crushing under a gradually applied compressive load. It helps assess the quality and suitability of aggregates for use in construction, especially in high-load-bearing applications. Comparison ofCrushing Value for Conventional and Lightweight Aggregates. Conventional Coarse Aggregatetypically consists of materials like crushed granite,basalt, or natural gravel.

Crushing values generally range between 20% and 30% for good quality aggregates used in road construction, as specified by IS 383:2016. Lower crushing values (e.g., below 20%) indicate higher strength and better suitability for construction.

Lightweight aggregates with crushing values between 14% and 19% have higher resistance to crushing than many conventional coarseaggregates.

8.6 IMPACT TEST

S.NO	MIX	IMPACT VALUE
1	MIX 1(8M mix)	**11.4**
2	MIX 2(10M mix)	**27.8**
3	MIX 3(12M mix)	**16**

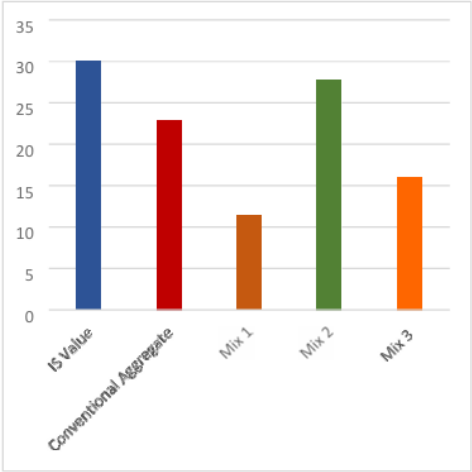

The impact value of an aggregate is a measure of its toughness and ability to resist impact forces, which is critical for determining its suitability in road construction and other load-bearing applications. Comparing the impact value of conventional coarse aggregates (like natural stones or crushed rocks) with lightweight aggregates Typical impact values: usually range from 10 to 30%. Conventional Aggregates: Typically higher values (e.g., 25- 30%) indicate good toughness for heavy-duty applications.

Lightweight Aggregates (9–11%): Lower values indicate higher resistance to impact, which is surprising for lightweight materials.

Lower impact values in lightweight aggregates could be attributed to uniform pore distribution andstrong bonding in geopolymer aggregates.

Discussion need to be made whether low impact values make lightweight aggregates suitable for specific applications (e.g., non-load-bearing structures, lightweight concretes, or precast panels). The use of lightweight aggregates with low impact values can reduce structural dead load while maintaining adequate durability.

Potential challenges in high-impact zones or heavily loaded pavements.

Lightweight aggregates with impact values of 9–11 are comparable or better than many conventional aggregates.

Study need to be done on relationship between impact value and other properties, such as compressive strength, durability, and density.

This comparison could emphasize that lightweightaggregates, especially those geopolymer-based, are not just alternatives but potential upgrades for specific applications. Their low impact values, while seemingly advantageous, need to be studied further to ensure they meet all practicalrequirements in construction.

9. SUMMARY AND CONCLUSION

In this study material properties such as flakiness index, elongation index, specific gravity, water absorption value, crushing value, impact value was found with tests as per the IS 2386:1963. The materials used in this project are copper slag, ground granulated blast furnace slag, Geopolymer. Three Coarse aggregate mixes with copper slag, ground granulated blast furnace slag, and different Molarities (8M, 10 M, 12M) of

geopolymer solutions were prepared. The dry materials were weighed separately and mixed together in the pelletizer equipment. The coarse aggregate mixes were prepared with GGBS (80%), copper slag (20%). The procedures for the tests were studied carefully and the tests were conducted for both conventional aggregates and three mixes with different Molarities of geopolymer. Test were conducted for manufactured aggregates prepared using different proportions of alkaline Solution such as 8M, 10M and 12M. The 8M Mix is observed to provide better impact and crushing strength compared to 10M and 12M mixes. The tests conducted were flakiness index test, elongation index test, specific gravity test, water absorption test, crushing value test, and impact value test. The results of tests were then comparedwith Indian standard as per IS 2386:1963. It is observed that the alkali aggregate irrespective of molarity satisfies the Indian Standards specification. The aggregate will be test for the influence of different curing temperature and the properties of concrete will be tested in the phase IIof the project.

REFERENCES

- K.M. Klima, Y. Luo, H.J.H. Brouwers, Qingliang Yu,Effects of mineral wool waste in alkali activated-artificial aggregates for high- temperature applications,Construction and Building Materials,Volume 401,2023
- Alaa M. Rashad, Youssef A. Mosleh, M.M. Mokhtar,Thermal insulation and durability of alkali-activated lightweight slag mortarmodified with silica fume and fly ash,Construction and Building Materials, Volume 411,2024
- Ling-Yu Xu, Lan-Ping Qian, Bo-Tao Huang, Jian-Guo Dai,Development of artificial one- part geopolymer lightweight aggregates by crushing technique,Journal of Cleaner Production,Volume 315,2021
- L.F. Fan, H. Wang, W.L. Zhong,Developmentof lightweight aggregate geopolymer concretewith shale ceramsite, Ceramics, International, Volume 49, Issue 10,2023
- Dongming Huang, Chenlong Lin, Zhenzhen Liu, Yiyan Lu, Shan Li,Compressive behaviors of steel fiber-reinforced geopolymer recycled aggregate concrete-filled GFRP tube columns,Structures,Volume 66,2024
- Wei, H.; Wu, T.; Yang, X. Properties of Lightweight Aggregate Concrete Reinforcedwith Carbon and/or Polypropylene Fibers. Materials 2020
- Bekkeri, G.B., Shetty, K.K. & Nayak, G. Performance of concrete produced with alkali-activated artificial aggregates. J Mater Cycles Waste Manag 26, 2024
- Hamsashree, Pandit, P., Prashanth, S. et al.Durability of alkali-activated fly ash-slag concrete- state of art. Innov. Infrastruct Solut. 9, 222 (2024)
- D.V.B. Desai, A. Sathyam, D.Sireesha, IOSR J.Mech. Civ. Eng., 11, 30 (2014).
- M. Gesoglu, E. Güneyisi, H. O. Oz, Mater. Struct., 45, 1535 (2012).
- R. Arellano Aguihr, O. Burciaga Diaz, J. I. Escalarte Garcin, Constr. Build. Mater.,24, 1166(2010).

- O. Abdulkareem, M. Abdullah, K. Hussin, K. Ismail, M. Binhussain, Materials, 6, 4450 (2013).
- A.R. Rafiza, Adv. Mater. Res., 626, 892-895 (2012). . M.M.Al Bakri Abdullah, et al. Int. J. Mol. Sci., 13, 7186-7198 (2012).
- 30. J.P. Ries, et al. Guide for Structural Lightweight-Aggregate Concrete Reported by ACI Committee 213. (2010).
- S. Akcaozoglu, K. Akcaozoglu, C. D. Atis, Composites Part B, 45, 721-726 (2013). 32. T.S. Yun, Y.J. Jeong, T. S. Han, K.S. Youm, Energ Buildings 61, 125-132 (2013).

CFD Simulation of Fire Dynamics in Textile Warehouses Using PyroSim and Fire Dynamics Simulator (FDS)

Simulare CFD a dinamicii incendiului în depozitele de textile folosind PyroSim și Simulatorul de dinamică a incendiului (FDS)

Emanuil-Petru Ovadiuc, Răzvan Calotă*, Ilinca Năstase

*CAMBI, Technical University of Civil Engineering in Bucharest, Building Services Department, 66 Avenue Pache Protopopescu, 020396, Bucharest, Romania

E-mail: *academicovadiuc@gmail.com, ilinca.nastase@cambi.ro, razvan.calota@utcb.ro*

DOI: 10.37789/rjce.2025.16.2.2

Abstract. *This study investigates the use of Computational Fluid Dynamics (CFD) simulations, employing PyroSim and the Fire Dynamics Simulator (FDS), to analyze fire dynamics in a textile warehouse. The research focuses on modeling a specific fire scenario to assess fire propagation, temperature distribution, smoke movement, and visibility conditions. The results are intended to inform fire safety strategies and evaluate the effectiveness of existing fire prevention measures in such facilities*

Keywords: *PyroSim, Fire Dynamics Simulator, statistical analysis, fire simulation, warehouse*

1. Introduction

In recent years, the use of advanced computational simulations, such as those performed using the PyroSim software, has significantly improved the way fire safety engineering is approached. These simulations provide engineers with deeper insights into fire behavior, helping them make informed decisions and develop robust strategies that effectively protect both lives and property. Studies [1-3] have demonstrated the capabilities of FDS in predicting fire behavior in various building types. Applying CFD simulations to fires in textile warehouses comes with a set of challenges, due to the significant quantity of combustible materials, and the fast and unpredictable nature of fire spread in such environments. These complexities require careful consideration in modeling and interpreting simulation results to ensure accurate outcomes.

The article was received on 17.03.2025, accepted on 15.05.2025 and published on 22.05.2025

Workspace definition for the present study

The first step in preparing a working model in PyroSim is to define the geometry through obstacles, represented by: floor, walls, support pillars, beams, ceiling, shelves, and in the case of each obstacle, to specify the nature of the material from which it is made is defined.

The building's resistance structure is designed to provide adequate fire protection and is built using fire-resistant materials and elements and it consists of:

- *Reinforced concrete frames* made of class A1 pillars, fire resistant for 120 minutes (R120), and class A1 beams, fire resistant for 45 minutes (R45).
- *The perimeter enclosures*, built of brick masonry with a thickness of 20-40 cm. This masonry is classified as A1, fire resistant for 240 minutes (REI240), providing an additional barrier against the spread of fire.
- *The floor* made of concrete, which ensures a strong and durable surface, also classified as A1, fire resistance.
- *The interior partitioning* between storage spaces with the same level of fire danger made of plasterboard-plasterboard with a thickness of 22 cm. These boards are classified as A2 - s1, d0, providing adequate protection against the spread of fire for 180 minutes (EI180).
- *Communication* within the same fire compartment is made through two fire-resistant doors with a fire resistance of 45 minutes (EI 45 - C), thus ensuring safety and fire insulation in the event of an emergency situation [4].

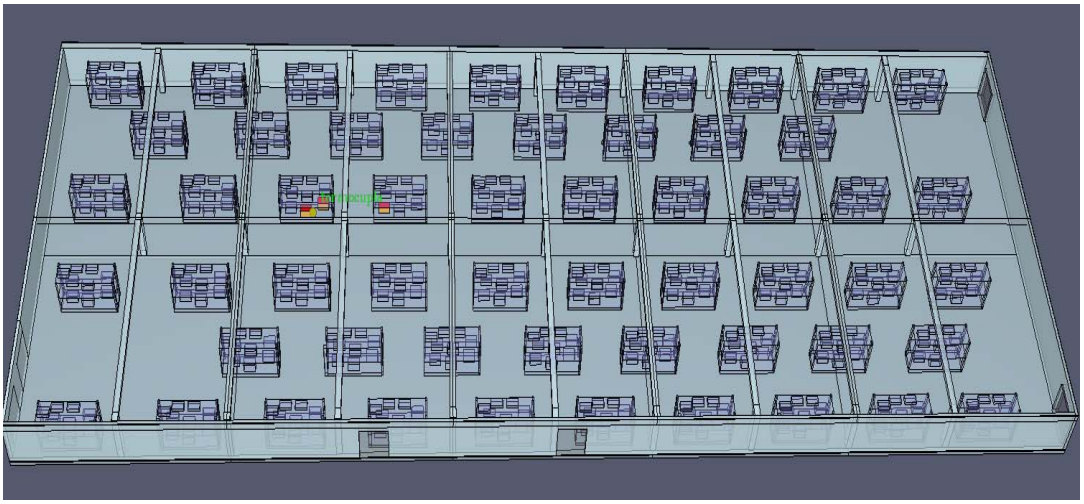

Fig. 1. Room geometry

Defining Fire

This step involves many engineering solutions based on the multitude of chemical reactions that can take place following the combustion process.

The outbreak can be achieved through two main components:

1. *Reaction:* parameters that define the combustion process and aim to define the way in which the molecules of atoms combine with each other to produce the by-products resulting from combustion and implicitly heat
2. *Surface:* parameters that define the physical and chemical characteristics of the combustible and non-combustible materials that go into the composition of the working model [5].

Size workspace-specific cells

As a general rule, the smaller the size of the cells that define the geometry of the model, the more the precision of the simulation increases, being as close to reality as possible. At the same time, this also leads to an increase in the running time of the program in order to process the data necessary to perform the analysis on the behavior of the existing combustion process.

This was done in order to obtain data that would express as much as possible the results of a fire in a real situation.

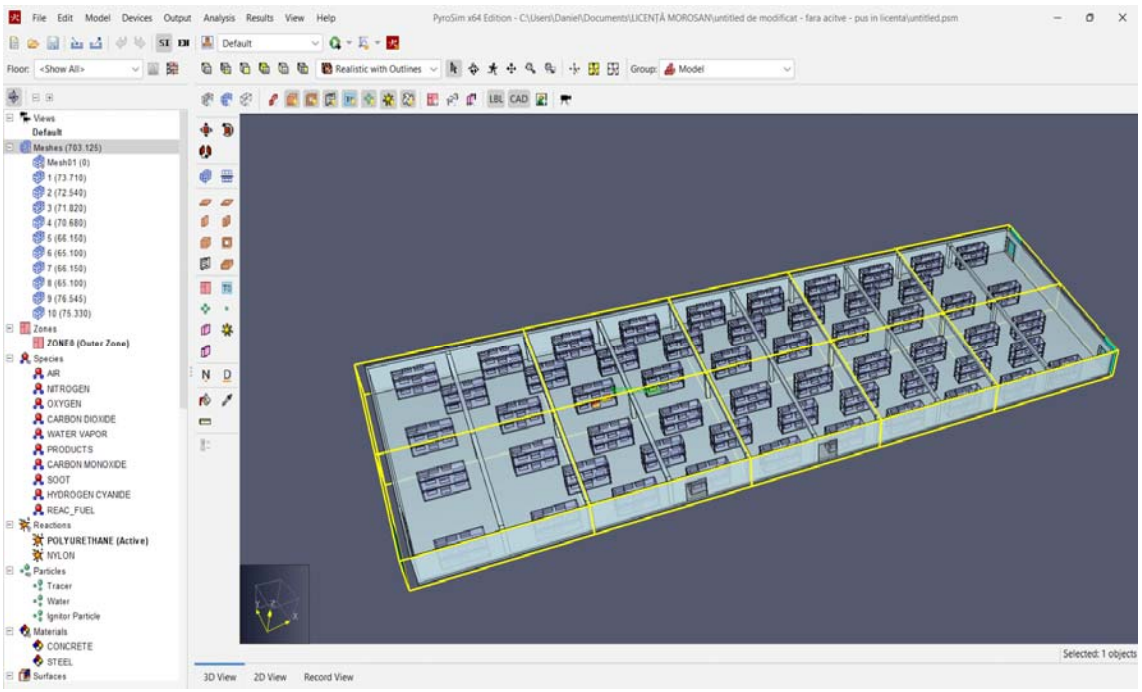

Fig. 2. Workspace Assignment

In order to establish a more detailed analysis of the fire parameters, 2D plans (slices) were introduced in the compartment.

These planes allow for the observation and interpretation of changes in temperature, visibility, and smoke movement velocity during the simulation.

By examining these plans at various points and at different points in the simulation, we can gain a deeper understanding of the evolution of the fire and its impact on the environment. This method helps us identify critical areas and develop effective fire response strategies.

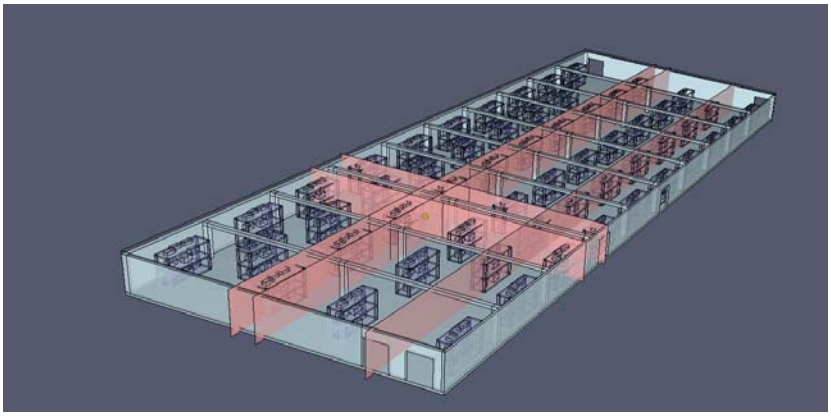

Fig. 3. Distribution of 2D planes

Definition of the simulation parameters:

There are many parameters that can be defined in Fire Dynamics Simulator (FDS), which influence the running time of the program depending on the duration of the fire simulation, radiation calculations, particle life, ambient configuration (temperature, pressure, concentration of gases in the air composition, humidity) [6].

The mesh resolution was selected based on a consideration of computational resources and the need to adequately resolve the key fire dynamics phenomena, particularly the flame height. A mesh sensitivity study was conducted to ensure that further refinement of the grid did not significantly alter the simulation results.

For the simulation, the following parameters of the ambient environment are established:

- Temperature: 20°C.
- Pressure: 101325 Pa.
- Mass fraction of oxygen: 0.2323.
- Relative humidity: 40%.
- Gravitational constant: 9.81 m/s^2

The particularities of the fire (temperature, visibility, smoke propagation in the respective space) will be analyzed for a period of 5-minutes, this time actually representing the duration until the intervention forces come into action according to the area of location of the warehouse within the intervention district specific to the detachment.

2. Scenario of the occurrence of the fire

The simulation focuses on a compartment intended for the storage of textile materials, in which the products are organized in boxes arranged on shelves, aligned in a single row. Inside this warehouse, there are about 60 tons of textiles and/or leather on an area developed by 1739.6 m^2.

Calculation of the thermal load [6,7]: The estimated thermal load of the compartment is determined according to the nature of the combustible materials present, as follows:

- According to MP008 Romanian norm *the calorific value* of finished textiles is:

$$Qi = 16{,}3\ Mj/kg.$$

- The thermal load of the storage space is:

$$60.000\ kg * 16{,}3\ Mj/kg = 978.000\ Mj$$

- The heat load density of the textile warehouse is:

$$\frac{978.000\ Mj}{1739{,}58\ m^2} = 562{,}2\ \frac{Mj}{m^2}$$

Fire risk: taking into account the purpose of the construction (textile warehouse), the fire risk is established in the case of production and/or storage buildings, thus resulting in a HIGH FIRE RISK [6,7].

Protection systems

The warehouse is subject to fire safety approval and/or authorization due to the developed area, which is greater than or equal to 600 sqm, in this case as 1739,6 sqm and as result the building must be equipped with active fire protection systems having [8,9]:

- indoor hydrant installations, being part of the category of fire limitation and extinguishing installations.
- fire detection, signaling and warning installations.
- hot gas smoke and exhaust installations for storage spaces with areas larger than 36 sqm.

The simulation scenario involves the negligence of an employee who throws a cigarette in the space, despite the strict smoking ban. The outbreak of the fire is initially formed in the packaging in which the textile products were kept, and the flames quickly spread to the adjacent boxes, thus creating an emergency situation.

Fortunately, the fire detection, signaling and warning installation worked at normal parameters, thus warning all the personnel in the building who managed to evacuate entirely and safely, thus there were no victims as a result of the emergency situation created. According to the reports of the own emergency intervention staff, the hydrant installation did not work with the supply valves stuck due to the lack of periodic maintenance, so the specific intervention staff had to evacuate, also noticing that the smoke extraction hatches were not opened. Thus, the worst case scenario was taken into consideration, to highlight the rapid spread of the smoke, even in the initial phase of the fire.

3. Interpretation and analysis of results

Based on the fire scenario, the analysis and interpretation of simulation results cover the first 5 minutes after ignition. This interval was selected because it represents the typical response time required for emergency services to arrive, allowing the study to effectively evaluate the conditions firefighters face upon entry.

At the same time, the non-functionality of the active fire protection systems in the facility's equipment (smoke extraction installation and indoor hydrant installation) will also be taken into account, due to various technical reasons caused by the lack of periodic maintenance.

The parameters of the fire are chosen according to their importance at the time

of the firefighters' intervention, which lead to an increase or decrease in the degree of difficulty of the mission itself.

Temperature

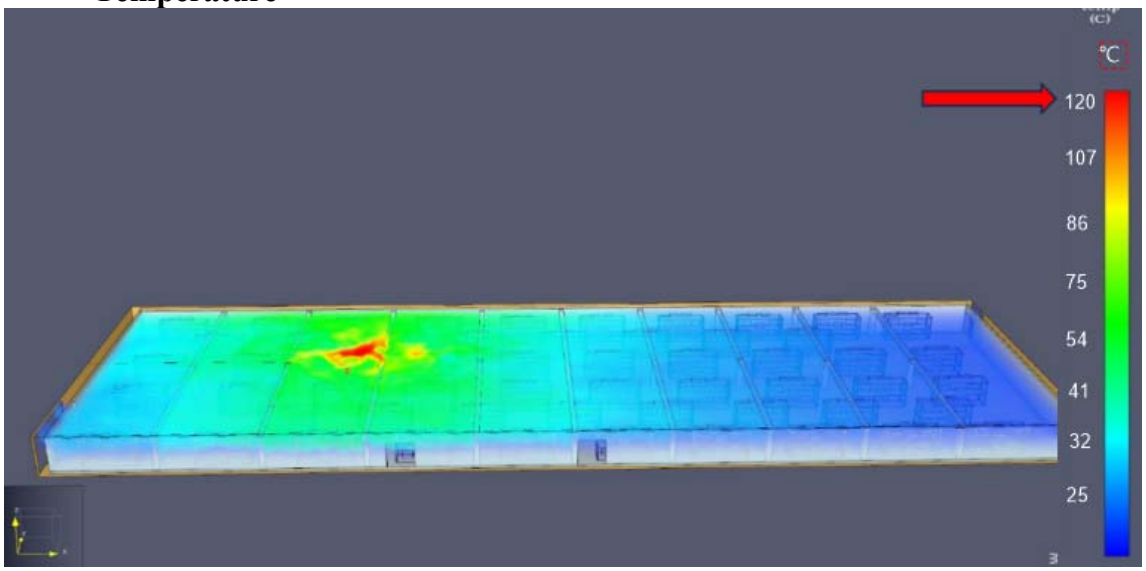

Fig. 4. Temperature of fire effluents

At ceiling level, in a fire compartment, the accumulated smoke and flue gases reach temperatures of over 120°C in the area of the firebox, after 5 minutes. This area is illustrated in Figure 4 in red. As the smoke moves horizontally over the entire surface of the ceiling, flooding the compartment, its temperature drops. This phenomenon is illustrated by the change in the color of the smoke to yellow, green and blue, respectively.

The ignition of textiles containing cotton involves the rapid transition from slow combustion to flame combustion. In the case of self-ignition, the carbonization of the inner layers occurs from a temperature of 160°C.

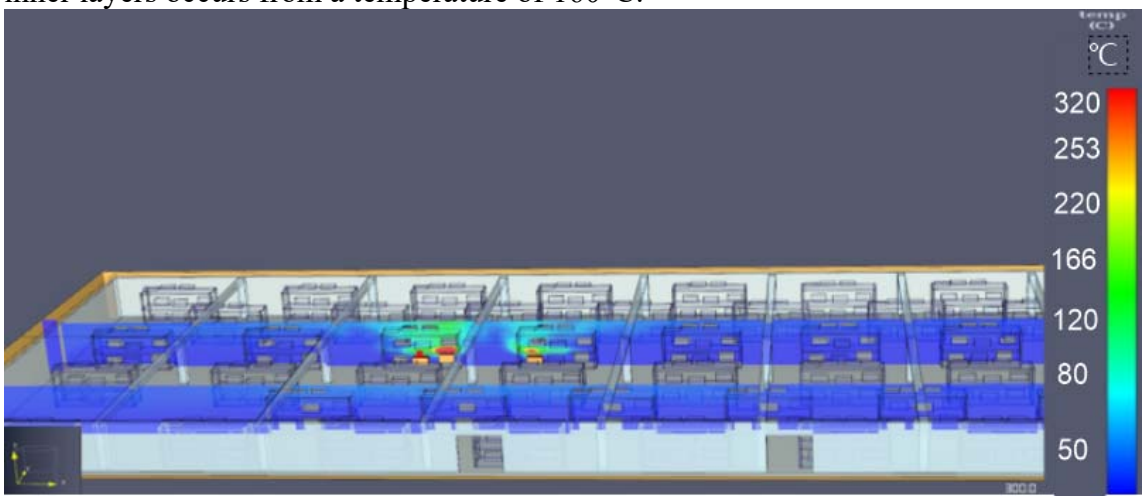

Fig. 5. Temperature in the area of the outbreak

On the other hand, synthetic fibers used in blends to make finished products have a lower fire hazard. These fibers melt under the action of heat. For example, nylon has a melting temperature between 200°C and 300°C [11].

Through experiments carried out, it has been shown that in the case of a combustion characterized by the presence of flames, about 70% of the energy generated by the fire is transferred to the environment through the convection process, while the remaining 30% is transmitted by radiation. This finding highlights the importance of the convection process in heat transmission in fires, where heated air rises and is replaced by cooler air, contributing to the spread and intensification of the fire [12-14].

Flue gas movement

In the absence of a smoke and hot gas evacuation system, the latter, being influenced by the upward force generated by the heat emanating during the fire, will rise vertically towards the ceiling of the room. Once in the ceiling area, the smoke will move horizontally towards the entire surface of the compartment, under the action of convection and turbulence.

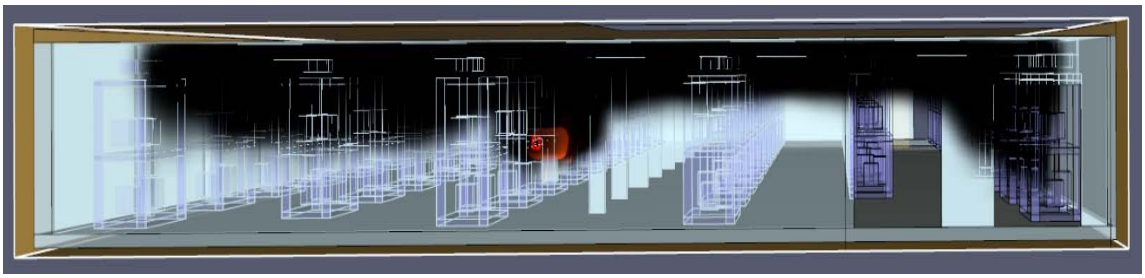

Fig. 6. Smoke stratification in the warehouse after 30 seconds

In this phase, the smoke forms a dense and coarse stratification that extends over the entire surface of the ceiling.

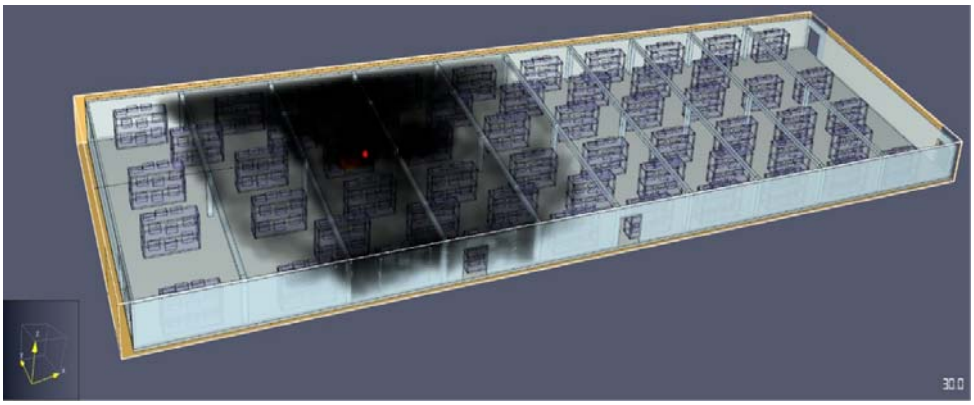

Fig. 7. Smoke propagation in the warehouse after 30 seconds

Fig. 8. Smoke propagation in the warehouse after 5 minutes

So, as can be seen from Figures 7 and 8, after 5 minutes the warehouse is flooded with smoke, greatly reducing visibility and making it difficult for firefighters to intervene.

Following the fire, due to the upward force generated by the heat emanating from the fires, the smoke and hot gases move vertically at a speed of around 1.5 meters per second, according to the indications shown in Figure 9, illustrated by a distinctive red color. Once they reach the top of the space, the smoke and flue gases slow down and begin to expand horizontally across the ceiling surface.

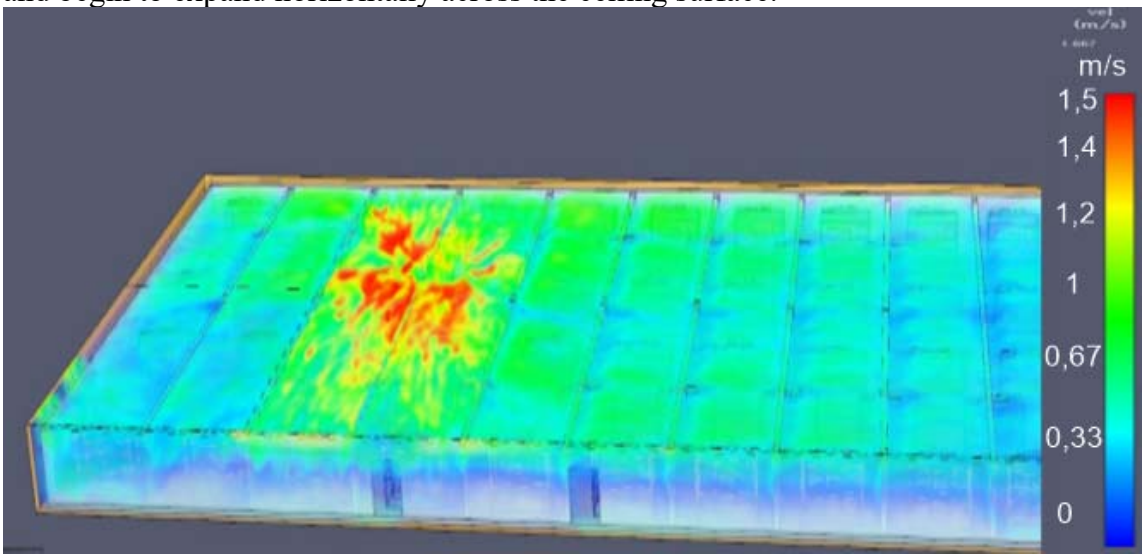

Fig. 9. Speed of smoke movement in the burned space after 5 minutes

As a result, the entire area of the warehouse is flooded with smoke, generating a dangerous situation in terms of safety and evacuation.

Factors influencing the rate of fire growth:

- *the amount of combustible dust* (such as in the textile or woodworking industry)
- *ventilation* because in closed spaces with low ventilation, the accumulation of smoke and heat is favored, accelerating the spread of the fire.
- *the composition of combustible materials* because fast-burning materials (such as textiles) will contribute to a faster spread of the fire

Visibility within the warehouse

Smoke stratification and vertical visibility:

- In an enclosed space, the smoke resulting from combustion tends to stratify, i.e. to accumulate in the upper part of the room.
- The smoke layer can greatly reduce vertical visibility. In many cases, vertical visibility can be completely lost in about 2 minutes.

It is important to emphasize that this aspect can become a significant threat to the safety of people and the building due to obstruction of visibility, increase in temperature and concentrations of toxic substances.

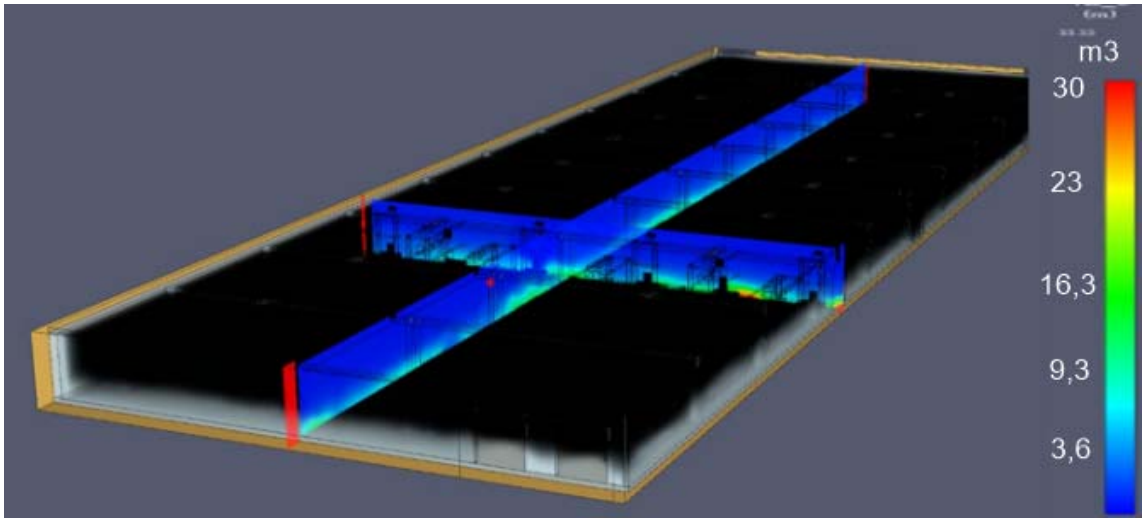

Fig. 10. Visibility in the warehouse at the time of the firefighters' intervention (5 minutes)

4. Conclusions

The use of simulations in the PyroSim program facilitates the obtaining of a general engineering perspective, clearly highlighting the parameters investigated in order to meet the fire safety requirements of the warehouse.

For the present study, the following values were obtained:

- maximum temperature of the fire effluents in the ceiling area, 120 °C.
- maximum temperature in the focus area, 320 °C.
- flue gas velocity around 1.5 m/s.

Visibility at the upper levels of the warehouse drops rapidly, becoming completely obscured within minutes due to heavy smoke accumulation. As time progresses, smoke gradually fills the entire space, significantly reducing visibility even at ground level by the 5-minute mark. This severely complicates firefighting efforts, making it difficult for intervention teams to navigate and perform rescue operations.

This study highlights the value of using CFD simulations to gain insights into fire dynamics within textile warehouses, together with improving fire safety strategies.

Future research should consider additional fire scenarios and perform detailed Heat Release Rate (HRR) analyses under varying conditions to study the heat transfer.

References

[1] Aditya Kumar Pandey, Manish Kumar Mishra, Application of Fire Dynamics Simulator in Warehouse Fires: A Case Study, International Research Journal of Engineering and Technology (IRJET), Volume: 07 Issue: 06 | June 2020, e-ISSN: 2395-0056

[2] Katarzyna Pawluk, Marzena Lendo-Siwicka et al., Sustainable Design and Construction Cost of Warehouse in the Light of Applicable Fire Regulations, Sustainability 2024, 16(7), https://doi.org/10.3390/su16073002

[3] Shifan Tao, Xuan Dong, Yaxin Tan, Yansong Wei, Bowen Wang, Yufeng Huang, Numerical simulation study on the smoke spread process under the influence of the hollow floorboard in the logistics warehouse, Case Studies in Thermal Engineering, Volume 15, November 2019, https://doi.org/10.1016/j.csite.2019.100517

[4] Thunderhead Engineering, https://support.thunderheadeng.com/docs/pyrosim/2024-2/user-manual/, Accessed on 01.09.2024

[5] Fire and Thermal Boundary Conditions in the FDS User Guide (McGrattan et al. 2021, 87)

[6] PyroSim Fundamentalas –https://files.thunderheadeng.com/support/documents/pyrosim-results-user-manual-2022-2.pdf, Accessed on 091.09.2024

[7] SR-10903-2016 - Calculation of Thermal Load Density

[8] Construction Fire Safety Regulations – P118, Romanian Norm, https://www.mdlpa.ro/subarticles/8/normativincediu032025

[9] HGR 571 – Government Decision on the approval of the categories of constructions and arrangements that are subject to fire safety approval and/or authorization

[10] ORDER no. 6.025/2018 for the modification of the technical regulation "Normative on fire safety of constructions, Part III - Detection, signaling and warning installations", indicative P 118/3-2015

[11] Diaconu-Şotropa D., Burlacu L., Phenomena of burning, Review AICPS no. 1/2007 Bucharest, 2007.

[12] Charlie Hopkin, Michael Spearpoint, Danny Hopkin, A Review of Design Values Adopted for Heat Release Rate Per Unit Area, Fire Technology, 55, 1599–1618, 2019, https://doi.org/10.1007/s10694-019-00834-8, Springer

[13] Drysdale, D. (2011). An Introduction to Fire Dynamics (3rd ed.). John Wiley & Sons.

[14] Society of Fire Protection Engineers (SFPE). (2016). SFPE Handbook of Fire Protection Engineering (5th ed.). Springer

Integrating Ice-Slurry Air Conditioning Systems with Renewable Energy Sources: A Sustainable Solution

Integrarea sistemelor de climatizare cu soluție de apă-gheață și surse de energie regenerabilă: O soluție sustenabilă.

Emil Iakaboș[1], Florea Chiriac[1], Alina Girip[1], Mădălina Teodora Nichita[1], Nicoleta Tanase[1,*],Eugen Badea[1] and Paul Dancă[1,2]

[1]Faculty of Building Services Technical University of Civil Engineering Bucharest
66 Pache Protopopescu Blvd, Bucharest, Romania
E-mail: mil.iakabos@eebc.ro, florea.chiriac@gmail.com, agirip4@yahoo.com, mtn_76@yahoo.com, wnicolw@yahoo.com, ebadea2010@gmail.com, paul.danca@utcb.ro,

[2]Department of Renewable Energy Sources, National Institute for Research and Development in Electrical Engineering ICPE-CA
313 Splaiul Independentei, Bucharest, Romania
E-mail: paul.danca@icpe-ca.ro

DOI: 10.37789/rjce.2025.16.2.3

Abstract. *The increasing demand for sustainable and energy-efficient cooling solutions highlights the potential of ice-slurry systems due to their high latent heat capacity and superior cooling performance. Integrating these systems with renewable energy sources, such as solar and wind power, further enhances their efficiency and sustainability. This study explores the theoretical principles, mathematical modeling, numerical simulations, and experimental validation of ice-slurry air conditioning powered by renewables. Additionally, it provides a detailed analysis of photovoltaic and wind energy utilization in conjunction with ice-slurry cooling. Findings demonstrate that this integration significantly reduces operational costs and carbon footprint while ensuring reliable and efficient thermal management in commercial and industrial buildings.*

Key words: *Ice-Slurry, Energy Storage, Renewable Energy*

1. Introduction

Thermal Energy Storage (TES) systems are gaining recognition as an effective solution for reducing energy costs and minimizing environmental impact, especially in air conditioning applications. These systems store thermal energy in the form of ice or chilled water during off-peak hours, typically at night when electricity rates are lower. The stored energy is then used during peak demand periods, reducing the need for electricity precisely when it's most expensive and the grid is under the greatest strain.

The article was received on 21.02.2025, accepted on 16.05.2025 and published on 22.05.2025

This approach not only lowers costs but also contributes to more efficient energy management overall [1].

One of the most valuable aspects of TES is its ability to shift energy consumption away from peak hours. At night, when grid demand is low, the system produces and stores ice or chilled water. The next day, as temperatures rise and air conditioning demand surges, the system taps into this stored energy to provide cooling, significantly reducing the need for on-the-spot electricity. This not only helps consumers avoid high electricity rates but also lessens the burden on power grids, reducing the need for fossil fuel-based energy production during peak hours [2].

The economic benefits of TES are hard to ignore, especially for buildings with high cooling needs like offices, shopping centers, and hospitals. By using cheaper nighttime electricity to generate cooling energy, businesses can drastically lower operating costs over time [3,4]. The financial savings are especially pronounced in regions with large differences between peak and off-peak electricity rates. Beyond cost savings, TES systems help improve the stability and reliability of the energy grid. Shifting large cooling loads to off-peak times smooths out electricity demand, reducing the likelihood of grid overloads and lowering the need for additional power plants or emergency energy reserves. This makes the entire energy system more resilient and sustainable in the long run [5].

Energy efficiency is another significant advantage. TES systems reduce the need for continuous operation of air conditioning units, which are typically energy-intensive. Instead, cooling is generated in advance and used as needed, cutting down overall energy consumption. Less energy use means fewer carbon emissions, and if the system is paired with renewable energy sources like solar or wind power, the environmental benefits are even greater [6,7]. What makes TES even more attractive is its flexibility. Systems can be tailored to different operational strategies, whether it's load-shifting—moving energy consumption to cheaper off-peak times—or load-leveling, which spreads energy use more evenly throughout the day. This adaptability makes TES suitable for a wide range of applications, from small residential buildings to massive industrial complexes [8].

In practice, TES is already making an impact across various sectors. Schools, hospitals, factories, and commercial buildings are increasingly adopting these systems to manage their cooling needs more sustainably. As technology advances, making TES systems even more efficient and affordable, their adoption is likely to grow, playing a crucial role in sustainable energy management for the future [9].

In summary, TES systems offer a practical, cost-effective, and sustainable approach to cooling. By optimizing energy use, reducing peak demand, and integrating seamlessly with renewable energy sources, they provide a pathway toward a greener and more resilient energy future. As energy demands continue to rise, these systems will become even more valuable in balancing sustainability with growing cooling needs. In this way in the current paper is presented a comparation regarding the efficiency of a conventional cooling system and an ice-slurry cooling system with TES powered from renewable energy sources.

2. Ice-Slurry System and Renewable Energy Integration

2.1 Ice-Slurry System Overview

An ice-slurry system is an innovative thermal energy storage solution that combines both ice and liquid phases to provide cooling. The system works by creating a suspension of fine ice particles in a liquid carrier, typically a mixture of water and glycol, that can efficiently absorb and transfer heat. Ice-slurry systems are particularly valuable in large commercial and industrial cooling applications, where they offer substantial energy savings and operational flexibility.

The key components of an ice-slurry system are as follows:

- Ice-Slurry Generator: This component is responsible for producing and maintaining the suspension of ice particles within the liquid medium. The generator operates by freezing a portion of the liquid carrier to form fine ice particles. These particles are then mixed evenly with the liquid to create a slurry that can be easily pumped and stored.
- Storage Tank: The storage tank holds the ice-slurry until it is needed for cooling. The size of the tank depends on the cooling requirements of the space and the duration for which cooling is required. The stored slurry can be used on-demand, providing flexibility in how and when cooling is applied.
- Distribution Network: This network consists of pumps and pipes that deliver the ice-slurry to the various cooling points within a building or facility. The distribution system is designed to ensure that the slurry reaches areas that require cooling efficiently, without significant losses of temperature.
- Heat Exchangers: Heat exchangers facilitate the heat transfer between the cooled space (such as a room or a machine) and the ice-slurry. They are crucial for ensuring that the cooling process is efficient, as they maximize the amount of heat extracted from the environment and transferred to the slurry.
- Overall, the ice-slurry system operates in a way that allows for highly efficient cooling while reducing reliance on traditional, energy-intensive air conditioning units. The use of thermal storage allows for cooling to occur when it is most cost-effective, typically during off-peak hours when electricity rates are lower.

2.2 Ice-Slurry Cooling Process and Calculations

The cooling effect of an ice-slurry system is achieved through two primary mechanisms: the sensible heat capacity of the liquid carrier and the latent heat of fusion of the ice particles. When the ice-slurry circulates through the system, the ice absorbs heat from the environment, causing it to melt. The phase change from solid to liquid requires energy, known as the latent heat of fusion, which results in the cooling effect.

The total cooling energy provided by the ice-slurry system is a combination of these two factors. The formula for calculating the total cooling energy is as follows:

$$Q_{total} = Q_{sensible} + Q_{latent} \quad (1)$$

Where:

Q_sensible represents the sensible heat energy absorbed by the liquid phase,
Q_latent represents the latent heat energy absorbed by the ice phase as it melts.
Let's take an example to understand the cooling requirement:
Example Calculation:

Consider a commercial space that requires 100 kW of cooling over a period of 10 hours. For simplicity, let's assume the ice-slurry has a 30% ice fraction and that the temperature drop required is 10°C. To calculate the mass of ice-slurry needed:
The latent heat of fusion for water (which is the most common liquid carrier) is approximately 334 kJ/kg. The total energy required for the cooling process is 100 kW × 10 hours = 1,000 kWh = 3,600,000 kJ. Since the ice fraction is 30%, the total mass of the slurry is distributed between ice and water. Assuming the energy required for cooling is split proportionally, approximately 30% of the total energy will be absorbed by the ice.

Using these values, approximately 17,240 kg of ice-slurry would be required to maintain the cooling over the 10-hour period.

3. Photovoltaic and Wind Energy Infrastructure for Ice-Slurry Systems

Integrating renewable energy sources like photovoltaic (solar) and wind energy into ice-slurry systems offers the potential for both reducing operational costs and improving environmental sustainability. These renewable sources provide a way to power ice-slurry systems with clean energy, reducing reliance on fossil fuels and lowering the carbon footprint of the entire cooling process.

3.1 Photovoltaic (PV) Infrastructure

Photovoltaic (PV) systems are widely used to convert sunlight into electricity. The solar panels used in these systems typically consist of semiconductor materials that produce electricity when exposed to light. The efficiency of a PV system depends on factors such as solar irradiance, the type of panels used, and environmental conditions like temperature.

The main components of a PV system that integrate with ice-slurry systems include:

- Solar Panels: These are the primary components that convert sunlight into electricity. Panels are generally made from monocrystalline or polycrystalline silicon and provide efficiency rates ranging from 15% to 22%, depending on the quality of the panel and sunlight exposure.
- Inverters: Solar inverters convert the direct current (DC) electricity generated by the solar panels into alternating current (AC), which is required for the operation of the ice-slurry system.
- Battery Storage: To handle fluctuations in solar energy availability, battery storage systems are used to store excess energy produced during peak sunlight hours. This

stored energy can then be used when the solar generation drops, ensuring that the ice-slurry system receives a constant power supply, even during cloudy periods or at night.

- Controllers and Monitoring Systems: These systems optimize the operation of the PV setup by monitoring energy production, consumption, and storage, ensuring maximum efficiency and performance.

The power generated by a PV system can be calculated using the following formula for a 200 m² panel area, 1000 W/m² solar irradiance, and 22% efficiency:

$$P = \text{Area} \times \text{Irradiance} \times \text{Efficiency}\ P = 200\ m^2 \times 1000\ W/m^2 \times 0.22 = 44\ kW \quad (2)$$

Thus, a PV system of this size would generate 44 kW of electricity under optimal conditions. This could be used to power the ice-slurry system during the day, with excess energy stored for use during off-peak hours.

3.2 Wind Energy Infrastructure

Wind energy is another renewable source that can complement the operation of ice-slurry systems. Wind turbines convert the kinetic energy from wind into electrical energy, which can be used to power the ice-slurry system or stored in batteries for later use. Wind turbines come in two primary designs: horizontal-axis turbines (more common for large-scale production) and vertical-axis turbines.

Key parameters for integrating wind energy into an ice-slurry system include:

- Cut-In Speed: The minimum wind speed at which the turbine begins to generate power. This is typically around 3-4 m/s.
- Rated Power Output: The maximum power the turbine can generate, which typically ranges from 5 kW for small turbines to over 100 kW for large turbines used in commercial setups.
- Capacity Factor: This represents the ratio of actual energy output to the theoretical maximum energy output, with typical values ranging from 25% to 45%, depending on the wind conditions.
- Energy Storage: Because wind energy is intermittent, energy storage systems are needed to balance the fluctuating supply and demand. Batteries or other storage solutions ensure that the energy generated during windy periods can be used when wind speeds are lower.

The power output of a wind turbine is given by the formula:

$$P = 0.5 \times \rho \times A \times v^3 \times Cp \quad (3)$$

Where:

ρ is the air density (approximately 1.225 kg/m³ at sea level),
A is the area swept by the turbine blades,
v is the wind velocity,

Cp is the power coefficient (a measure of the efficiency of the turbine, typically around 0.35-0.45 for modern turbines).

For a wind turbine with a 10 m blade radius and a wind speed of 8 m/s, the power output can be calculated to understand how much energy can be generated. These calculations are crucial in assessing the overall efficiency and viability of integrating wind energy with an ice-slurry system.

4. Efficiency Comparison: Ice-Slurry vs. Conventional Cooling Systems

One of the main advantages of ice-slurry systems is their efficiency compared to conventional cooling systems. These systems have shown to offer higher performance in terms of energy efficiency, cost savings, and environmental impact.

4.1 Energy Efficiency Metrics

Coefficient of Performance (COP): Ice-slurry systems typically achieve COP values between 4 and 6, which is significantly higher than traditional air conditioning systems, which typically range from 2.5 to 4. This means that ice-slurry systems provide more cooling per unit of energy consumed, leading to lower energy costs and reduced demand on the power grid.

Energy Consumption: Ice-slurry systems generally require 30-50% less energy than conventional cooling methods. This reduction in energy consumption translates directly into cost savings, especially when integrated with renewable energy sources like solar or wind power.

Carbon Footprint: By utilizing renewable energy such as solar and wind power to run the ice-slurry system, the carbon dioxide emissions can be reduced by up to 60% compared to fossil fuel-based cooling systems. This makes ice-slurry systems an environmentally friendly alternative, particularly in regions focused on sustainability and carbon reduction.

Overall, integrating ice-slurry systems with renewable energy sources not only provides significant economic benefits but also contributes to a greener, more sustainable future for cooling technologies.Prezentarea va fi clară şi concisă, iar simbolurile utilizate vor fi definite în cadrul unei liste de simboluri (dacă este cazul). Se va folosi Sistemul Internaţional (SI) de unităţi de măsură.

5. Conclusions

The integration of ice-slurry air conditioning systems with renewable energy sources such as photovoltaic and wind energy presents a highly efficient and sustainable cooling solution. By leveraging the unique thermal properties of ice-slurry, these systems provide superior cooling performance while significantly reducing energy consumption and operational costs compared to conventional cooling methods. The ability to store and utilize thermal energy during peak demand periods allows for better

load management, ultimately easing the strain on electrical grids and enhancing overall energy efficiency.

The efficiency analysis conducted in this study demonstrates that ice-slurry systems, when combined with renewable energy, can achieve substantial reductions in carbon emissions—up to 60% compared to traditional cooling methods. The high coefficient of performance (COP) and lower energy requirements make ice-slurry technology an attractive option for commercial and industrial applications, particularly in regions where electricity costs are high and sustainability initiatives are prioritized.

Furthermore, the integration of solar photovoltaic and wind energy infrastructure enhances the feasibility of these systems by providing a clean and renewable power source. Solar panels, with efficiency rates of up to 22%, can generate substantial electricity during peak sunlight hours, while wind turbines offer a complementary power supply that can be utilized even during periods of low solar availability. The inclusion of battery storage systems further improves reliability, ensuring a consistent and uninterrupted cooling supply.

Looking ahead, advancements in energy storage technology and intelligent control strategies will play a crucial role in optimizing the performance of ice-slurry systems. Improved battery storage solutions, real-time monitoring, and automated control mechanisms will enhance energy efficiency, making these systems even more attractive for widespread adoption. Additionally, further research into optimizing ice-slurry generation and distribution methods will contribute to increasing system efficiency and reducing operational costs.

In conclusion, ice-slurry air conditioning systems integrated with photovoltaic and wind energy sources offer a viable, cost-effective, and environmentally friendly alternative to conventional cooling technologies. As energy demands continue to rise and the transition toward sustainable energy accelerates, these systems will play an essential role in shaping the future of energy-efficient cooling solutions across commercial and industrial sectors.

Acknoledgement

This work was carried out through the NUCLEU program of the National Plan for Research, Development and Innovation 2022-2027 carried out with the support of the Romanian Ministry of Research Innovation and Digitization, contract number 42N/2023 project number PN23140101

References

[1]. Beijneveld, T., J. Alpízar-Castillo, and L. Ramírez-Elizondo, Photovoltaic thermal system design including aquifer thermal energy storage in a fifth generation district heating network in Hilversum. Case Studies in Thermal Engineering, 2025. 68: p. 105854.

[2]. Alva, G., Y. Lin, and G. Fang, An overview of thermal energy storage systems. Energy, 2018. 144: p. 341-378.

[3]. Kamal, R., et al., Strategic control and cost optimization of thermal energy storage in buildings using EnergyPlus. Applied Energy, 2019. 246: p. 77-90.
[4]. Iakabos, E., et al., Enhancing the performance of a heating, ventilation, and air conditioning system using ice slurry. E3S Web Conf., 2025. 608: p. 01006.
[5]. Deka, P. and A. Szlęk, Thermal energy storage in buildings: opportunities and challenges. Archives of Thermodynamics, 2022. vol. 43(No 4): p. 21-61.
[6]. Calotă, R., et al., Bridging the gap: Discrepancies in energy efficiency and smart readiness of buildings. Energy Reports, 2024. 12: p. 5886-5898.
[7]. Danca, P.A., et al., A possibility of harnessing the heat discarded into the environment using thermoelectric generators. IOP Conference Series: Earth and Environmental Science, 2023. 1234(1): p. 012006.
[8]. Vérez, D., et al., Thermal energy storage co-benefits in building applications transferred from a renewable energy perspective. Journal of Energy Storage, 2023. 58: p. 106344.
[9]. Talebjedi, B., T. Laukkanen, and H. Holmberg, Integration of thermal energy storage for sustainable energy hubs in the forest industry: A comprehensive analysis of cost, thermodynamic efficiency, and availability. Heliyon, 2024. 10(17): p. e36519.

About sustainable installations

Despre instalații sustenabile

Dr. Ing. Adrian Retezan[1], Ing. Florin Bumbar[2], Dr. Ing. Remus Retezan[2]
[1] University Politehnica Timișoara, Civil Engineering Faculty, Civil Engineering and Building Services Department, Romania
e-mail: adrian_retezan@yahoo.com

[2] SC SOMIAL CONSTRUCT SRL
Com. Dumbrăvița, Str. Petofi Sanor 1C, Jud. Timiș, Romania
e-mail: florin.bumbar@somial.ro, remus.retezan@somial.ro

DOI: 10.37789/rjce.2025.16.2.4

Abstract
The paper presents the importance and approach of sustainability, with particularization for the construction works. A way of determining by score and qualitative appreciation of sustainability is provided.

Keywords: *sustainability, installations, construction*

1. Preliminary considerations – generalities

MAN is (should be) considered as the ultimate beneficiary of all socio-political, scientific-technical, cutural-artistic and sporting activities, of all human activities (of individuals, groups, professional associations, etc., governments, parliaments, international organizations); humanity is, in substance, the sum of all individuals/ people.

MAN (if he is HUMAN) must live (to live) in harmony with Heaven and Earth (fig.1)

MAN is understood both as an individual and as a society (to whom it is incumbent upon the task/debt of giving thanks/to ensure the well-being of the individual) and has an obligation to respect the laws that make him a partner with the universe [1].

For good ”knowledge” in the universe, man has a duty to know them and take into account its laws by issuing its own laws (at all levels) and their correct application.

The level of knowledge of these laws differentiates (intellectually and in terms of obligations) individuals, maintaining their equality in front of life.

Reaching ”perfection” is the purpose of all human activities (including laws), to which everyone must knowingly participate.

The article was received on 22.04.2025, accepted on 21.05.2025 and published on 22.05.2025

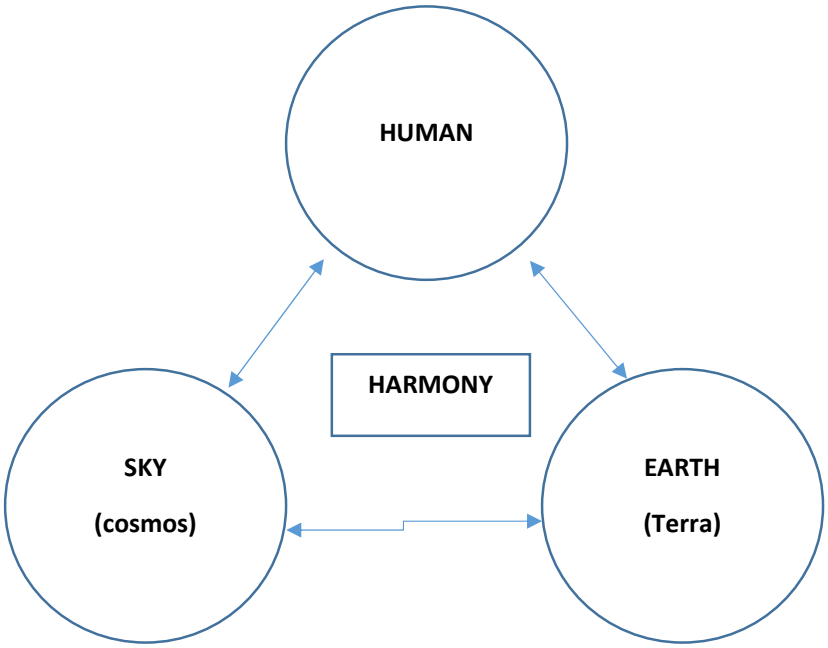

Fig. 1. Premise of life

Harmonization ”legalized” OM-NATURE is provided in Law 10/1995 (with subsequent additions), for constructions and related installations, at Art.5 lit.g) ”s sustainable use of natural resources”, and at pct.2) Specification is made:”fundamental requirements are established by domains/subdomains and categories of constructions and by specialties for installations related to constructions.”.

According to DEX, sustainability is ”the quality of an anthropogenic activity to unfold without depletion of available sources and without destroying the environment, so without compromising the satisfaction of the needs of future generations”.

2. Method of approach

The constructions/buildings are differentiated in:

a) Existing;

b) New, that is, in the design/preparation phase of the execution work.

For the existing works, the possibility of interventions (the case of maintenance works, capital repairs, change of destination, demolitions) is analyzed.

The new works will take into account (and will take into account) technological progress, raw materials, human health (and other living things).

For construction installations, sustainability will be analyzed from ”source”, which can be warehouse/store/warehouse/manufacturer (in no case sand quarry or iron extraction moun/coal, etc., or dam that provides water to a hydorcentral, etc.).

Functions of construction installations (fig.2), specific to the buildings/ constructions served, are defining in the selection/preference of beneficiaries.

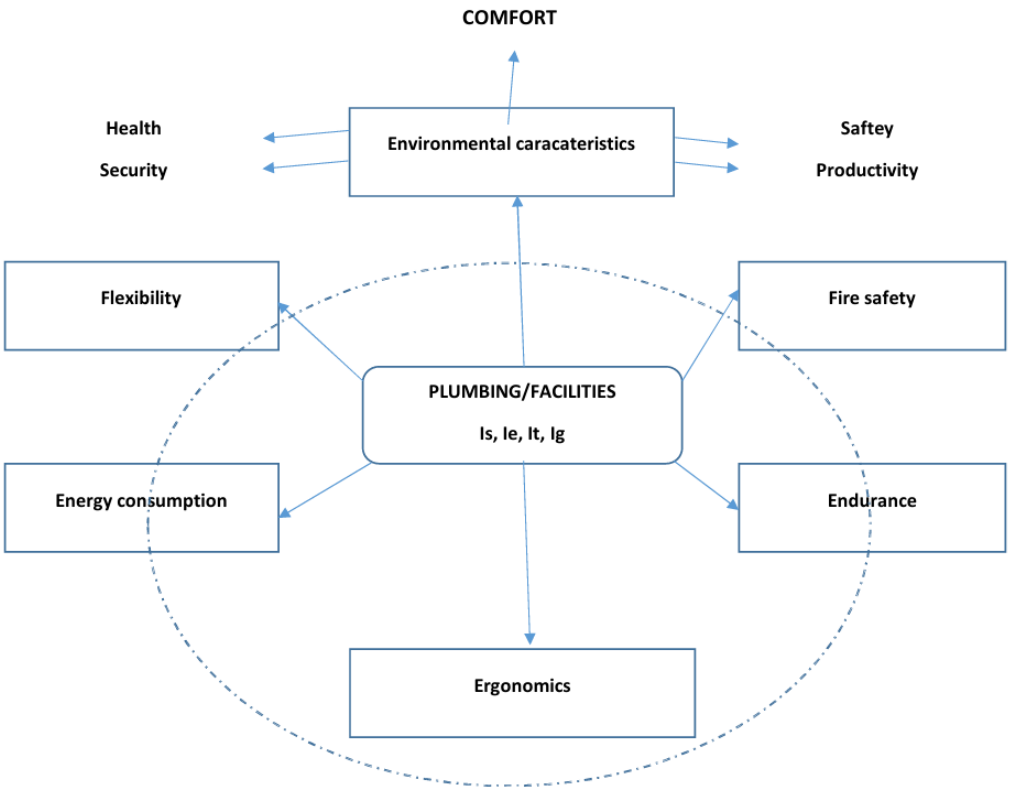

Fig 2.

The sustainability of the installations can be approached (characterized) globally, or by specialties by:

a) Defining footprint: ecological; carbon; water;

b) Methodologies (drafted by authorized companies) based on weighted criteria/ parameters (influenced by the importance of the objective, but also by the ”interest of the developer).

Location, through climatic parameters, requires the determination of the approach to sustainability.

3. Technical aspects

The conceptual/functional realization of the installations [2] aims at ensuring:

1) Reducing energy consumers ”classic” by renewable energy replacement, as well as by increasing yields (through new constructive concepts) to consumers;

2) Environmental protection (ambientally by noise reduction, air quality assurance, optimized lighting, but also by what and how ”transfer” to the outside environment):

3) Insured comfort (removal of excesses/”sclavagism” comfort);

4) Ensuring sustainability.

The expected help from the architect is essential for both the installer and the structurist, so a correct collaboration is required, taking into account existing

technologies and equipment of the executor and taking into account the directives, the, normlatives, standards that propose ”Save life on Terra”.

Each specialist, by what he does, is considering reducing waste, reusing materials (”circular economy”) and promoting new materials/equipment/technologies/principles of approach, but also refurbishments/modernizations.

Problems/weights arise when the price factor appears (which contributes to the depth of the social and economic gaps - real sources of ”sabotare” global sustainability.

Criteria/parameters of ””/”precise”/”recise” sustainability, specific to each methodology (BREEAM-Building Research Establishment Environmental Aaassment Metot, LEED-Leadriding in Energy and Environmental Design, etc, DGNB-Deutsche Gesellshoft fur Nachhaltiges Bauer etc.) have in common:

- Energy – required and consumed;
- Location – access and facilities;
- Water assurance – quality, assurance, recirculation and reuse, etc.;
- Embedded materials – quality, provenance, characteristics;
- Ecology – land use, additional works, etc.;
- Pollution reduction – in any form;
- Innovation – with positive functional and environmental effects;
- Health and comfort/well-being;
- Priorities – local, regional – in fact interests;
- Management etc.

Obs.1) These specific constructions/parameters, respectively buildings, are also to be taken into account the installations, for construction – global approach or specialties - .

The parameters/criteria taken into account must characterize the reality (desired/ existent), operation, operation and maintenance.

No time (respectively criterion/parameter) should be considered except in correlation with the environment.

The complexity of the objective/installations, if they do not reduce the negative impact on the environment, does not affect sustainability.

Installations, equipment, materials (which give ”life” buildings) have their sustainability according to their production, virtually unknown to the installer (the manufacturer does not pass it in the technical book) – it will not take it into account.

Table 1 proposes/shows the table head for establishing the sustainability of a goal (building installations, ventilation installations – air conditioning, lighting/ force/ signalling installations, water supply installations, etc.).

Sustainability. Objectively

Table 1

Nr. crt.	Parameter (criterion)	% participatory (П)	Note parameter / criterion	Score
0	1	2	3	4
TOTAL		100	-	0....10

Obs. 1) The parameters/characteristics (n) defining sustainability are determined by the holder of the methodology, by distinct types of objectives (eg installations).

Obs. 2) The participatory percentage [3] established by the holder shall take into account the contribution made by the parameter/criterion in protecting the environment.

Obs. 3) note the parameter Ni, i=1..n; is recommended as n≤12 with exceptions being contained/represented by the note.

Obs. 4) The P score is calculated with the relations:

Pi=(·Ni)/100 and P=ni

Depending on the score obtained, sustainability can be assessed by the scale shown in Table 2.

Sustainability scale

Table 2

Score	≥9	8,9÷7,5	7,4÷6,1	6÷5	4,9÷4	≤
Sustainability	Exceptional	Great	Better	Satisfactory	Unsatisfactory	Unacceptable
	Platinum	Gold	Silver	Bronze	Mud	Manure/Compost

The calculation of sustainability depends on the good definition of the objective, the degree of accuracy of the determination of parameters and their weighting equally the grade given to them that depends on quality, physical and functional condition.

For a subject – objective: man, building, locality, area etc. – can determine (taking into account the sum of activities, behavioural etc.) the ecological, carbon, carbon footprint, water with which it is possible to decide and sustainability.

4. Conclusions

SUSTAINABILITY and SUSTAINABLE DEVELOPMENT do not equal, sustainability includes sustainability.

MAN, the recipient of all activities in society, has the purpose/debt of living in harmony with Heaven and Earth to understand and recognize/apply their laws.

The legislation is intended to ensure progress in compliance with the needs of life factors.

Installations in construction, through equipment, operation and maintenance, reflect the degree of education, civilization and responsibility of man and society.

For construction installations it is recommended to assess sustainability by starting from ”source” (warehouses, manufacturers, distributors) of materials and equipment (which could also provide information about sustainability (useful of choice).

The definition of the sustainability of a concrete objective (for example, the indoor heating installation of an educational building) depends on the parameters (criteria) envisaged (e.g. heat source – district heating system; own heating system operating on natural gas/wood/electricity/unconventional sources).

For each of the parameters/criteria, depending on the environmental effects, the weight is specified and it receives a note – from 1 to 10 – (taking into account the yield/functional quality; with these the score is determined.

Based on the score the appreciation appears in the sustainability scale by providing information to those interested.

References

[1] Retezan A., Doboși I.S.-The optimized thermal comfort prevision for public buildings with multiple functionalities, health Buildings, vol.2, Esspo, August 2000, Finland.

[2] Bob C., Bob L.-Sustenability in Science Engineering, Timișoara, May 27-29, 2009.

[3] Retezan A., Bob C., Tamas D.-Considerații referitoare la sustenabilitate și economia de energie, România Instalații, nr. 3-4 2012.

Characteristics of a thunderstorm downburst measured in a suburban area

Caracteristicile unei furtuni măsurate în zonă suburbană

Ileana Calotescu[1], Daniel Bîtcă[2]

[1]Technical University of Civil Engineering Bucharest.
Bd. Lacul Tei nr. 122 - 124, cod 020396, Sector 2, București, Romania
E-mail: ileana.calotescu@utcb.ro

[2]Technical University of Civil Engineering Bucharest.
Bd. Lacul Tei nr. 122 - 124, cod 020396, Sector 2, București, Romania
E-mail: dan.bitca@utcb.ro

DOI: 10.37789/rjce.2025.16.2.5

Abstract. *This paper analyses a thunderstorm downburst record measured by a monitoring system installed on a 50 m high telecommunication lattice tower. The structure is located in the suburbs of Afumați, Ilfov County, approximately 15 km from Bucharest, the capital city of Romania. The monitoring system was developed under the SEVAST research project which aims at identifying the full-scale behaviour of a telecommunication lattice tower subjected to synoptic and non-synoptic winds. Since its implementation, the system has captured more than 10 thunderstorms. In this paper, the statistical parameters of the wind velocity measured during a thunderstorm downburst measured on May 7th 2024 are evaluated.*

Key words: *thunderstorm downburst, full-scale monitoring, lattice tower, wind*

1. Introduction

Research on thunderstorms and their effect on structures has been developed for more than forty years around the world in an effort to identify their characteristics and establish guidelines for design practice [1]. However, current wind loading codes still make use of traditional techniques developed based on the synoptic extra-tropical cyclone model which assumes statistical stationarity and logarithmic wind velocity profiles [2]. This is partly due to the scarcity of quality full-scale data and partly to the lack of consensus regarding the characteristics of thunderstorms needed for engineering design. Thunderstorms show considerable differences from boundary layer winds, both in terms of meteorological phenomena producing each type of wind and in terms of wind flow characteristics relevant for structural response, such as velocity profiles, turbulence intensity gust factors. Field detection and instrumentation

The article was received on 31.03.2025, accepted on 15.05.2025 and published on 22.05.2025

of real structures is of paramount importance in evaluating these differences and advancing the knowledge in thunderstorm research.

One of the first field programs to study thunderstorms, namely NIMROD (Northern Illinois Meteorological Research on Downbursts), was carried out by Fujita in 1978 [3] with the aim to depict the structure of downbursts by using Doppler radars and anemometers installed in the suburbs of Chicago, USA. Subsequently, a second monitoring network named JAWS (Joint Airport Weather Studies) was established in 1982, to understand the mechanism of microbursts which were the cause of a number of accidents involving aircrafts at the time [3]. More recent studies have focused on identifying thunderstorm characteristics based on downbursts measured by classical meteorological weather stations [4-6] or anemometric records [7-9] as well as differences between downburst and atmospheric boundary layer (ABL) induced loading on low-rise buildings [10] or slender steel structure [11,12].

This paper describes the characteristics of a thunderstorm downburst measured by a wind and structural monitoring system installed on a 50 m tall telecommunication lattice tower located in a suburban area approximately 20 km North-West of Bucharest, the capital city of Romania. Section 2 presents the site and tower characteristics. In Section 3, the monitoring system is described while Section 4 presents the characteristics of the thunderstorm record. Finally, Section 5 presents the main conclusions of the paper.

2. Site and tower characterization

The tower is located on the outskirts of Afumați (Fig. 1a), the site being characterized by different terrain categories according to the Romanian wind code CR1-1-4/2012 [13] i.e. terrain category II (roughness length z_0=0.05m) for North-East and South-West directions and terrain category III (roughness length z_0=0.3m) for South-East and North-West directions, the reference wind velocity being v_b=25.30 m/s. Assuming a logarithmic mean wind profile, the design wind parameters evaluated on a 10-min interval at heights of 10 m and 50 m are summarized in Table 1.

Table 1

Design wind parameters at the Afumați site evaluated based on CR 1-1-4/2012 [13]

Parameter	H=10 (m)		H=50 (m)	
	Category II	Category III	Category II	Category III
Mean wind velocity, v_{m10}^0 (m/s)	25.47	19.10	33.02	27.87
Peak wind velocity, v_p^0 (m/s)	43.12	37.05	50.82	45.82
Gust factor, G_{10}^0	1.70	1.93	1.54	1.64
Turbulence intensity, I_v	0.20	0.26	0.15	0.18

The monitored structure is a 50 m high telecommunication lattice tower having a triangular in-plane section (Fig. 1b). The tower is divided into 10 sections of approximately equal heights. The bottom 5 sections are made up of inverted V-bracing systems whereas the upper 5 sections are made up of N-bracing systems. All the structural elements of the tower are made of hollow circular cross-sections. Along the

tower height there are two resting platforms at 15 m and 27.50 m as well as two working platforms at 40 m and 47.50 m. Various ancillary elements are supported by the tower amounting to approximately 4.5 tons. The total mass of the structure comprising structural and ancillary elements is 13.7 tons.

(a)

(b)

Fig. 1. (a) Location of monitoring system (North aligned vertically) and (b) the monitored tower

3. The monitoring system

The monitoring system (Fig. 2) is made up of (*i*) meteorological sensors, comprising an ultrasonic anemometer and a four-camera video system, (*ii*) structural monitoring sensors, including three strain gauges and one triaxial accelerometer, (*iii*) data acquisition system, comprised of a datalogger and modules located in the shelter at the base of the structure. The ultrasonic anemometer has a sampling frequency of 10 Hz and is able to measure wind speed, wind direction and ambient temperature. It is installed on a leg member at the top of the tower. A four-camera video system was installed on the tower to complement the meteorological sensors. Three cameras were installed at 12 m and are pointing to the horizon to capture cloud formations and evolution whereas one camera was installed at 15 m and is pointing towards the shelter for surveillance aim. Each video camera has a 120^{o} angle range approximately centered on the North-East, South-West and North-West directions. The triaxial accelerometer is installed at 50 m on a tower leg and has a sampling rate of 125 Hz. Finally, the strain gauges are installed at the tower base on the three leg members and have a sampling frequency of 100 Hz. The datalogger is installed in the shelter located at the base of the tower. It stores the data corresponding to all sensors on a continuous basis and transmits it to the server located at the Technical University of Civil Engineering Bucharest (UTCB).

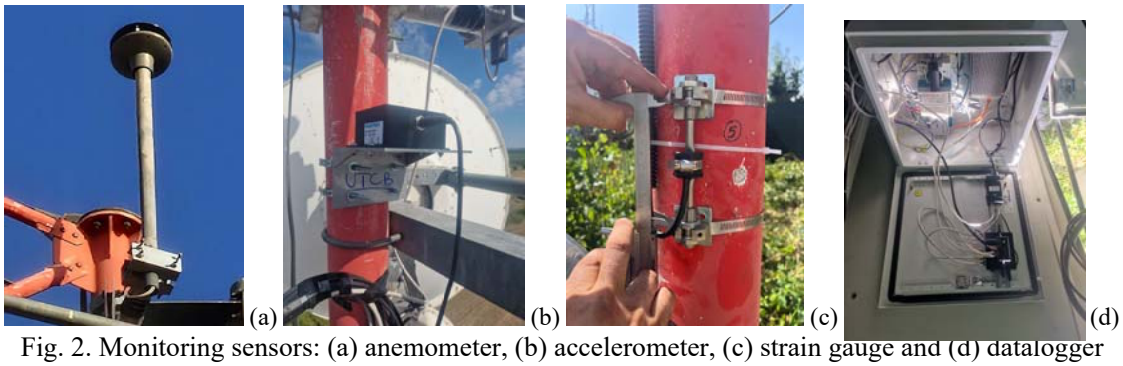
(a) (b) (c) (d)

Fig. 2. Monitoring sensors: (a) anemometer, (b) accelerometer, (c) strain gauge and (d) datalogger

4. Thunderstorm characteristics

Thunderstorm records are generally characterized by a sudden increase (ramp-up) and decrease (ramp-down) in wind velocity observed in a short interval of time; sometimes it is coupled with a sudden drop in temperature and a change in wind direction. A thunderstorm record may also be characterized by large peak velocities and gust factors defined as the ratios between the peak and the mean wind speed on the specified averaging time interval.

Classification and separation of records from anemometric data [14] may be done by means of quantitative controls mainly based on expert judgement of the wind velocity time history patterns and qualitative controls expressed in terms of gust factor ratios defined as G_1/G_{10}, G_{10}/G_{10}^0 and G_{60}/G_{60}^0 where 10 and 60 represent the wind speed averaging time interval expressed in minutes and 0 indicates the reference values (Tab. 1). Three categories of records are considered: depressions (D), gust fronts (F) and thunderstorms (T) determined by considering a threshold of 15 m/s of the peak wind velocity averaged on 1-s.

In this paper, a thunderstorm record measured on May 7th 2024 extracted based on the above-mentioned procedure [14] is analysed and its main statistical parameters are evaluated. Figure 2 shows the cloud formation during the event as recorded by the video cameras. The downdraft is mostly visible in the NW direction which is in agreement with the direction measurements acquired by the anemometer. The radar images captured at the time of the event and published on the website of the Romanian National Meteorological Administration confirm the occurrence of the thunderstorm.

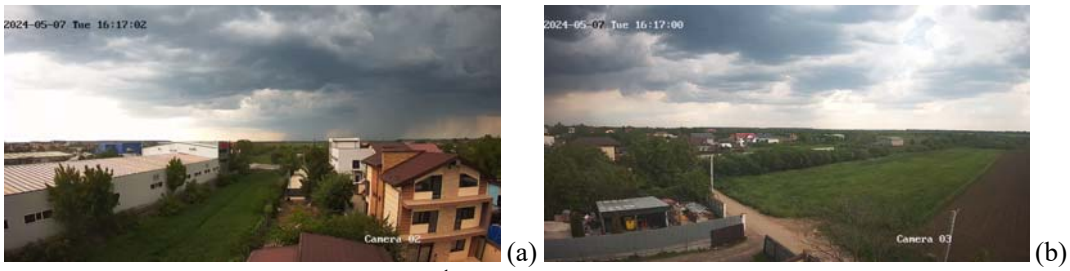

(a) (b)

Fig. 3. Snapshots taken during the May 7th 2024 event at 16:17 EEST (a) NW and (b) NE directions

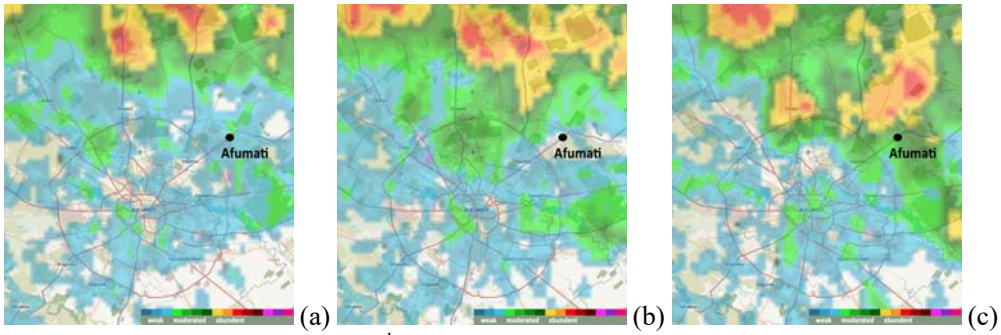

(a) (b) (c)

Fig. 4. Radar images on May 7th 2024 at: (a) 16:21, (b) 16:31 and (c) 16:41 EET (https://www.meteoromania.ro/)

Figure 5 shows the variation of the wind speed and wind direction together with their respective Probability Density Functions (PDF) within a 10-min interval centered around the peak velocity. The ramp-up and ramp-down of this thunderstorm are clearly visible in the 10-min interval. The total duration of the event was approximately 5 minutes. The temperature dropped by approximately 5 ºC and the wind direction changed gradually from 180 to 270 degrees. The registered instantaneous peak wind speed was v_{max} = 20.3 m/s whereas the 10-min mean wind speed was $\overline{v}_{m10}$ = 9. 82 m/s. The skewness and kurtosis resulted s=0.83 and k=3.28 respectively which deviate considerably from the normal distribution. Finally, the 10-min gust factor defined as $G_{10} = v_{max}/\overline{v}_{10}$ resulted G_{10}=2.07 which much larger that the code-recommended one (Tab. 1).

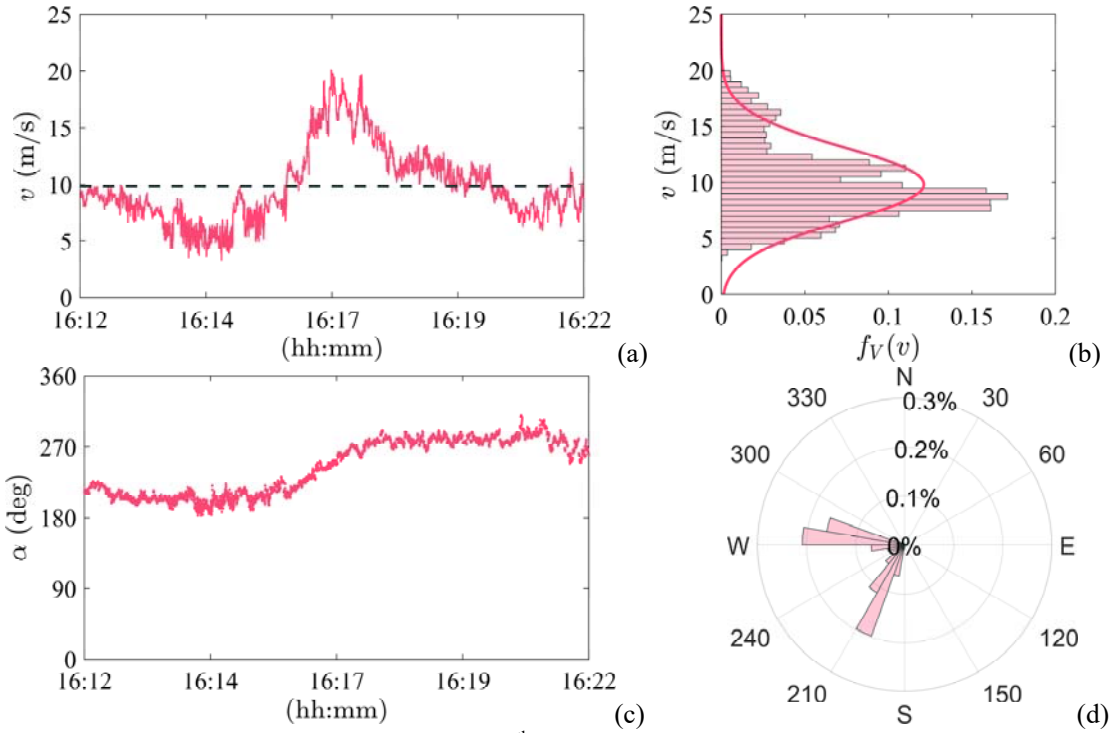

Fig. 5. Thunderstorm event recorded on May 7th 2024: (a) wind speed, (b) wind direction, (c) PDF of wind speed and (c) PDF of wind direction in 10-min

The decomposition of the velocity records associated with thunderstorms is expressed as [15]:

$$v(t) = \overline{v}(t) + v'(t) = \overline{v}(t) + \sigma_v(t)\tilde{v}'(t) = \overline{v}_{\max}\gamma(t)\left[1 + \overline{I}_v\mu(t)\tilde{v}'(t)\right] \quad (1)$$

where t is the time, $\overline{v}$ is the slowly varying mean wind velocity and v' is the residual fluctuation extracted by making use of the moving average filter considering a moving average period T = 30 s [15], σ_v is the slowly varying standard deviation of v', $\tilde{v}'$ is the reduced turbulent fluctuation, I_v represents the slowly varying turbulence intensity and γ and μ represent two non-dimensional ratios defined as:

$$\gamma(t) = \overline{v}(t)/\overline{v}_{\max} \quad (2)$$

$$\mu(t) = I_v(t)/\overline{I}_v \quad (3)$$

where $\overline{v}_{\max}$ is the maximum value of the slowly-varying mean wind velocity of $\overline{v}$ and $\overline{I}_v$ is the value of I_v averaged on a 10-min interval. Some noteworthy wind velocity ratios of thunderstorm records are given by [15]:

$$R = v_{\max}/\hat{v} \quad (4)$$

$$G_{\max} = v_{\max}/\overline{v}_{\max} \quad (5)$$

$$\hat{G} = \hat{v}/\overline{v}_{\max} \quad (6)$$

where $\hat{v}$ is the 1-s peak wind velocity. The wind velocity decomposition of the selected thunderstorm record is shown in Figure 6.

The turbulence characteristics of thunderstorm wind record were evaluated based on the residual fluctuation component, v' (Eq. 1) obtained from the wind velocity decomposition in 10-min (Fig. 6). The mean value of the slowly varying turbulence intensity resulted $\overline{I}_v$ = 0.08. The integral length scale of turbulence, L_u, was determined by fitting the experimental PSD to the model proposed by Solari and Piccardo [16] resulting L_u = 19.25 m. Figure 7 shows the Power Spectral Density Functions (PSD) of the residual fluctuation component, v' (Eq. 1) and the normalized PSD corresponding to the May 7th 2024 thunderstorm record. A good fit is obtained in the inertial sub-range as emphasized by the slope of the curve n-5/3 shown with black continuous line on Figure 7a. Moreover, a good fit match me be observed between the normalized PSD obtained from measurements and the theoretical PSD [16].

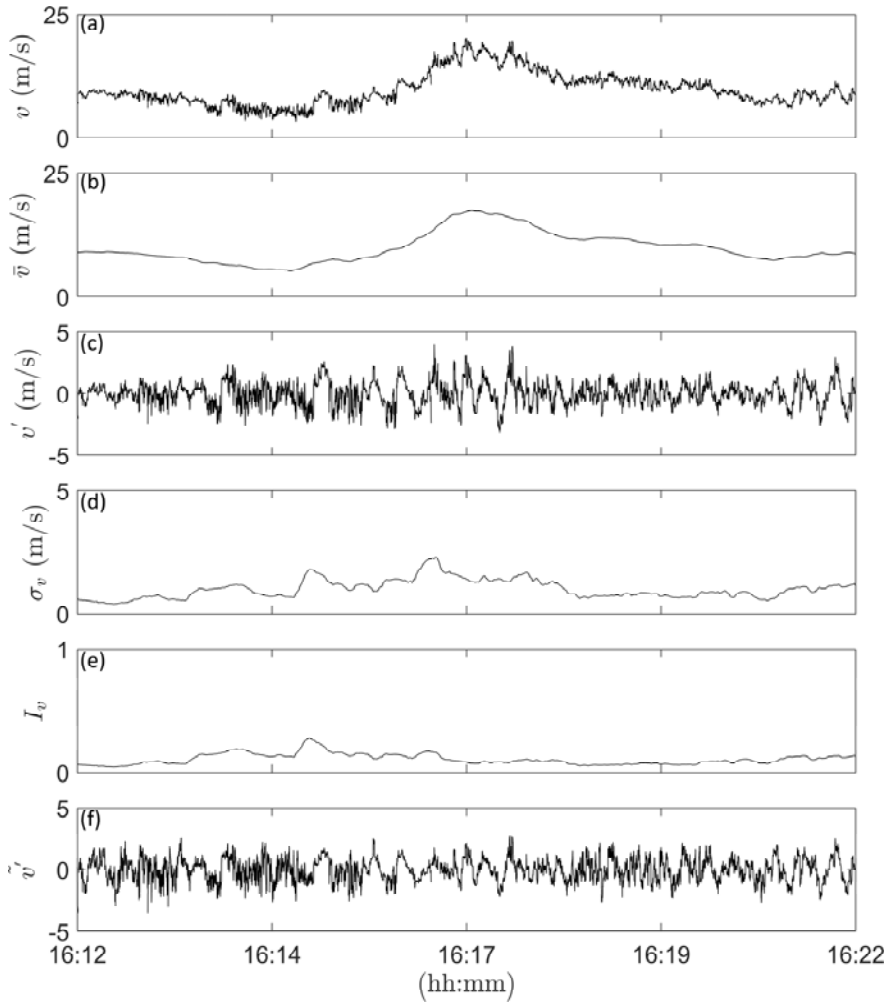

Fig. 6. Wind velocity decomposition in 10-min: (a) v, (b) $\overline{v}$, (c) v', (d) σ_v, (e) I_v and (f) $\tilde{v}'$

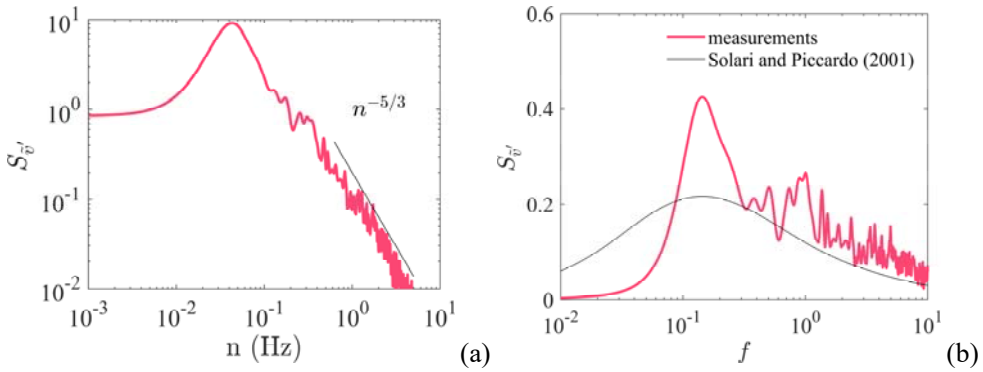

Fig. 7. (a) PSD and (b) matching between the measured and the theoretical normalized PSD

The time period during which thunderstorms develop their maximum intensity may be defined in terms of the non-dimensional γ function (Eq. 2) shown in Figure 8a.

The maximum value of the slowly-varying mean wind velocity, $\overline{v}_{max}$ occurs at t=0 while t_i and t_d indicate the conventional limiting values of t for which the most intense part of the thunderstorm occurs [15]; these values correspond to γ = 0.6 which represents a wind velocity pressure equal to 36% of its maximum value. The total duration of the most intense part of the May 7th 2024 thunderstorm resulted 200 s which is in agreement with literature results [15]. Finally, Figure 8b shows the μ function of the selected thunderstorm record which is a measure of turbulence intensity.

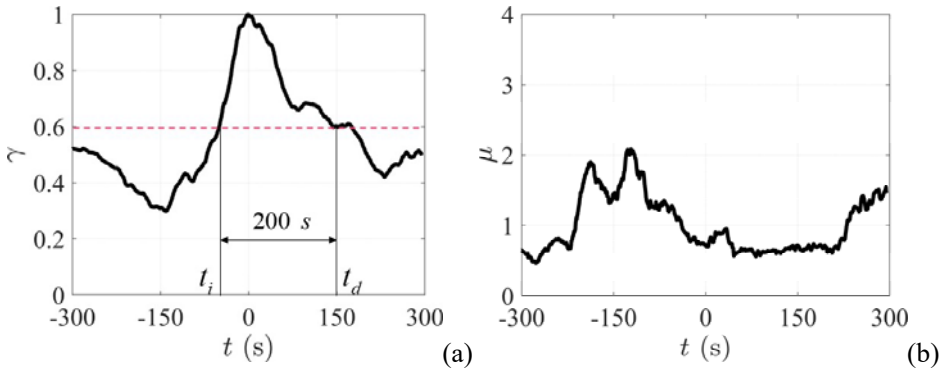

Fig. 8. (a) γ function and (b) μ function for the May 7th 2024 thunderstorm record

Finally, Table 2 shows the values of the noteworthy parameters of the wind velocity record measured on May 7th 2024 compared to similar results provided in literature. As it may be seen, very similar results are obtained between the May 7th 2024 record and thunderstorms measured in Romania [12] while a slight difference may be noticed when results are compared to thunderstorms measured in Italy [15]. This might be caused by the different climate and location of the anemometric stations. The monitoring system described in [12] is located in a flat, open field while the monitoring systems described in [15] are located near costal regions.

Table 2

Comparison between noteworthy parameters of the wind velocity record measured on May 7th 2024 and literature results

Parameter	v_{max} (m/s)	$\hat{v}$ (m/s)	$\overline{v}_{max}$ (m/s)	$\overline{v}_{m10}$ (m/s)	$\overline{I}_v$	L_u (m)	R	G_{max}	$\hat{G}$
Value	20.3	20.15	17.83	9.82	0.08	19.3	1.00	1.14	1.13
Solari et. al, 2015 [15]					0.12	34.6	1.06	1.27	1.20
Calotescu et. al, 2025 [12]					0.08	54.5	1.03	1.15	1.12

5. Conclusions and prospects

This paper presents the statistical characteristics of a thunderstorm record measured near Bucharest, Romania in a suburban terrain category. The record was captured by a wind and structural monitoring system installed on a 50 m

telecommunication lattice tower which has been continuously running since September 2023.

The thunderstorm record was measured on May 7th 2024 and was extracted based on a separation and classification methodology which makes use of gust factor ratios and expert judgement in order separate synoptic from non-synoptic wind records. In this paper, video camera images of the cloud formation during the event together with radar data was used in order to validate the identified thunderstorm record. The resulted thunderstorm characteristics such as gust factor ratios, turbulence intensity, integral length scale of turbulence and thunderstorm duration show good agreement with similar results available in literature, especially for monitoring systems located in similar climatic conditions and terrain category.

The monitoring system presented in this paper is the second developed by the authors in Romania in an effort to collect long term continuous and synchronous wind and structural thunderstorm data. The first system was installed in Sânnicolau Mare, Romania [12] on a 50 m lattice tower identical to the one presented in this paper with the only difference being the number and position of ancillary elements. Prospects of this study include identifying similarities and differences between the two monitoring systems both in terms of thunderstorm wind velocities as well as the thunderstorm-induced response of the two towers.

Acknowledgements

This work was supported by a National Research Grants of the UTCB, project number $GnacC_{2023}^{ARUT}$-UTCB-06, SEVAST (Studii experimentale asupra comportării la vânt a stâlpilor de telecomunicații). The authors acknowledge the kind generosity of TECHNO VOLT company (https://www.technovolt.ro/) who donated the accelerometer used within this project.

References

[1] T. Fujita, „Downbursts: meteorological features and wind field characteristics”, Journal of Wind Engineering and Industrial Aerodynamics, 36, 1990, pp. 75-86.

[2] A.G. Davenport, „The application of statistical concepts to the wind loading of structures”, Proceedings of the Institution of Civil Engineers 19, 1961, pp. 449–472. https://doi.org/10.1680/iicep.1961.11304

[3] T.T. Fujita, „The downburst microburst and microburst. Report of Projects NIMROD and JAWS”, 1985.

[4] F.T. Lombardo, J.A. Main, E. Simiu, „Automated extraction and classification of thunderstorm and non-thunderstorm wind data for extreme-value analysis”. Journal of Wind Engineering and Industrial Aerodynamics 97, 2009, pp. 120–131. https://doi.org/10.1016/j.jweia.2009.03.001

[5] N.J. Cook, „Automated classification of gust events in the contiguous USA”, Journal of Wind Engineering and Industrial Aerodynamics 234, 2023, 105330. https://doi.org/10.1016/j.jweia.2023.105330

[6] I. Calotescu, A.S. Chitez, M.V. Birsan, D. Micu, A. Dumitrescu, „Assessment of thunderstorm-prone areas in Romania based on wind damage occurrence and surface observation data", Journal of Wind Engineering and Industrial Aerodynamics 250, 2024, D https://doi.org/10.1016/j.jweia.2024.105765

[7] G. Solari, M. Burlando, M.P. Repetto, „Detection, simulation, modelling and loading of thunderstorm outflows to design wind-safer and cost-efficient structures", Journal of Wind Engineering and Industrial Aerodynamics 200, 2020, 104142. https://doi.org/10.1016/j.jweia.2020.104142

[8] S. Zhang, Q. Yang, G. Solari, B. Li, G. Huang, „Characteristics of thunderstorm outflows in Beijing urban area", Journal of Wind Engineering and Industrial Aerodynamics 195, 2019, 104011. https://doi.org/10.1016/j.jweia.2019.104011

[9] G. Huang, Y. Jiang, L. Peng, G. Solari, H. Liao, M. Li, „Characteristics of intense winds in mountain area based on field measurement: Focusing on thunderstorm winds", Journal of Wind Engineering and Industrial Aerodynamics 190, 2019, 166–182. https://doi.org/10.1016/j.jweia.2019.04.020

[10] F.T. Lombardo, M.S. Mason, A.Z. de Alba, „Investigation of a downburst loading event on a full-scale low-rise building", Journal of Wind Engineering and Industrial Aerodynamics 182, 2018, pp. 272–285. https://doi.org/10.1016/j.jweia.2018.09.020

[11] M.T. Mengistu, A. Orlando, M.P. Repetto, „Wind and structural response monitoring of a lighting pole for the study of downburst effects on structures", Journal of Wind Engineering and Industrial Aerodynamics 240, 2023, 105447. https://doi.org/10.1016/j.jweia.2023.105447

[12] I. Calotescu, D. Bîtcă, M.P. Repetto, „Full-scale monitoring of a telecommunication lattice tower under synoptic and thunderstorm winds", Journal of Wind Engineering and Industrial Aerodynamics, 258, 2025, 106022. https://doi.org/10.1016/j.jweia.2025.106022

[13] Cod de proiectare. Evaluarea acțiunii vântului asupra construcțiilor, indicativ CR1-1-4/ 2012, Monitorul Oficial al României nr 704bis/15.X.2012.

[14] P. De Gaetano, M.P. Repetto, T. Repetto, G. Solari, „Separation and classification of extreme wind events from anemometric records", Journal of Wind Engineering and Industrial Aerodynamics 126, 2014, pp. 132–143. https://doi.org/10.1016/j.jweia.2014.01.006

[15] G. Solari, M. Burlando, P. De Gaetano, M.P. Repetto, „Characteristics of thunderstorms relevant to the wind loading of structures", Journal of Wind Engineering and Industrial Aerodynamics, 20(6), 2015, pp. 763–791. https://doi.org/10.12989/was.2015.20.6.763

[16] G. Solari, G. Piccardo, „Probabilistic 3-D turbulence modelling for gust buffeting of structures", Probabilistic Engineering Mechanics 16, 2001, pp. 73–86. https://doi.org/10.1016/S0266-8920(00)00010-2

Potable water: a potential national security issue in the near future

Apa potabilă, în viitorului apropiat, o posibilă problemă de securitate națională

Nicolae Iordan, Ioan Boian, Alexandru Bulmez, Ioan Căldare

Transilvania University of Brasov, B-dul Eroilor nr. 29, Cod postal 500036, Brașov, România
e-mail: nicolae.iordan@gmail.com, boian.ioan@gmail.com, bulmez.alexandru@gmail.com, megavoxconfort@yahoo.com

DOI: 10.37789/rjce.2025.16.2.6

Abstract
The paper presents the political, economic, and social trends pertaining to water demand, extraction, and management in the EU countries and beyond, alongside the measures taken by the Romanian government to align with EU policies. Information sourced from international organizations, research, and documents from European and national agencies has been synthesized. In the current context of globalization, as the global population continues to increase, the demand for food and water is anticipated to escalate, precipitating instability, poverty, and the globalization of insecurity. Hence, there is a pressing need to heighten focus on the efficient utilization, conservation, pollution mitigation of water sources, and augmenting their reuse percentage.

Key-words*: potable water, issue, globalization*

Rezumat
Articolul prezintă tendințele politice, economice și sociale legate de cerința, prelevarea și managementul apei în țările UE și nu numai precum și acțiunile întreprinse de statul român pentru alinierea la politicile UE. Au fost sintetizate informații din documente elaborate de organisme internaționale, cercetări și documente ale unor agenții europene și naționale. În contextul actual al procesului de globalizare, pe măsură ce populația globului continuă să crească, va crește și cererea de hrană și apă, care vor genera instabilitate, sărăcie și globalizarea insecurității. De aceea se dorește creșterea atenției acordate utilizării eficiente a apei, a economisirii ei, reducerea poluării surselor de apă și creșterea procentului de reutilizare a ei.

Cuvinte-cheie*: apă potabilă, problemă, globalizare*

1. Introduction

"Water is not merely a commercial commodity but a heritage that must be protected, defended, and treated as such (Directive 2000/60/EC, Article 1)".

The article was received on 15.05.2025, accepted on 21.05.2025 and published on 22.05.2025

Three-quarters of Europeans rely on groundwater for their water supply, and 20% of surface waters are at high risk of pollution. Furthermore, 60% of European cities exploit their groundwater resources unsustainably.

Almost half of the EU population lives in countries experiencing "water stress" - a situation where water demand exceeds available supply during a certain period or when poor water quality restricts its use. Water stress leads to the degradation and depletion of water resources.

Water consumption is distributed among various sectors: 44% for energy generation, 24% for agriculture, 21% for domestic use, and 11% for industry. These consumption patterns vary geographically, with some regions using up to 60-80% of their water for agriculture. Reused water accounts for 2.4% of urban effluents, i.e., 964 million cubic meters with 347 million cubic meters for Spain for Spain and 233 million cubic meters for Italy, both leading in reuse, primarily for agriculture. Romania's water resources are relatively scarce and unevenly distributed in time and space, totaling 134.6 billion cubic meters, as surface and groundwater. According to the degree of hydrographic basin development the usable amount is around 39.5 billion cubic meters. Romania's endogenous resources, i.e., formed from precipitation falling on the country's territory rated to the population number is 1,894 cubic meters per year and per capita. As a result, Romania is one of the countries with the lowest water resources in Europe, as shown in Figure 1.

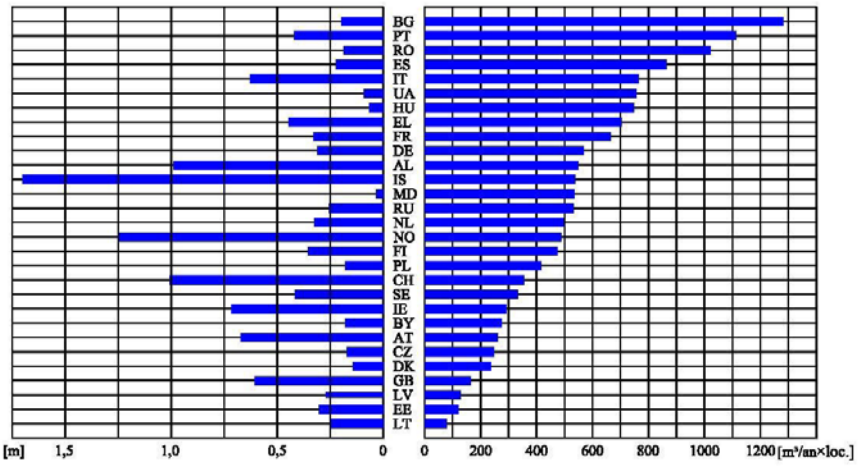

Fig.1. Specific water resources (left) and specific water consumption (right) in European states (according to the European Environment Agency)

2. Romania's Water Resources and Requirements

Considering exogenous water resources, such as the Danube and rivers from the upper Siret basin, equivalent to 170 cubic kilometers per year, Romania's total water resources amount to 212 cubic kilometers per year. The country heavily relies on upstream water resources from other countries, which are not entirely usable. Unlike

Western and Northern Europe, insufficient water resources could hinder Romania's economic development unless a strict water management policy is implemented.

Due to variable water regimes, excess water during floods and low flow during droughts necessitate measures like the construction of reservoirs to retain excess water for dry periods. The National Administration "Romanian Waters" plans new hydrological basin projects, including reservoirs, to increase usable water resources and storage capacities during floods.

The quality and quantity of water in urban areas are critical for potable water supply, yet urban pollution contributes significantly to water quality degradation, according to specialists from the World Water Organization. Daily, two million tons of wastewater enter watercourses globally without adequate treatment. Urban population growth and inefficient water use in cities exacerbate these issues, leading to significant water wastage. Efficient management could provide potable water to millions more people.

Global statistics also indicate that "every second, the urban population grows by two people, meaning that every month, five million people move to cities, while 27% of the urban population worldwide does not have access to water supply systems.

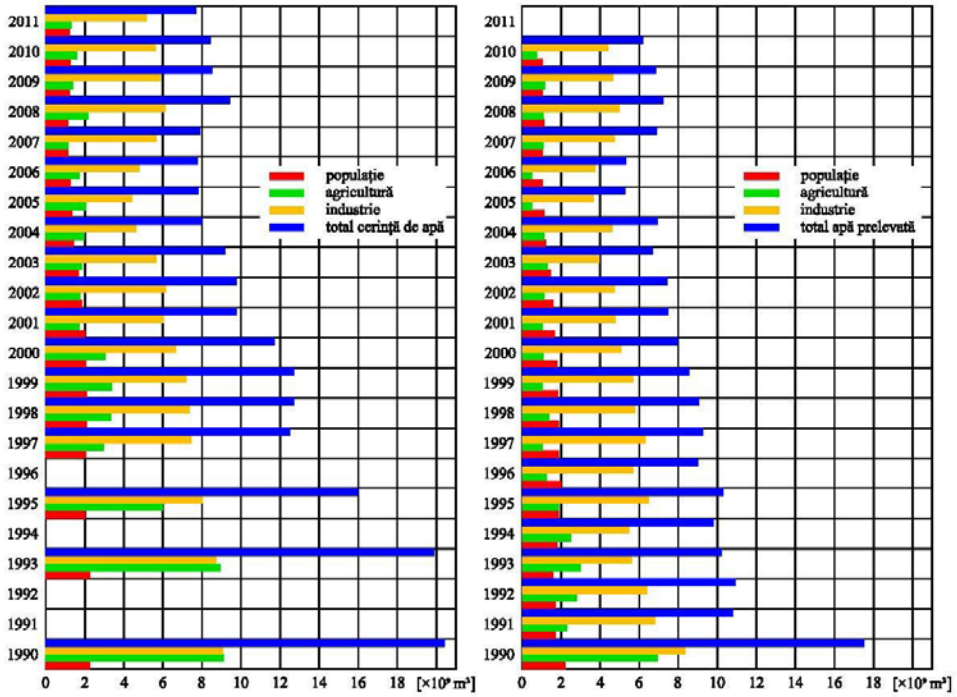

Fig.2. Evolution of water demand (left) and water withdrawals (right) in the period 1990-2010 (according to data provided by ANAR).

Every year, between 250–500 cubic meters of potable water are wasted in large cities globally. If this quantity of water were no longer wasted, an additional 10–20 million people could have potable water in the world's large 2008–2009) and short

periods of slight growth (2004–2005, 2007–2008). Domestic water demand has steadily decreased, indicating reduced distribution losses and improved efficiency.

Reality demonstrates that globalization is the most significant and powerful force in shaping a new matrix of international security, being associated with the increase of insecurity, mainly due to one of its characteristics, namely the increase of interdependencies.

The issue of resources and competition for resources represents another important aspect of the globalization of insecurity. The interdependencies between resources, on one hand, and development, prosperity, and power, on the other hand, have decisively shaped the political evolution of the world. The most powerful motivation for war is the acquisition, access, or control of critical resources. As the planet's population continues to increase, so will the consumption of vital resources, leading to poverty, inequality, and both intra- and interstate violence. The scarcity of resources such as water and food can lead to dysfunctionality at the level of the entire international community.

According to the Human Development Report "Beyond Water Crisis: Power, Poverty, and Global Water Shortage," in many developing countries, unsafe water represents a greater threat to human security than violent conflicts.

The authors of the report argue that annually 1.8 million children die from diarrhea, a disease that could be prevented by consuming a glass of water and ensuring sanitary conditions; due to water-related diseases, approximately 443 million school days are lost; and nearly 50% of the population in developing countries suffer from illnesses caused by the lack of water and sanitation at the same time. Moreover, the water and sanitation crisis hinder economic development, with sub-Saharan African countries losing 5% of GDP annually, more than the aid they receive.

According to researchers from the World Resources Institute, water will be considered the primary asset of the 21st century, much like oil was considered in the last century. The causes of conflicts and insecurity are multiple, complex, and well-integrated.

It is increasingly evident that environmental degradation and resource depletion play a significant role in the generation and exacerbation of human insecurity.

cities. "Compared to 1990, there have been two dramatic decreases in water demand. The first occurred between 1990 and 1999, when water demand for the three main categories decreased from 20.4 billion cubic meters in 1990 to 11.74 billion cubic meters in 2000. The second decrease occurred between 2001 and 2010, with water demand reaching 8.45 billion cubic meters in 2010, compared to the year 2000. Figure 2 presents the decrease in water demand and withdrawals. The water requirement for industry has halved, from 9.06 billion cubic meters, as it was in 1990, to 4.4 billion cubic meters, in 2005. Agricultural water demand has been volatile, reflecting hydrological conditions and irrigation capacity, experiencing years of sharp decline (1990–1997, 2000–2001.

3. Environmental Security and Water Sources Security are Integral Components of National Security

Annual economic growth, once quantified in billions of dollars, is now measured in trillions of dollars. However, as the economy grows exponentially, the Earth's natural capacities have not kept pace. In other words, humanity's global demands have surpassed the Earth's regenerative power. Today, global demands on natural systems exceed their sustainable capacity by over 25%.

From a more nuanced perspective, some specialists argue that the link between the environment (biodiversity loss, soil erosion, climate change) and security is so complex that it requires a new way of thinking. The consequences of global environmental crises will be so significant that protecting the global environment will need to become a matter of national security.

According to some, the Earth has environmental capacity limits, which is why they anticipate an increase in environmental crises leading to refugee crises and authoritarian regimes. As many states will face these challenges, non-state paramilitary structures and conflicts over energy and water resources will proliferate.

Global water scarcity is the result of tripling demand over the past half-century. Beyond traditional causes of water supply insecurity, climate change also affects water resources. Higher temperatures increase evaporation rates, alter precipitation patterns, and melt glaciers that feed rivers, as the Earth's climate system and the hydrological cycle are very closely linked.

Among the most visible manifestations of diminishing water resources are the drying up of rivers and the disappearance of lakes. The connection between water and food is strong; 70% of the total volume of water used is for irrigation, 22% in industry, and 8% for domestic purposes. Due to the increasing water demand in all three categories, competition between sectors is becoming more intense, with agriculture almost always losing out.

According to United Nations data, the total volume of water on Earth is 1.4 billion km³, of which 97.5% is salt water, and the remaining 2.5%, or 35 million km³, is fresh water.

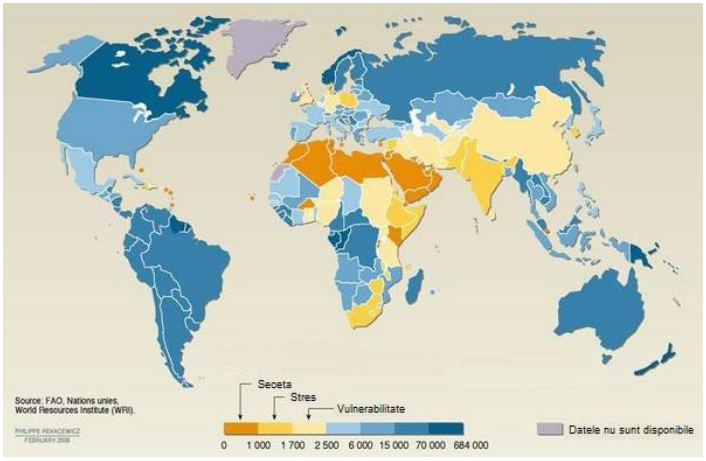

Fig.3. Availability of potable water (cubic meters per person per year, 2007).

In Europe, 44% of water resources are allocated to energy production, 24% to agriculture, 21% to population supply, and 11% to industry.

On the European continent, lakes and rivers supply 81% of the total freshwater, serving as the primary source of water for industry, energy, and agriculture. Conversely, the water supply for the population is primarily dependent on groundwater.

Romania's most significant water resources are surface waters-rivers, lakes, the Danube River, and groundwater. A special category of resources includes mineral waters (carbonated, sulfurous, ferruginous, etc.) and geothermal waters. These resources are relatively scarce and unevenly distributed in time and space, theoretically totaling 134.6 billion cubic meters, of which the usable resource, according to the degree of development of the hydrographic basins, is about 40 billion cubic meters.

The World Bank study, titled "Romania – Functional Review of the Environment, Water and Forestry Sector," revealed that half of the population is not connected to potable water supply and sewerage networks (compared to over 70%, the EU average), resulting in high levels of pollution that exceed the European average, including nitrate contamination of groundwater and land.

Romania's accession to the EU was a challenging exercise in complying with European environmental protection standards, reflected in the numerous transition periods in key areas such as water quality, water supply and sewerage networks, and the development of wastewater treatment plants.

The risk factors for potable water supply systems (conveyance, treatment, purification, sewerage) are:

- The conduct of economic activities in the sanitary protection zones of potable water resources (raw water intakes from surface sources, as well as groundwater sources) or the conveyances to consumers;
- The lack of necessary human resources to ensure the guarding of facilities (stations, pipelines, aqueducts, reservoirs);
- The lack of demarcation of sanitary protection zones and hydrological protection perimeters at some groundwater sources;
- The lack of specialized equipment and competent personnel at the public health directorates for verifying potable water quality, in accordance with community provisions necessary to ensure continuous testing of water from groundwater sources or reservoirs.

4. Conclusions

The interconnected challenges posed by water and food shortages, energy needs, population growth, climate change, biodiversity loss, and economic interdependence represent a potential "tsunami" for the entire world. These challenges are "unusual" in that they have a scale and level of complexity unprecedented in human history.

Understanding their importance and taking appropriate actions are among our common dilemmas regarding security.

Concerning the impact of environmental issues, which can exponentially and directly affect social, physical, and economic security, we can highlight extreme weather events and "shocks" related to water and energy supply, as well as the acceleration of risks and threats such as: precipitation caused by soil erosion and structural instability, degradation of water quality or destruction of water supply sources, the spread of new diseases, degradation of energy supply capacity, pest invasions, destruction of agriculture and fishing, new "causes" of armed conflict, and the amplification of abuses and crimes.

The water crisis is becoming an increasingly acute and noticeable process over time, which, according to researchers, currently represents the second largest global problem of the 21st century, the first being, indisputably, the planet's population growth. The current problem is not one of resources but rather of the efficient distribution and management of water at a global level.

Bibliography

[1] Agiu, Ana-Maria, Informare de presă, Biroul de presă, Administraţia Naţională Apele Române, 2011, pp. 3-4.

[2] Dalby, Simon, Environmental Security, University of Minnesota Press, Mineapolis London, 2002, pp. 209-211.

[3] Leaua, Ana Ligia, Provocări de mediu la adresa securităţii naţionale – calitatea şi gestionarea resurselor de apă, Annals of the University of Bucharest, Political science series 14 (2012), 1, pp. 99-116.

[4] Watkins, Kevin, Human Development Report, Published for the United Nations Development Programme, New York, 2006, pp. 159-169.

[5] http://www.eea.europa.eu/

[6] http://www.worldbank.org

Ensuring sustainability of thermal energy conservation in traditional houses in the Republic of Moldova

Asigurarea sustenabilității conservării energiei termice la casele tradiționale din Republica Moldova

Ion Albu, Doina-Cezara Albu

Technical University of Moldova, Faculty of Construction, Geodesy and Cadastre, av. Dacia, 41, Chisinau, Republic of Moldova
e-mail: *ion.albu@fcgc.utm.md, doinacezara.albu@emi.utm.md*

DOI: 10.37789/rjce.2025.16.2.7

Abstract
The conservation of thermal energy in traditional winter homes in rural areas of the Republic of Moldova represents a current challenge due to the sustained increase in the prices of thermal energy resources. The construction industry is witnessing a shift towards greater energy efficiency, with minimal or even near-zero consumption. The main aim of this study is to conduct a comprehensive examination of current technologies and methodologies designed to enhance the energy efficiency of traditional residential structures while adhering to sustainability principles. The authors aim to carry out the analysis of thermal insulation materials for walls and to recommend practical solutions to help promote traditional energy-efficient housing.

Rezumat
Asigurarea conservării energiei termice în casele tradiționale de locuit pe timp de iarnă în localitățile rurale din Republica Moldova constituie o problemă actuală pe motiv ce prețurile la resursele de creare a energiei termice sunt în permanentă creștere. Progresele din industria construcțiilor indică o schimbare spre eficiență energetică cu consum minim sau chiar aproape de zero. Autorii își propun să efectueze o analiză amănunțită a tehnologiilor și metodelor actuale care vizează sporirea eficienței energetice a caselor tradiționale de locuit, respectând principiile de sustenabilitate. Studiul își propune analiza materialelor de izolare termică a pereților și recomandarea de soluții practice, care să contribuie la promovarea locuințelor tradiționale eficiente din punct de vedere energetic.

Keywords: *thermal energy, traditional house, sustainability*

Cuvinte cheie: *energie termală, casă tradițională, sustenabilitate*

1. Introduction

In the context of mounting concerns about the environment and energy efficiency, the conservation and optimisation of heat consumption in traditional houses

The article was received on 23.02.2025, accepted on 21.05.2025 and published on 22.05.2025

is a topic of significant interest. [1, 2, 3, 4]. It is evident that traditional houses, in particular those constructed from adobe bricks, have significant cultural and historical value. However, it is also apparent that these structures frequently encounter difficulties with thermal insulation and excessive energy consumption. It is of paramount importance to enhance the energy efficiency of these dwellings if they are to remain viable in the long term. The utilisation of appropriate materials and technologies enables the optimisation of the thermal insulation of traditional houses, thereby reducing energy consumption and enhancing the comfort of residents.

The concept of sustainability is of paramount importance, particularly in light of the pressing issues of climate change and our dependence on finite energy sources. The term 'sustainability' is defined as the capacity to maintain an action or system over an extended period of time. In the field of construction, energy efficiency is of paramount importance. The traditional adobe house is a pertinent topic in this context.

The Republic of Moldova Ministry of Energy, the Consolidated Unit for the Implementation and Monitoring of Energy Projects (UCIPE), and the United Nations Development Programme (UNDP) are currently conducting an investigation into the potential of new approaches to thermal energy conservation in modern [5] and traditional residential buildings. This initiative, which has the support of international partnerships and recent legislative changes, has the potential to make a significant contribution to local energy efficiency and sustainable community development in the Republic of Moldova.

The Republic of Moldova has a long tradition of building houses from natural materials, but faces significant challenges in terms of sustainability and energy efficiency of traditional housing [6]. Traditional houses, constructed from adobe bricks, stone or wood, have a relatively low environmental impact. However, they are prone to significant heat loss, which results in high heating and cooling costs.

The study addresses the question of ensuring sustainability of thermal energy conservation in traditional houses in the Republic of Moldova. The study analyses the main characteristics of traditional houses in terms of energy performance, identifying potential solutions for sustainable thermal insulation of the envelope of traditional houses.

The objective of this study is to provide a comprehensive analysis of existing technologies and methodologies to improve the energy performance of traditional houses while respecting the principles of sustainability. Furthermore, the study will present effective solutions that will contribute to the promotion of more energy-efficient traditional housing, thus contributing to a more sustainable future for the Republic of Moldova.

2. Brief history

The construction of adobe houses in the Republic of Moldova has a long history, spanning centuries. The construction technique has been influenced by historical, geographical, and cultural factors, becoming an integral part of the architectural identity of the area.

Archaeological evidence indicates that the use of clay in combination with straw or straw in construction has been identified since the Bronze Age (3rd millennium BC). This evidence demonstrates a long tradition of the use of this material in construction.

The construction of adobe houses became more widespread in the 13th-16th centuries, coinciding with the emergence of urban centres and more developed rural communities.

In the 19th and 20th centuries, the construction of adobe houses continued to be a widespread practice, influenced by the architectural trends of the time. The construction of traditional adobe houses was adapted to the specific characteristics of each region, reflecting the distinct geographical and cultural characteristics of the area in question.

In terms of architectural design, traditional adobe houses were divided into three categories. The first was a one-room house, which was usually found in more remote villages or as a secondary summer accommodation. The second was the two-chambered house, which consisted of a truss and a pantry, with a four-sided hipped roof. The third was the three-chamber house, which was characterised by the addition of a new living room to the central space, with the aim of creating a clean room with valuables (Figure 1) [7]. They were perfectly adapted to the climatic conditions of the Republic of Moldova, providing protection against the cold and excessive heat.

The external appearance of the houses was created by plastering the walls with lime, which gave the impression that they were built of stone [8].

Patio, a platform in front of the house, was a common architectural element. The purpose of the patio was twofold: first, to protect the foundation from rain and second, to serve as a resting place.

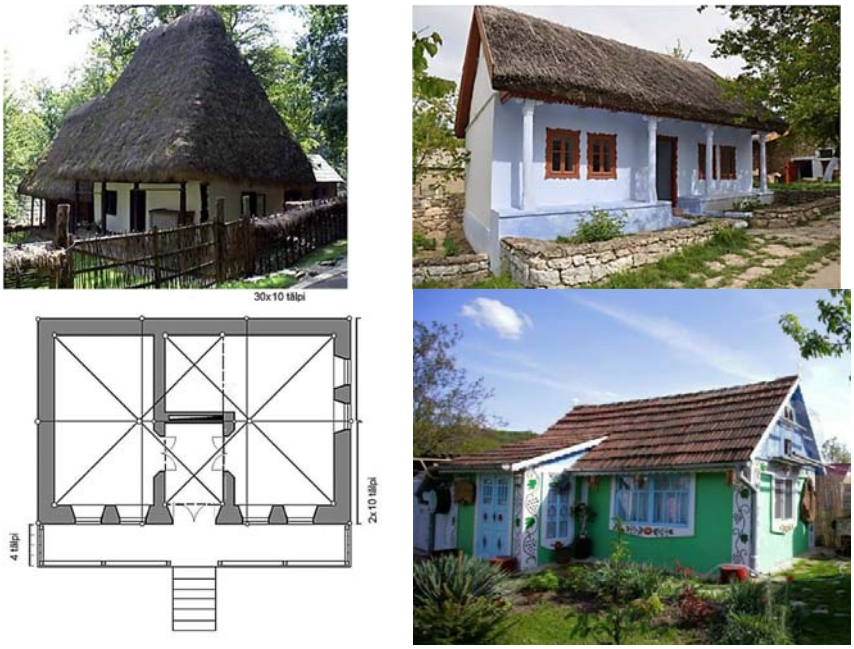

Figure 1. Traditional houses in the Republic of Moldova

The construction of the adobe houses was achieved using a straightforward and cost-effective methodology. Wall construction was carried out manually, with adobe bricks laid in layers and glued together with clay mortar (Figure 2). The clay, which was mixed with straw, was readily available and could be easily handled. The incorporation of straw into the composition imparted strength and elasticity to the material. Once the walls were erected, they were improved by applying a layer of clay plaster with horse chaff or baleen and glazing. This not only added a smooth and visually appealing finish, but also served as a protective barrier against moisture, ultimately contributing to the strength and longevity of the walls [9].

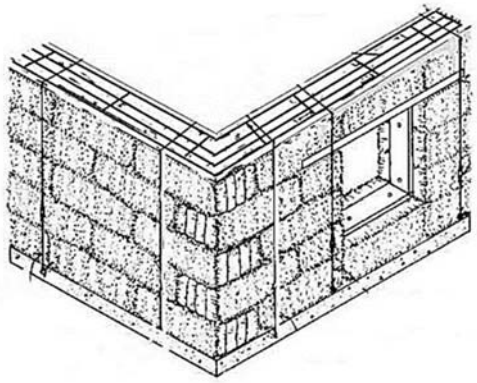

Figure 2. The structure of adobe walls [9]

The traditional adobe houses of the Republic of Moldova are imbued with a profound cultural significance, symbolising a rich heritage and a profound connection with nature. Such structures exemplify an ingenious adaptation to local resources, a respect for local traditions, and a sense of community.

3. Material and technology

In the present era, traditional adobe houses are confronted with a multitude of challenges, including those pertaining to energy efficiency and the adaptation of these structures to the prevailing standards of modern construction. Modernisation of these houses necessitates the implementation of intelligent solutions with the objective of improving thermal insulation and reducing energy losses, whilst simultaneously preserving the authentic characteristics of traditional construction.

In order to maintain the architectural integrity of the facade, an investigation was conducted to ascertain the suitability of natural materials for insulating the interior walls (Figure 3).

Figure 3. Types of sustainable insulation materials

In order to identify suitable insulation materials for traditional houses in the Republic of Moldova, a comparative analysis (Table 1) of the six materials shown in Figure 3 was carried out.

Table 1

Analysis of sustainable insulation materials

No.	Insulating material	Criteria							
		Breathability	Biodegradable	Fire resistance	Toxicity	Sound insulation	Cost	Country of production	Others
1	Sheep wool board	The material allows water vapour to pass through it, thereby preventing condensation and mould formation in the walls.	The material in question decomposes naturally, thereby reducing the environmental impact.	Sheep wool is fire resistant, contributing to a safe home.	The product does not emit any harmful chemicals into the atmosphere.	The material serves to absorb sound, thereby reducing noise from external sources.	12.50-13.00 euro/sq m	Romania	Sheep wool is a suitable choice for people with allergies as it is natural and hypoallergenic.
2	Cellulose board			Treated with mineral salts, cellulose is non-combustible, contributing to the safety of the home.			10.60 euro/sq m 38 euro/sq m	Finland Moldova	

No.	Insulating material	Criteria							
		Breathability	Biodegradable	Fire resistance	Toxicity	Sound insulation	Cost	Country of production	Others
3	Wood fibre board			Wood fibres are treated with fire retardant to reduce the risk of fire.			12.50-44.50 euro/sq m	Germany	Wood fibres are a suitable choice for people with allergies as they are natural and hypoallergenic.
4	Hemp board			Hemp boards are flame retardant treated to reduce the risk of fire.			14 euro/sq m	Netherlands - Romania	Hemp absorbs CO_2 from the atmosphere, helping to combat climate change.
5	Cork board			Cork is fire resistant, contributing to the safety of the home.			29.00-42.80 euro/sq m	Portugal	Cork is a suitable choice for people with allergies as it is natural and hypoallergenic.
									Cork is a durable material that can last for decades.
6	Microfibre straw board			Microfibre straw is flame retardant treated to reduce the risk of fire.			10.65 euro/sq m	Poland	Straw microfibres are a suitable choice for people with allergies as they are natural and hypoallergenic.
									Straw absorbs CO_2 from the atmosphere, helping to combat climate change.

The utilisation of sustainable insulation materials in the construction of adobe-walled houses confers a plethora of advantages, both in terms of environmental impact and the well-being of those who reside therein. These natural materials are environmentally friendly, biodegradable, non-toxic, and have the capacity to regulate humidity and temperature within the home. Furthermore, the use of these materials can

help reduce the energy expenditure required for the heating and cooling of buildings, thus reducing the environmental impact. The utilisation of these sustainable insulation materials facilitates the construction of a healthier and more balanced environment, with long-term sustainable benefits.

Figure 4 shows the fundamental technology utilised to implement interior thermal insulation utilising environmentally friendly materials. The process begins with the attachment of OSB plywood to the adobe wall, followed by the attachment of the wooden casing. Subsequently, the insulation material is installed in conjunction with a vapour barrier and plasterboard. The final step in the process is the application of decorative plaster to complete the wall.

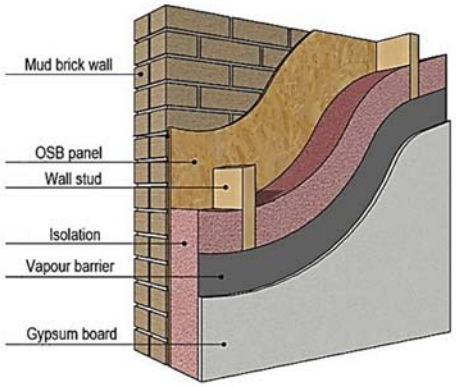

Figure 4. Technology of thermal insulation of adobe walls

The advantages of such insulation include the reduction of energy consumption, an improvement in the thermal efficiency of the home, and a reduction in the carbon footprint.

4. Improving wall energy efficiency

There is a growing focus on energy efficiency in buildings, with a shift towards near zero energy buildings (NZEB) and a strong emphasis on promoting environmental sustainability and resource efficiency. This trend reflects a wider move towards more sustainable and greener practices in the construction industry. In order to bring traditional houses up to the new requirements by incorporating modern technologies and sustainable materials, calculations on thermal resistance and thermal transmittance were proposed and are presented in Table 2.

Given that the typical thickness of adobe walls is 40 cm, and that the thermal conductivity of clay blocks with straw is 0.40 W/mK, the thermal resistance [10] was calculated to be 1.00 m^2K/W, while the thermal transmittance was found to be 1.00 W/m^2K. In accordance with European standards, houses should aspire to achieve NZEB [11], where the thermal resistance should be a minimum of 4 m^2K/W and the thermal transmittance a maximum of 0.25 W/m^2K.[12].

Table 2

Energy efficiency of sustainable solutions for thermal insulation of adobe walls

No	Type of thermal insulation	Input data Thermal conductivity (λ), W/mK	Thickness, cm	Thermal resistance (R), m^2K/W	Thermal transmittance (U), W/m^2K
1	*Thermal insulation with wool boards*			**4.687**	**0.213**
	with αe + αi			0.175	
	Adobe wall	0.400	40.00	1.000	1.000
	OSB board	0.130	1.50	0.115	8.667
	Wool board	0.038	10.00	2.632	0.380
	Vapour barrier	0.400	0.02	0.001	1818.182
	Gypsum board	0.250	1.25	0.050	20.000
	Aerogel plaster	0.028	2.00	0.714	1.400
2	*Thermal insulation with cellulose boards*			**4.619**	**0.216**
	with αe + αi			0.175	
	Adobe wall	0.400	40.00	1.000	1.000
	OSB board	0.130	1.50	0.115	8.667
	Cellulose board	0.039	10.00	2.564	0.390
	Vapour barrier	0.400	0.02	0.001	1818.182
	Gypsum board	0.250	1.25	0.050	20.000
	Aerogel plaster	0.028	2.00	0.714	1.400
3	*Thermal insulation with wood fibre boards*			**4.121**	**0.243**
	with αe + αi			0.175	
	Adobe wall	0.400	40.00	1.000	1.000
	OSB board	0.130	1.50	0.115	8.667
	Wood fibre board	0.040	8.00	2.000	0.500
	Vapour barrier	0.400	0.02	0.001	1818.182
	OSB board	0.130	1.50	0.115	8.667
	Aerogel plaster	0.028	2.00	0.714	1.400
4	*Thermal insulation with hemp boards*			**4.107**	**0.244**
	with αe + αi			0.175	
	Adobe wall	0.400	40.00	1.000	1.000
	OSB board	0.130	1.50	0.115	8.667
	Hemp board	0.039	8.00	2.051	0.488
	Vapour barrier	0.400	0.02	0.001	1818.182
	Gypsum board	0.250	1.25	0.050	20.000
	Aerogel plaster	0.028	2.00	0.714	1.400
5	*Thermal insulation with cork boards*			**4.643**	**0.215**
	with αe + αi			0.175	
	Adobe wall	0.400	40.00	1.000	1.000
	Cork board	0.037	10.00	2.703	0.370
	Vapour barrier	0.400	0.02	0.001	1818.182
	Gypsum board	0.250	1.25	0.050	20.000
	Aerogel plaster	0.028	2.00	0.714	1.400
6	*Thermal insulation with microfibre straw boards*			**4.217**	**0.237**
	with αe + αi			0.175	
	Adobe wall	0.400	40.00	1.000	1.000
	OSB board	0.130	1.50	0.115	8.667
	Microfibre straw board	0.037	8.00	2.162	0.463
	Vapour barrier	0.400	0.02	0.001	1818.182
	Gypsum board	0.250	1.25	0.050	20.000
	Aerogel plaster	0.028	2.00	0.714	1.400

A summary of the findings is presented in Figure 5, which illustrates that the use of thermal insulation materials, including sheep wool boards, cellulose boards, and cork boards, results in enhanced energy performance of traditional houses in the Republic of Moldova.

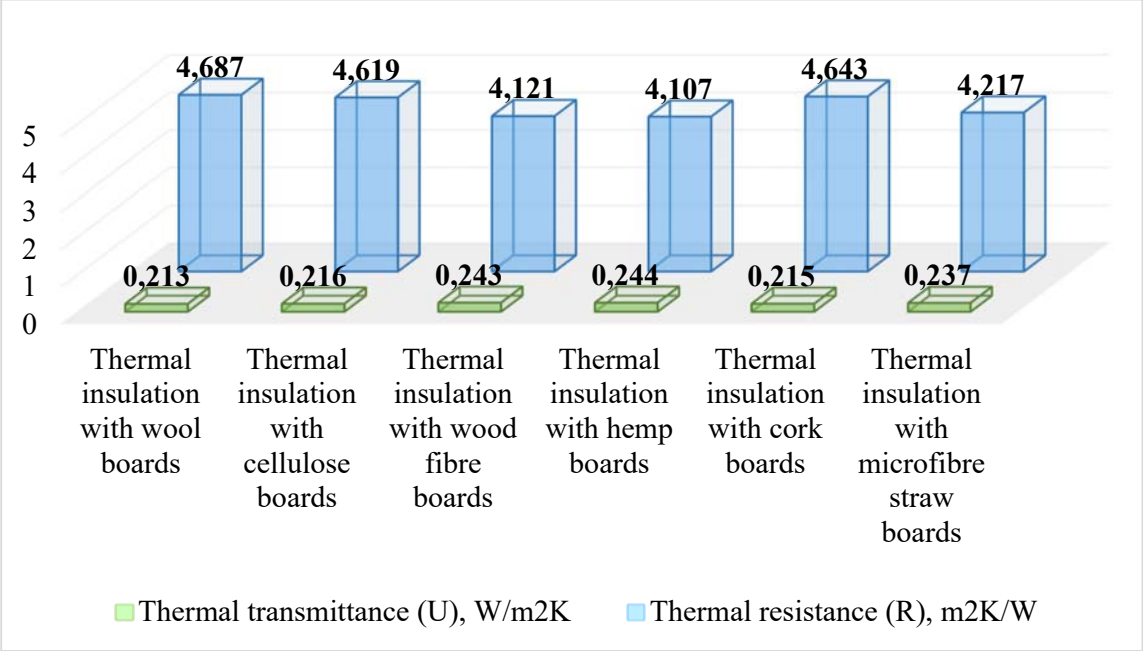

Figure 5. Presentation of data on the energy efficiency of thermal insulation for adobe walls

To gain a more comprehensive understanding, calculations were carried out on the energy efficiency of adobe walls with thermal insulation using the most common materials, including mineral wool, expanded polystyrene and polyurethane foam.

Table 3

Energy efficiency of solutions for thermal insulation of adobe walls

No.	Type of thermal insulation	Input data		Thermal resistance (R), m^2K/W	Thermal transmittance (U), W/m^2K
		Thermal conductivity (λ), W/mK	Thickness, cm		
1	*Thermal insulation with expanded polystyrene*			**4.367**	**0.229**
	with αe + αi			0.175	
	Adobe wall	0.400	40.00	1.000	1.000
	Adhesive	0.080	2.00	0.250	4.000
	Expanded polystyrene EPS100	0.034	10.00	2.941	0.340
	Aerogel plaster	0.400	0.02	0.001	1818.182
2	*Thermal insulation with mineral wool*			**4.199**	**0.238**
	with αe + αi			0.175	
	Adobe wall	0.400	40.00	1.000	1.000
	OSB board	0.130	1.50	0.115	8.667

No.	Type of thermal insulation	Input data: Thermal conductivity (λ), W/mK	Thickness, cm	Thermal resistance (R), m^2K/W	Thermal transmittance (U), W/m^2K
	Mineral wool	0.035	10.00	2.857	0.350
	Vapour barrier	0.400	0.02	0.001	1818.182
	Gypsum board	0.250	1.25	0.050	20.000
	Aerogel plaster	0.400	0.02	0.001	1818.182
3	*Thermal insulation with polyurethane foam*			**4.198**	**0.238**
	with αe + αi			0.175	
	Adobe wall	0.400	40.00	1.000	1.000
	OSB board	0.130	1.50	0.115	8.667
	Polyurethane foam (closed-cell)	0.021	6.00	2.857	0.350
	Gypsum board	0.250	1.25	0.050	20.000
	Aerogel plaster	0.400	0.02	0.001	1818.182

The insulation of adobe walls with expanded polystyrene or mineral wool will require a thickness of 10 cm to achieve the necessary energy efficiency requirements, whereas the use of closed-cell polyurethane foam will necessitate a thickness of 6 cm.

5. Conclusion

The research presents potential technologies for thermal insulation of adobe walls of traditional houses in the Republic of Moldova, with a focus on energy performance analysis.

A critical analysis of the six types of sustainable solutions for thermal insulation of adobe walls reveals the following conclusions:

- The proposed solutions permit the passage of water vapour, thereby preventing condensation and mould formation in the walls. Furthermore, they are composed of biodegradable materials that do not emit toxic substances into the environment and provide effective sound insulation;
- The proposed solutions are fire-resistant, having undergone a flame retardant treatment;
- Sheep wool board, wood fibre board, cork board and microfibre straw board solutions are suitable for allergy sufferers as they are manufactured from hypoallergenic materials;
- The analysis of the energy efficiency of sheep wool, cellulose and cork solutions indicates a thermal resistance of greater than 4.6 W/m^2K and a thermal transmittance of less than 0.22 m^2K/W. In comparison to the most commonly utilised materials, the proposed solutions demonstrate superior energy performance with a thickness of 10 cm;
- From a financial perspective, the thermal insulation solution comprising cellulose boards imported from Finland is likely to be more cost-effective than the other proposed solutions.

In conclusion, it is of paramount importance to prioritize the sustainability of thermal energy conservation in traditional houses in the Republic of Moldova. This will facilitate a reduction in energy consumption, the conservation of natural resources, and

the protection of the environment. The study demonstrated that there is a wide range of practical and effective solutions to improve thermal energy conservation in traditional houses without affecting their authenticity. The implementation of the sustainable solutions presented will result in traditional homes becoming more energy efficient, thereby reducing heating costs, carbon emissions and negative environmental impacts. Furthermore, it will ensure the comfort of residents and contribute to the preservation of cultural heritage.

BIBLIOGRAPHY

[1] S. E. Șerban, T. Catalina, R. Popescu, and L. Popescu, "The Intersection of Architectural Conservation and Energy Efficiency: A Case Study of Romanian Heritage Buildings," *Applied Sciences*, vol. 14, no. 11, p. 4835, Jun. 2024, doi: 10.3390/app14114835.

[2] İ. Yüksek and T. Esin, "Analysis of traditional rural houses in Turkey in terms of energy efficiency," *International Journal of Sustainable Energy*, vol. 32, no. 6, pp. 643–658, Dec. 2013, doi: 10.1080/14786451.2013.769992.

[3] M. Philokyprou and A. Michael, "Environmental Sustainability in the Conservation of Vernacular Architecture. The Case of Rural and Urban Traditional Settlements in Cyprus," *International Journal of Architectural Heritage*, vol. 15, no. 11, pp. 1741–1763, Nov. 2021, doi: 10.1080/15583058.2020.1719235.

[4] Pallaska Elvida, Haugen Tore, Hoxha Visar, Finochiaro Luca, and Temeljotov Salaj Alenka, "Sustainability by improving energy efficiency in traditional housing in Kosovo," in *Proceedings of the CIB World Building Congress*, Kähkönen Kalle and Keinänen Marko, Eds., Tampere: Tampere University of Technology, 2016, pp. 506–517.

[5] Albu Svetlana and Panevski Sashe, "Guidelines for the implementation of energy efficiency measures and the use of renewable energy sources in the residential sector," May 2024.

[6] Șevicuc Lina, "Eficiența energetică a clădirii (Energy efficiency of the building)," in *Conferința Tehnico-Ştiinţifică a Colaboratorilor, Doctoranzilor şi Studenţilor: consacrată celei de-a 50-a Aniversări a U.T.M.*, Chisinau: Tehnica-UTM, Oct. 2014, pp. 290–293. [Online]. Available: http://repository.utm.md/bitstream/handle/5014/2563/Conf_UTM_2014_II_pg290_293.pdf?sequence=1

[7] MOISEENKO Z., *Архитектура сельских жилых домов молдавии (Architecture of rural dwellings in moldavia)*. Chisinau: CARTEA MOLDOVENASCA, 1973.

[8] M.-L. Marian, "THE TRADITIONAL MOLDOVAN DWELLING FROM THE SEC. XVIII-XX FROM THE PERSPECTIVE OF THE CONSTRUCTION MATERIALS AND SOLUTIONS USED," *Journal of Social Sciences*, vol. 4, no. 3, pp. 71–78, Sep. 2021, doi: 10.52326/jss.utm.2021.4(3).08.

[9] Albu Doina-Cezara and Serbanoiu Ion, *Utilizarea materialelor locale pentru construcţii de locuinţe (Use of local materials for housing construction)*. Iasi: Editura Societăţii Academice "Matei - Teiu Botez," 2024.

[10] E. și M. în C. Centrul de Inginerie, "NCM M.01.02:2016 Performanța energetică a clădirilor Metodologia de calcul al performanței energetice a clădirilor," Chișinău, 2016.

[11] L. P. ȘI A. MINISTERUL DEZVOLTĂRII, *METODOLOGIE DE CALCUL AL PERFORMANȚEI ENERGETICE A CLĂDIRILOR*. România, 2022, p. 602.

[12] D.-C. Albu and I. Serbanoiu, "Ensuring Sustainability of Residential Buildings by using Local Materials in the Conditions of the Republic of Moldova," *WSEAS TRANSACTIONS ON ENVIRONMENT AND DEVELOPMENT*, vol. 20, pp. 59–65, Jan. 2024, doi: 10.37394/232015.2024.20.7.

How do we see climate changes regarding refrigerants

Cum vedem schimbările climatice cu privire la agentii frigorifici

Gratiela Tarlea[1], Virgil Tomosoiu[1], Mioara Vinceriuc[2], Livia Antofi[1]

[1]Technical University of Civil Engineering Bucharest, 66 Blv. Pache Protopopescu, Bucharest,Romania
E-mail: *gratiela.tarlea@gmail.com*

[2]The Romanian General Association of Refrigeration, 66 Blv. Pache Protopopescu, Bucharest, Romania
E-mail: *vinceriuc@gmail.com*

DOI: 10.37789/rjce.2025.16.2.8

Abstract
In this paper, is presented our opinion regarding „How do we see Climate Changes in Refrigeration" focussed by comparative study of refrigerants.
Decarbonization is the goal of EU by 2050. Reduction of carbon dioxide emissions by using low-carbon energy sources, resulting in less production of greenhouse gases in the atmosphere is an important target.

Rezumat
În această lucrare, este prezentată opinia noastră cu privire la "Cum vedem schimbările climatice în refrigerare", axată pe studiul comparativ al agenților frigorifici.
Decarbonizarea este obiectivul UE până în 2050. Reducerea emisiilor de dioxid de carbon prin utilizarea surselor de energie cu emisii reduse de carbon, este un obiectiv important, ceea ce duce la o producție mai mică de gaze cu efect de seră în atmosferă.

Key words: *decarbonization, climate changes, greenhouse*

Cuvinte cheie: *decarbonizare, schimbări climatice, seră*

1. Refrigerants Situation

In the last ten years, a lot of research has been done in the field of AF, at international level, taking into consideration the severe restrictions stipulated by law: Kyoto Protocol, Regulation (EU) 2024/573, Paris Agreement/2015, Kigali Amendment/ 2016 / Montreal Protocol [1,3,4,5]. Other important events in connection with CC: January 1, 2019 the Kigali amendment imposed regulations to reduce the production an usage of hydrofluorocarbons (HFC's), greenhouse gases (temperature increase 0.4°C)

All countries signing the Montreal Protocol agreed to phase out HFC's by more than 80% over the next 30 years (replacing environmentally friendly alternatives).

Kigali amendment (elimination of up to 80 billion tons of CO2 emissions by 2050)

The article was received on 19.03.2025, accepted on 21.05.2025 and published on 22.05.2025

Significant contribution to the objective of the Paris Agreement to limit the increase in global average temperature to a maximum of 2°C.

Figure 1. Climate changes [9,10]

In figure 2 it is shown the situation of climate impact of cooling sector.

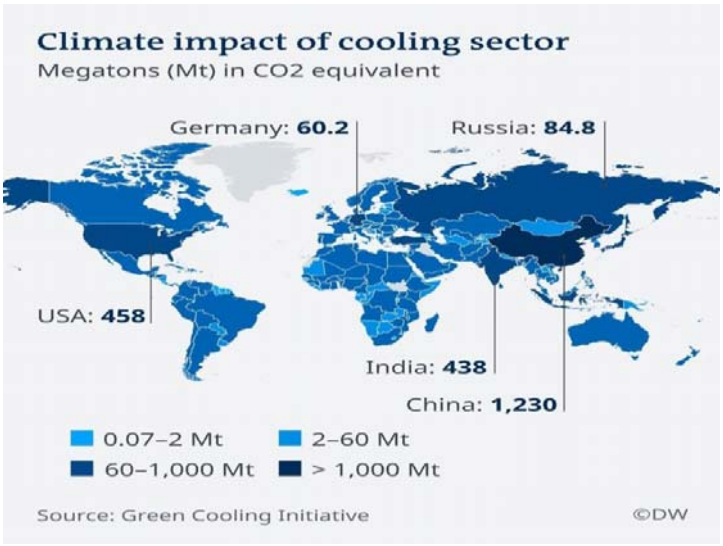

Figure 2. Cooling Sector

Decarbonization

Decarbonization is the reduction of carbon dioxide emissions by using low-carbon energy sources, resulting in less production of greenhouse gases in the atmosphere [2,5,6,7]. In our field must be done some important measures:

▶ Use of low GWP (global warming potential) refrigerants while maintaining energy efficiency;

▶ Calculated TEWI (Total Equivalent Warming Impact) Factor for the refrigeration systems (heat pump).

2. Using Low GWP Refrigerants

Using low GWP refrigerants, we could minimize the risk of deteriorating the ozone layer from refrigerant leaks.

Figure 3. Low GWP refrigerants

Two of the lowest GWP refrigerants are R-744 (CO2), with a GWP of 1 and R-717 (Ammonia) with a GWP of 0.

In our opinion R-717 it is better than the R-744 for many reasons [8].

Ammonia has better efficiency than CO2 so it would use less electrical power to operate.

Ammonia has lower operating pressure than CO2 and also could reach higher condensation temperatures, so it would be a good alternative for heating as well.

3. Starting from our homes

Almost every house in Europe has at least one air conditioning unit and most of these units are using outdated refrigerants and without proper maintenance could appear leaks contributing at the depletion of the ozone layer.

It would be a more efficient way to centralize the cooling of our homes. Using this method, we can keep the refrigeration systems in a district cooling point and use an intermediary cooling agent to cool our homes. This system could be used for heating as well.

In this way we could use the old but reliable R-717 (Ammonia) which has GWP 0 and it is very efficient. Indeed, it is toxic for people, but the system would be in a closed environment and would be equipped with a leak detection system.

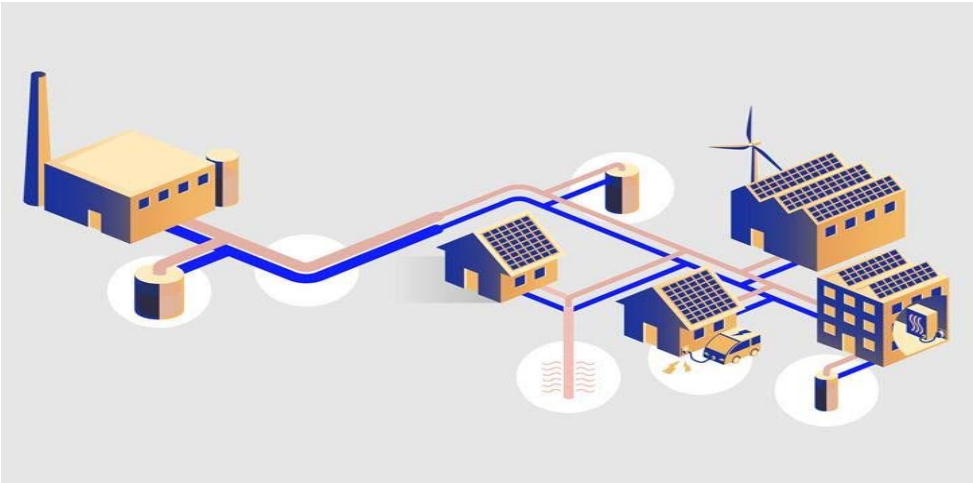

Figure 4. Connection of HVAC systems starting from our homes

At the moment the cooling sector still has a huge impact in the climate change. The big and developed countries around the world have pretty high CO2 emissions.

One of the many solutions is decarbonization, which basically means to reduce CO2 emissions using low-carbon energy sources. Two main solutions are use of low GWP refrigerants while maintaining energy efficiency and using in the designing stage the TEWI factor for refrigeration. Using low GWP refrigerants we could minimize the risk ofdeteriorating the ozone layer, but we have to keep in mind that energy efficiency is also important. Like better efficiency than CO2, which means lower power consumption, a factor that also contributes at lowering the CO2 emissions, given that about 60% of the electric energy is produced from burning coal. Another advantage is lower operating pressure. And the higher condensation temperature makes it suitable for usage in heat pumps.

4. Conclusions

We could start this change from our homes. Given that almost every house in Europehas at least one air conditioning unit, in many cases they use outdated refrigerants which without proper maintenance could lead to leaks.

In our opinion a better alternative would be centralization of the cooling system. With this method smaller district cooling plants could be created. This kind of system would use an intermediary cooling agent to cool our homes and it would be much safer. In the cold season this system could be used in a heat pump setup and supply heat to our houses.

For industrial application we think it would be suitable to use Ammonia, it is a natural refrigerant with a GWP of 0 and has high efficiency. Because Ammonia is toxic for people, the district plant would be equipped with safety systems for leak detection.

BIBLIOGRAPHY

[1]. ASHRAE – Thermophysical Properties of Refrigerants, -Chapter 20, 2009

[2]. Codul bunelor practici – Domeniul frigului si aerului conditionat, Editura AGIR, Bucuresti, 2008-2009

[3]. Regulation (EU) 2024/573 of the European Parliament and of the Council of 7 February 2024 on fluorinated greenhouse gases

[4]. Bitzer - Refrigerent Report 2023

[5]. Communication from the Commission to the European Parliament, the European Council, the Council, the European Economic and Social Committee and the Committee of the Regions, The European Green Deal, 2019, https://eur-lex.europa.eu/legal-content/EN/TXT/?uri=CELEX%3A52019DC0640&qid=1717936088805

[6]. Zabet I., Tarlea G., Vinceriuc M. and Ţârlea A., - Comparative study of hydrocarbons, ammonia and HFC mixture alternatives for retrofitting ourposes, published at the Conference COFRET 2012, 11-13 Iunie 2012, Sozopol, Bulgarie, ISBN 978-619-460-008-3

[7]. Ţârlea G., Zabet I., Vinceriuc M. and Ţârlea A., - Theoretical eco-efficiency comparative study case, hydrocarbons, ammonia and HFC mixture alternatives retrofit, published at The 5th International Conference on Advanced Concepts in Mechanical Engineering June 14-15, 2012

[8] Vinceriuc, M., Tarlea, G., Tarlea, A., Zabet, I., - NH3 and CO2 study cases-refrigeration applications, International Multidisciplinary Scientific GeoConference Surveying Geology and Mining Ecology Management, Bulgaria, SGEM 2018, Conference Proceedings, ISSN 1314-2704, DOI: 10.5593/SGEM_GeoConference

[9] Tarlea G., Vinceriuc M. - AGENTI FRIGORIFICI vol I, 2024, Editura Matrix Rom, ISBN: 978-606-25-0908-8

[10] Vinceriuc M., - Cercetări privind contribuția sistemelor frigorifice, de aer condiționat și pompe de căldură la încălzirea globală, 2024, Editura Matrix Rom, 978-606-25-0904-0

NH3/H2O absorption cycle – mathematical model

Ciclul de absorbție NH3/H2O - model matematic

Cătălin-George Popovici[1], Emilian-Florin Țurcanu[1], Vasilică Ciocan[1], Nelu-Cristian Chereches[1], Sebastian-Valeriu Hudișteanu[1], Ana Diana Ancas[1], Marina Verdeș [1], Marius-Vasile Atanasiu[2]

[1] Technical University "Gheorghe Asachi" of Iasi, Faculty of Civil Engineering and Building Services, Department Building Services, D. Mangeron 67 str., 700050, Romania;
[2] Technical University "Gheorghe Asachi" of Iasi, Faculty of Mechanical Engineering, Department of Mechanical Engineering and Road Automotive Engineering, D. Mangeron 67 str., 700050, Romania;
e-mail: florin-emilian.turcanu@academic.tuiasi.ro, seby_hudisteanu@yahoo.com

DOI: 10.37789/rjce.2025.16.2.9

Abstract:
The rising interest in absorption cycles for refrigeration and air conditioning systems is driven by their significant benefits in reducing carbon emissions. Among these cycles, the NH3/H2O absorption cycle is particularly appealing. This paper provides a comprehensive overview of the system process, simulation methodology, and mathematical NH3/H2O cycle model, including a detailed description of the modeling technique.

Key-words: *absortion cycle, carbon emissions*

1. Introduction

There has been a significant surge in interest in refrigeration or air conditioning systems absorption cycles in recent times. It possesses substantial benefits that help decrease carbon emissions. The NH3/H2O cycle is the most appealing absorption cycle. This paper presents a concise overview of the system process, simulation methodology, and the NH3/H2O mathematical model. The modeling technique is also executed concisely.

1.1 Working principles & system description

An absorption refrigerator utilizes a heat source, such as solar energy, a flame fed by fossil fuels, waste heat from manufacturers, or district heating systems, to generate the necessary energy for the cooling process. The system employs two coolants, with the first coolant carrying out evaporative cooling and subsequently being

The article was received on 24.08.2024, accepted on 20.05.2025 and published on 22.05.2025

absorbed by the second coolant. The restoration of the two coolants to their original states requires heat input. The method can also be applied to cool buildings by utilizing the excess heat generated by a gas turbine or water heater. Absorption refrigerators are frequently employed in recreational vehicles, campers, hotels, and caravans due to their ability to operate on propane fuel instead of electricity. Conventional absorption refrigerators employ a refrigerant that has a shallow boiling point, similar to compressor refrigerators, which is below -18°C (0 °F). Compression refrigerators commonly utilise HCFC or HFC refrigerants, whilst absorption refrigerators typically employ ammonia or water as the primary coolant. Absorption refrigerators also require a secondary fluid capable of absorbing the coolant, such as water (for ammonia) or brine (for water). Both kinds employ evaporative cooling, where the refrigerant undergoes evaporation (boiling), thereby extracting heat and producing the desired cooling effect. The primary distinction between the two systems lies in the method by which the refrigerant undergoes a transformation from a gaseous state to a liquid state, enabling the cycle to be repeated. An absorption refrigerator utilises a heat-based process to convert the gas back into a liquid, without the need for any moving elements other than the fluids involved. The absorption cooling cycle can be delineated into three distinct phases: Evaporation is the process in which a liquid refrigerant transforms into a gas in a low-pressure environment, thereby absorbing heat from its surroundings, such as the compartment of a refrigerator. Due to the low partial pressure, the temperature required for evaporation is correspondingly low. Absorption: The second fluid, which is in a state of reduced quantity, draws out the refrigerant that has now become gaseous, thereby creating a low partial pressure. As a result, a liquid saturated with refrigerant is generated, which subsequently moves on to the following stage: Regeneration: The liquid saturated with refrigerant is heated, causing the refrigerant to transition into a gaseous state.

Evaporation takes place in the lower section of a narrow tube, where the bubbles of refrigerant gas propel the liquid that has been depleted of refrigerant into a higher chamber. From there, the liquid will flow downward due to gravity into the absorption chamber. The hot gaseous refrigerant moves through a heat exchanger, releasing its heat to the environment (such as the surrounding air at ambient temperature), and condenses at an elevated location. The liquid refrigerant will flow downwards due to gravity to provide the evaporation process.

1.2 System description

The operation of the ammonia-water absorption refrigeration system is founded on the fundamental principles of vapour absorption refrigeration. Ammonia serves as the refrigerant, while water functions as the absorbent in this system. The ammonia-water absorption system (NH3/H2O) is utilised in both residential and commercial settings where temperatures exceeding 32 degrees Fahrenheit are necessary. An important benefit of the ammonia-water solution is that water exhibits a high affinity for ammonia, allowing them to dissolve in one other under a wide range of operating conditions commonly

encountered in various refrigeration applications. In addition, the ammonia-water solution exhibits exceptional stability and compatibility with various materials, with the exception of copper and its alloys, which are susceptible to corrosion in the presence of ammonia. Figure (1) illustrates the standard NH3/H2O absorption cycle. The NH3-H2O absorption process includes the following components:Air conditioning serves as a cooling load and is connected to the evaporator unit. The fan cooling unit is connected to the air cooler unit. The cooling effect is produced in the evaporator by the liquid condition of the refrigerant, which is pure ammonia (NH3). It absorbs thermal energy from the substance to be cooled and undergoes evaporation. Subsequently, the ammonia transitions to the absorber in its gaseous form.The weak solution of ammonia-water is already present in the absorber. The water, acting as the absorbent in the solution, is not fully saturated and has the ability to absorb additional ammonia gas. Upon entering the absorber, the ammonia from the evaporator is quickly absorbed by water, resulting in the formation of a concentrated solution of ammonia and water. Heat is released during the absorption process, which might decrease the ability of water to absorb ammonia. Therefore, the absorber is cooled using cooling water. The absorber creates a concentrated solution of ammonia-water as a result of ammonia absorption. The generator unit is connected to the solar component. The flash evaporation tank will provide sufficient steam to power the generator unit. The concentrated solution of ammonia refrigerant and water absorbent is heated using an external heat source, such as steam or hot water. Additionally, it can be heated by alternative sources such as natural gas, electric heaters, waste exhaust heat, and so on. As a result of being heated, the refrigerant ammonia undergoes vaporisation and exits the generator. As a result of the cooling process, the water vapour that is left mixes with the ammonia refrigerant and undergoes condensation, along with some ammonia particles. The dilute solution of water and ammonia flows downwards into the condenser and then into the generator. The vaporised ammonia refrigerant, in its pure form, is subjected to high pressure and subsequently directed into the condenser. In this component, the refrigerant is effectively cooled through the utilisation of water. Ammonia, a refrigerant, undergoes a phase change into a liquid form and then flows through the expansion valve, causing a dramatic decrease in both its temperature and pressure. The ammonia refrigerant is introduced into the evaporator, where it generates the desired cooling effect. This loop perpetually repeats without interruption. Meanwhile, while ammonia undergoes vaporization in the generator, a dilute solution of ammonia and water remains within it. The solution undergoes expansion in the expansion valve and is then returned to the absorber, where the cycle is repeated. The cycle is regarded as a closed system in relation to the flow of work passing through it.

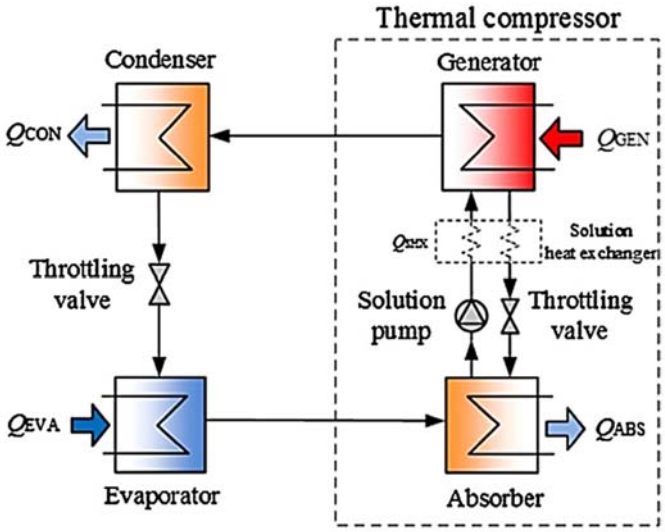

Figure (1) Typical NH3/H2O absorption cycle.

2.1 Modelling & simulation

2.2 The Modelling Methodology & assumptions

The characteristics that are not known include the areas, dimensions, mass flow rates, and the overall process temperatures, as well as any other computed physical qualities. In absorption operations, it is crucial to define the cooling load capacity in order to accurately calculate the thermal loads on the evaporator, absorber, condenser, and generator. In this work, the desired refrigerant load capacity in ton refrigerant $TR = \frac{Q_{evp},\ kW}{3.517}$ is specified as a known parameter in order to calculate all design aspects and mass flow rate through the cycle.

By specifying the system cooling load, one may determine the necessary thermal load. In addition, the necessary design constraints and performance estimates would be immediately approved. The modelling assumptions can be found in Table 1. The modelled blocks and lookup tables contain data for the saturated liquid and vapour phases, including information on pressure, temperature, enthalpy, specific volume, and specific entropy. The NIST [1] web chemistry book is the primary source for obtaining physical characteristics. Table 1 presents the design operating conditions and the assumptions that have been taken into account in this study. Table 2 presents the mathematical model utilised in this study. The suggested model control panel (refer to Figure 2) is a graphical user interface designed to manage the system inputs. All units have been created with a consistent approach, taking into account the behaviour of input and output streams that connect them. An iteration loop has been implemented to calculate the forward and backward streams. The model browser was developed using the Matlab/Simulink model environment. It possesses several characteristics,

including:The model facilitates the effortless modification of plant factors and adaptation to various operating situations, while providing maximum flexibility in stream allocation. The stream connection will be crucial in establishing connections between various units.

Table 1

Data assumptions for the ETC/PTC-H2O/LiBr and NH3/H2O configurations.

Unit Process	Assigned Data	Calculated Data
NH3/H2O: - **Absorption working fluid is NH3-H2O**	✓ Absorber temperature, ºC=30-35 ✓ Generator temperature, ºC=80-90 ✓ Condenser temperature, ºC=40-45 ✓ Hot air temperature, ºC=35 ✓ Target cooled air temperature, ºC=20 ✓ Evaporator temperature, ºC=5-10 ✓ Cooling load, TR=varying ✓ Condenser effectiveness, %=80 ✓ Cooling tower effectiveness, %=60 ✓ Fan system efficiency, %=85 ✓ Pumping system efficiency, %=75	**Absorption Unit:** ➢ Weak & strong solutions, kg/s ➢ *Design data ➢ Thermal power, kW ➢ Total cycle flow rate, kg/s ➢ Generator power, kW ➢ Cooling fan power, kW ➢ COP ➢ Relative performance ➢ Exergy destruction, kW
Notes:	▪ Data are run out based on steady state operating conditions. ▪ Ambient temperature is fixed as 25ºC for all process runs. ▪ *Design data means area, length, width, etc…	

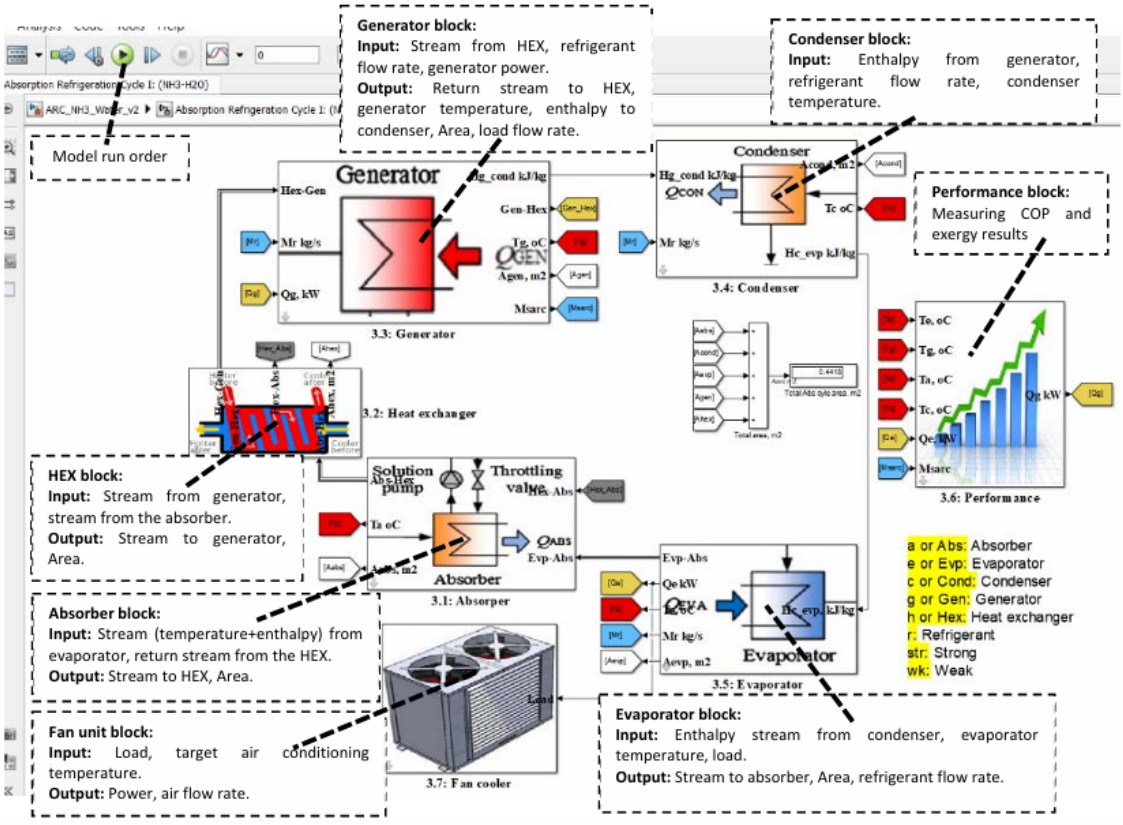

Figure (2) NH3/H2O model browser control panel under matlab/simulink toolbox.

3. The mathematical model

The process modelling via MATLAB/Simulink toolbox has been performed based on the following mathematical model that been presented in Table 2.

Table 2

The mathematical model of the system units.

Absorption unit [2, 5]:
1. The absorber unit [2, 4]: For absorber unit, the flow factor parameter is an especially important parameter in the calculation procedures of the thermal power through the mode. The flow rate ratio factor *f* is calculated based on the absorber temperature as following [2]: $f = 0.4067 \times exp(0.05606 \times T_a) + 5.09e-07 \times exp(0.3293 \times T_a)$ ….. (1) The strong solution mass flow rate, kg/s, M_{str} is calculated based on total refrigerant flow rate and the flow factor: $M_{str} = M_r \times f$ ….. (2) The weak solution mass flow rate, kg/s: $M_{wk} = M_{str} - M_r$ ….. (3) The Absorber thermal power, kW is calculated based on the energy balance across the absorber between inlet and outlet streams, where *H* denotes to enthalpy, kJ/kg: $Q_a = M_r \times \left(H_{e-abs} + (M_{wk} \times H_{hex-a}) - (M_{str} \times H_{a-hex})\right)$ ….. (4) Overall heat loss, kW/m^2°C [5]: $U_a = 1.6175 + 0.1537e-3 \times T_a + 0.1825e-3 \times T_a^2 - 8.026e-8 \times T_a^3$ ….. (5) The absorber area, m^2: $A_a = \frac{Q_a}{U_a \times \Delta T}$ ….. (6)
2. Heat exchanger unit [2-5]: For heat exchanger unit, the mass flow ratio is obtained as following: $f = \frac{M_{str}}{M_{str} - M_{wk}}$ ….. (7) The NH3 concentration percentage [2, 3]: $XNH3 = \frac{\frac{M_{str}}{f}}{M_r + M_{wk}}$ ….. (8) The outlet heat exchanger stream temperature towards the absorber unit, °C is calculated based on the heat exchanger effectiveness: $T_{hex\_a} = T_g - \left(\varepsilon_{hex} \times \left(T_g - T_a\right)\right)$ ….. (9) Outlet heat exchanger temperature to the generator unit, °C: $T_{hex\_g} = T_a + \left(\varepsilon_{hex} \times \left(T_g - T_a\right)\right)$ ….. (10) The enthalpy of NH3/H2O solution outlet to the absorber unit, kJ/kg is calculated based on temperature, °K and specific heat capacity, kJ/kg°K: $H_{hex\_a} = Cp_{NH3}(T_{hex-a} + 273) \times (T_{hex-a} + 273)$ ….. (11) Where the specific heat capacity for NH3, kJ/kg°K: $Cp_{NH3} = \frac{27.31 + 0.02383 \times T + 1.707e-5 \times (T^2) - 1.185e-8 \times (T^3)}{17.0305}$ ….. (12) The enthalpy of NH3/H2O solution outlet to the generator unit, kJ/kg: $H_{hex\_g} = Cp_{NH3}\left(T_{hex-g} + 273\right) \times \left(T_{hex-g} + 273\right)$ ….. (13)

The heat exchanger thermal power is then calculated based on the thermal energy balance between inlet and outlet streams, kW:

$Q_{hex} = (M_{str} - M_{wk}) \times (f-1) \times \left(H_{g-hex} - H_{hex-a}\right) \ldots\ldots (14)$

Enthalpy stream from the absorber towards the heat exchanger, kJ/kg:

$H_{a-hex} = H_{hex-g} - \left(\left(\frac{f-1}{f}\right) \times \left(H_{g-hex} - H_{hex-a}\right)\right) \ldots\ldots (15)$

Mean temperature, °C:

$T_{hex_m} = \frac{T_{hex-a} + T_{hex-g}}{2} \ldots\ldots (16)$

Overall heat loss, kW/m^2°C:

$U_{hex} = 1.6175 + 0.1537e-3 \times T^1_{hex_m} + 0.1825e-3 \times T^2_{hex_m} - 8.026e-8 \times T^3_{hex_m} \ldots\ldots (17)$

Heat exchanger area, m^2:

$A_{hex} = \frac{Q_{hex}}{U_{hex} \times \Delta T} \ldots\ldots (18)$

3. Generator unit [3-5]:

Outlet enthalpy to the HEX, kJ/kg is calculated based on energy balance between both units and flow rate ratio:

$H_{g\_hex} = \frac{\left(\frac{Q_g}{M_r}\right) - H_{g-cond} + (f \times H_{hex-g})}{f-1} \ldots\ldots (19)$

Overall heat loss, kW/m^2°C through the generator tubes is calculated as following [4]:

$U_g = 1.6175 + 0.1537e-3 \times T^1_g + 0.1825e-3 \times T^2_g - 8.026e-8 \times T^3_g \ldots\ldots (20)$

Generator area, m^2:

$A_g = \frac{Q_g}{U_g \times \Delta T} \ldots\ldots (21)$

Inlet driving steam mass flow rate, kg/s is calculated based on the latent heat, kJ/kg from the heat source:

$Ms = \frac{Q_g}{0.95 \times h_{fg}} \ldots\ldots (22)$

Where, h_{fg} is the latent heat of distillate vapor evaporation (pure Ammonia) [2-5]:

$h_{fg} = -46.53 \times exp(0.02096 \times T) + 1305 \times exp(-0.001835 \times T) \ldots\ldots (23)$

4. Condenser unit:

Condenser thermal power, kW:

$Q_c = M_r \times \left(H_{g-cond} - H_{cond-e}\right) \ldots\ldots (24)$

The overall heat loss, kW/m^2°C:

$U_c = 1.6175 + 0.1537e-3 \times T^1_c + 0.1825e-3 \times T^2_c - 8.026e-8 \times T^3_c \ldots\ldots (25)$

The condenser area, m^2:

$A_c = \frac{Q_c}{U_c \times \Delta T} \ldots\ldots (26)$

Inlet cooling water enthalpy, kJ/kg:

$H_{c_{cwi}} = 421.2 \times exp\left(0.004008 \times T_{c_{cwi}}\right) - 435.9 \times exp\left(-0.007559 \times T_{c_{cwi}}\right) \ldots\ldots (27)$

Outlet cooling water enthalpy, kJ/kg:

$H_{c_{cwo}} = \left(\frac{Q_c}{M_{cw}}\right) + H_{c_{cwi}} \ldots\ldots (28)$

5. Evaporator unit:

Thermal load on evaporator unit, kW [6]:

$Q_e = Load_{TR} \times 3.517 \ldots\ldots (29)$

Refrigerant mass flow rate, kg/s can be calculated based on the energy balance across the evaporator:

$M_r = \frac{Q_e}{H_{e-abs} - H_{cond-e}} \ldots\ldots (30)$

Fan unit [5]:

Cooling air mass flow rate, kg/s is calculated based on thermal power (Q_e, kW), specific heat capacity of the air, C_p, kJ/kg°C and the temperature difference between input and outlet cases, °C:

$$M_{air} = \frac{Load \times 3.517}{C_p(T_{a_m}) \times \left(T_{a_i} - T_{a_o}\right)} \ldots\ldots (28)$$

Air flow velocity, m/s based on air duct diameter, D_{ta}, m mass flow rate, and air density:

$$V_{air} = \frac{M_{air}}{\rho_a(T_{a_m}) \times \left(\left(\frac{\pi}{4}\right) \times \left(D_{t_a}{}^2\right)\right)} \ldots\ldots (29)$$

Pressure drop across the air-cooled condenser, kPa based on air density, air velocity, and mean air temperature, Ta_m, °C:

$$\Delta P = \frac{\sqrt{\left(\frac{V_{air} \times \rho_a(T_{a_m})}{0.85}\right)}}{2 \times 9.81 \times \rho_a(T_{a_m})} \ldots\ldots (30)$$

Fan Power, kW:

$$FHP = \frac{\left(\left(\frac{\pi}{4}\right) \times D_{t_a}{}^2\right) \times V_{air} \times \Delta P}{\eta_{fan}} \ldots\ldots (31)$$

Exergy & Performance [7-9]:

For any system goes under steady state, the mass, energy, and entropy balances equations under steady state condition should be developed as following.

$$\sum \dot{m_{in}} - \sum \dot{m_{out}} = 0, kg/s$$
$$\sum \dot{e_{in}} - \sum \dot{e_{out}} = 0, kJ/kg$$
$$\sum \dot{s_{in}} - \sum \dot{s_{out}} = 0, kJ/kgoC$$

The general form of the availability is defined by the following equation.

$$A_2 - A_1 = A_q + A_w + A_{fi} - A_{fo} - I$$

Where A_2-A_1=0 is the non-flow availability change in steady state condition, $A_q = \sum_J (1 - T_{amb}/T_J) Q_J$ is the availability transfer due to the heat transfer between the control volume and its surroundings, $A_w = -W_{cv} + P_o(V_2 - V_1)$ is equal to the negative value of the work produced by the control volume but in most cases the control volume has a constant volume, therefore Aw can be further simplified. And I=$T_{amb} \times S_{gen}$ is the availability destruction in the process. The flow availability expressed as$A_{fi,o} = \sum_{i,o} \dot{m}_{i.o}\, a_{fi,o}$. So, the general form in steady state condition would become;

$$0 = A_q + A_w + A_{fi} - A_{fo} - I$$

For performance calculations, the C.O.P is calculated based on evaporator and generator thermal powers, $COP = \frac{Q_e}{Q_g}$, where the Max C.O.P is found as $COP_{max} = \frac{(T_e + 273.15) \times (T_g - T_a)}{(T_g + 273.15) \times (T_c - T_e)}$, and the relative performance ratio could be then estimated as $RPR = \frac{COP}{COP_{max}}$

4. Conclusion

A model and presentation of an absorption refrigeration cycle utilizing NH3/H2O has been developed. The components of the cycle include the evaporator unit, absorber, condenser heat exchanger unit, and generator. The following highlights can be retracted: A description of the process has been provided. The model code has been executed and showcased. The outcome of processing the data has been demonstrated.

Bibliography

[1] https://webbook.nist.gov/chemistry/name-ser/

[2] M Conde, Theoritical Analysis of Nh3-H2o Refrigeration System Coupled with Diesel Engine: A Thermodynamic Study, Zurich, 2004.

[3] Y.T. Ge, S.A. Tassou, I. Chaer, Modelling and performance evaluation of a low-temperature ammonia–water absorption refrigeration system, International Journal of Low-Carbon Technologies 2009, 4, 68–77.

[4] N. Shankar Ganesh, T. Srinivas, Evaluation of thermodynamic properties of ammonia/water mixture up to 100bar for power application systems, Journal of Mechanical Engineering Research Vol. 3. (1), pp. 25-39, January 2011.

[5] CECIL E. VANDERZEE, DELBERT L. KING, The enthalpies of solution and formation of ammonia, J. Chem. Thermodynamics 1972, 4, 675-683.

[6] S. Bittanti, A. De Marco, M. Giannatempo, V. Prandoni, A Dynamic Model of an Absorption Chiller for Air Conditioning, https://doi.org/10.24084/repqj08.428

[7] Abdul Rahman Mallah, Mohd Nashrul Mohd Zubir, Omer A. Alawi, Kazi Md Salim Newaz, Ahmad Badarudin Mohamad Badry, Plasmonic nanofluids for high photothermal conversion efficiency in direct absorption solar collectors: Fundamentals and applications, Solar Energy Materials and Solar Cells 201 (2019) 110084.

[8] F. L. Lansing, Computer Modeling of a Single-Stage Lithium Bromide/Water Absorption Refrigeration Unit, JPL DEEP SPACE NETWORK PROGRESS REPORT 42-32, In it's The Deep Space Network p 247-257 (SEE N76-23304 14-12)

[9] A.S. Nafey, M.A. Sharaf, Lourdes Garcia-Rodriguez, A new visual library for design and simulation of solar desalination systems (SDS), Desalination 259 (2010) 197–207.

About the overall heat transfer coefficient of plate heat exchangers

Despre coeficientul de transfer termic global al schimbătorului de căldură cu plăci

Florin Iordache[1], Florin Băltărețu[1]

[1]Technical University of Civil Engineering Bucharest
Bd. Lacul Tei nr. 122 - 124, cod 020396, Sector 2, Bucharest, Romania
E-mail: fliord@yahoo.com, florin.baltaretu@utcb.ro

DOI: 10.37789/rjce.2025.16.2.10

Abstract. *The present work seeks to establish some practical working relationships for determining the values of overall heat transfer coefficient, k, related to plate heat exchangers. This problem is experimentally solved by the manufacturers of such heat exchangers in the world, so our work has more of an educational-research character, which can serve to some users of plate heat exchangers in district heating systems or indoor central heating installations.*

Key words: *plate heat exchanger, overall heat transfer coefficient*

1. Introduction

For some years, plate heat exchangers are the most used heat exchangers in district heating systems, as well as in indoor heating systems, as they are equipment with high energy performance and a high degree of compactness. As it is known, there are various constructive plate heat exchanger types, regarding the plates from which the exchanger is made up, the coupling of the plates being done either in a removable system (with gaskets) or in a fixed, non-removable system. The energy performance of these heat exchangers is dependent on their overall heat transfer coefficient, which is the object of our concern in this work.

An important influence on the value of the overall heat transfer coefficient is of course the type of circulation of thermal fluids within the heat exchanger, mainly counter-current or co-current. It is known that the energy performances of the counter-current heat exchanger are superior to the co-current one. In the present work, the case of a counter-current type plate heat exchanger will be analysed.

The article was received on 16.06.2024, accepted on 21.05.2025 and published on 22.05.2025

Another important influence on the value of the overall heat transfer coefficient is due to the dependence on temperature for the physical parameters of thermal fluids (density ρ, specific heat c, thermal conductivity λ and kinematic viscosity ν).

2. Description of the problem. Calculation relations

The basic relationship used to evaluate the global thermal transfer coefficient of the heat exchanger is:

$$\frac{1}{k}=\frac{1}{\alpha_1}+\frac{\delta_p}{\lambda_p}+\frac{1}{\alpha_2} \tag{1}$$

In order to determine the convective heat transfer coefficients related to the two thermal fluids circulating in counter-current through the heat exchanger, relationships based on the values of the Nusselt criteria (Nu_1 and Nu_2) were used. Therefore:

$$Nu_1=\frac{\alpha_1\cdot l_c}{\lambda_f};\quad Nu_2=\frac{\alpha_2\cdot l_c}{\lambda_f} \tag{2}$$

From relations (2) it follows:

$$\alpha_1=\frac{Nu_1\cdot\lambda_f}{l_c};\quad \alpha_2=\frac{Nu_2\cdot\lambda_f}{l_c} \tag{3}$$

For plate heat exchangers, a relationship used for the Nusselt criterion is:

$$\mathrm{Nu}=C\cdot\mathrm{Re}^n\cdot\mathrm{Pr}^m\cdot\left(\frac{\mu}{\mu_p}\right)^p \tag{4}$$

with coefficients m = 1/3 and p = 0.17. Some values of the coefficients C and n are presented in table 1 (as presented in [1], [2]), for different plate chevron angles β.

β	Re	C	n
≤ 30°	> 10	0.348	0.663
45°	> 100	0.300	0.663
50°	> 300	0.130	0.732
60°	> 400	0.108	0.703
≥ 65°	> 500	0.087	0.718

Table 1. Values of coefficients C and n for plate heat exchangers

In the present paper, we considered a plate heat exchanger with a chevron angle β = 60°, and a Reynolds number Re > 400. Neglecting the effect of viscosity, one obtains:

$$Nu=0{,}108\cdot\mathrm{Re}^{0{,}703}\cdot\mathrm{Pr}^{0{,}333} \tag{5}$$

where we have the following expressions for the Reynolds and Prandtl numbers:

$$\mathrm{Re}=\frac{w\cdot l_c}{\nu};\quad \mathrm{Pr}=\frac{\nu}{a};\quad a=\frac{\lambda_f}{\rho\cdot c} \tag{6}$$

The physical parameters of thermal fluids (water) were considered to be dependent on temperature [3], their expressions in the specific interval for heating systems being:

$$\begin{aligned}
&\rho=-0,0031\cdot t_m^2-0,1098\cdot t_m+1001\\
&c=0,0134\cdot t_m^2-1,2129\cdot t_m+4203,7\\
&\lambda_f=-10^{(-5)}\cdot t_m^2+0,0024\cdot t_m+0,5533\\
&\nu=10^{(-6)}\cdot\begin{pmatrix}-2,0406\cdot 10^{(-10)}\cdot t_m^5+8,3863\cdot 10^{(-8)}\cdot t_m^4-\\-1,3650\cdot 10^{(-5)}\cdot t_m^3+1,1548\cdot 10^{(-3)}\cdot t_m^2-\\-5,7371\cdot 10^{(-2)}\cdot t_m+1,7857\end{pmatrix}
\end{aligned} \tag{7}$$

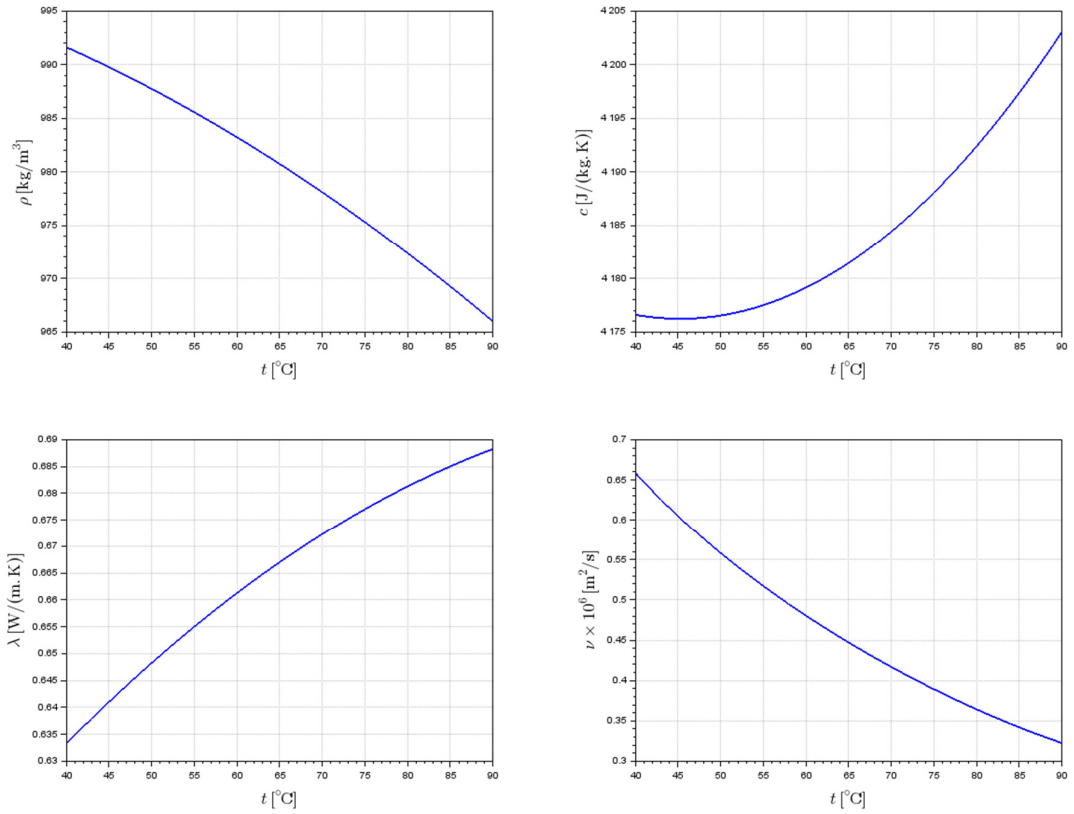

Fig. 1. The correlations for water density ρ, specific heat c, thermal conductivity λ and kinematic viscosity ν

It follows that for the evaluation of the convective thermal transfer coefficients α_1, α_2 it is necessary to evaluate the criteria Nu_1, Nu_2 and therefore of the criteria Re_1, Re_2 and Pr_1, Pr_2.

This involves the evaluation the physical parameters of the thermal fluids corresponding to the average temperatures of the thermal fluids. According to the theory presented at large in [4] in the chapter of heat exchangers, the determination of the average values of the temperatures of the thermal fluids for counter-current heat exchangers can be done using the relations:

$$\begin{aligned} t_{m1} &= C_1 + C_2 \cdot F \\ t_{m2} &= C_1 + y \cdot C_2 \cdot F \end{aligned} \tag{8}$$

where the constants C_1 and C_2 have the expressions:

$$\begin{aligned} C_1 &= \frac{-y \cdot E}{1 - y \cdot E} \cdot t_{11} + \frac{1}{1 - y \cdot E} \cdot t_{21} \\ C_2 &= \frac{1}{1 - y \cdot E} \cdot t_{11} - \frac{1}{1 - y \cdot E} \cdot t_{21} \end{aligned} \tag{9}$$

and F is the heat transfer co-module, which, together with the heat transfer module, E, have the expressions:

$$\begin{aligned} y &= \frac{G_1}{G_2} = \frac{a_1}{a_2} \\ NTU_1 &= \frac{k \cdot S}{G_1 \cdot \rho \cdot c} = \frac{k}{a_1 \cdot \rho \cdot c} \\ E &= \exp\left(-NTU_1 \cdot (1 - y)\right) \\ F &= \frac{1 - E}{-\ln(E)} \end{aligned} \tag{10}$$

In order to carry out the assessments presented, an iterative procedure is proposed, which starts with an initially proposed value for the global heat transfer coefficient for the heat exchanger, k_0. The nominal values of sizing parameters t_{110}, t_{210}, t_{120} and t_{220} are also considered known. Based on them, the values of the specific volumic flow rates of the thermal fluids are established:

$$\begin{aligned} a_1 &= \frac{k_0}{\rho \cdot c} \cdot \frac{\Delta t_{ml0}}{(t_{110} - t_{120})} \\ a_2 &= \frac{k_0}{\rho \cdot c} \cdot \frac{\Delta t_{ml0}}{(t_{220} - t_{210})} \end{aligned} \tag{11}$$

The iterative procedure involves the determination of the values *NTU*, *y*, *E*, *F*, and the average temperatures of the thermal fluids on the two circuits, t_{m1} and t_{m2}.

The values of convective heat transfer coefficients, α_1, α_2 are obtained, according to those presented, as well as the value of the overall heat transfer coefficient, *k*. With the new value obtained for *k*, the points in the procedure are followed again and so on, until a certain maximum imposed error is attained. Basically, the values of the inlet temperatures of the thermal fluids of the heat exchanger are proposed and the corresponding value of the overall heat transfer coefficient, *k*, is determined iteratively.

The circulation velocities of the thermal fluids between the heat exchanger changer plates were considered to have the same ratio given by the value of *y*, respectively 0.4 m/s on the primary circuit and 0.6 m/s for the secondary circuit.

Three values for the distance between the heat exchanger plates were considered for this analysis, namely $\delta = 0.002$, 0.004 and 0.006 m. The obtained results proved that this is an important constructive parameter.

3. Obtained results

In order to carry out this analysis, an automatic calculation tool was built in SCILAB, that allow for a couple of values (t_{11}, t_{21}) to quickly provide the values of the global heat transfer coefficient of the heat exchanger, *k*.

It was observed that the values of the overall heat transfer coefficient, *k*, depend quite a lot on the average value of the couple of input temperature values, which is why an attempt was made to correlate the output values, *k*, with the input ones, (t_{11}, t_{21}), more precisely, the correlation between *k* and $t_{med} = (t_{11} + t_{21})/2$ and $dt = t_{11} - t_{21}$.

Some of the obtained results are presented below.

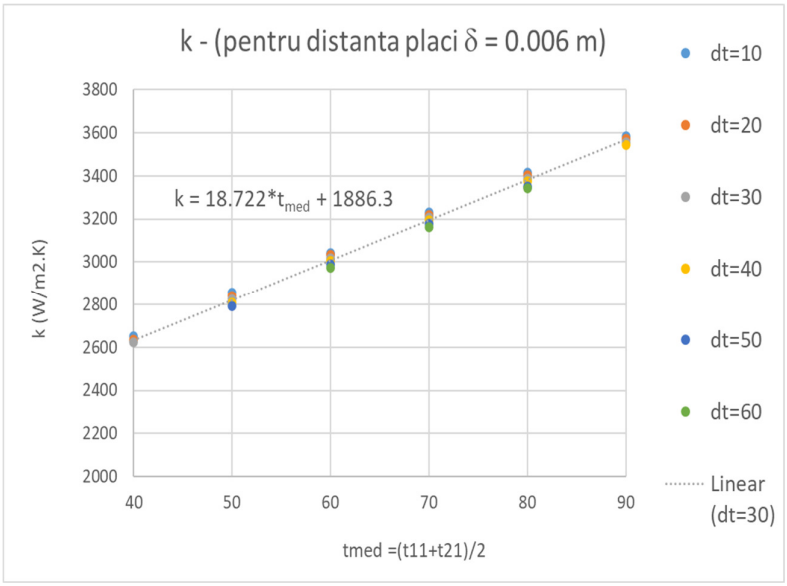

Fig. 2. The correlation for *k* ($\delta = 0.006$ m)

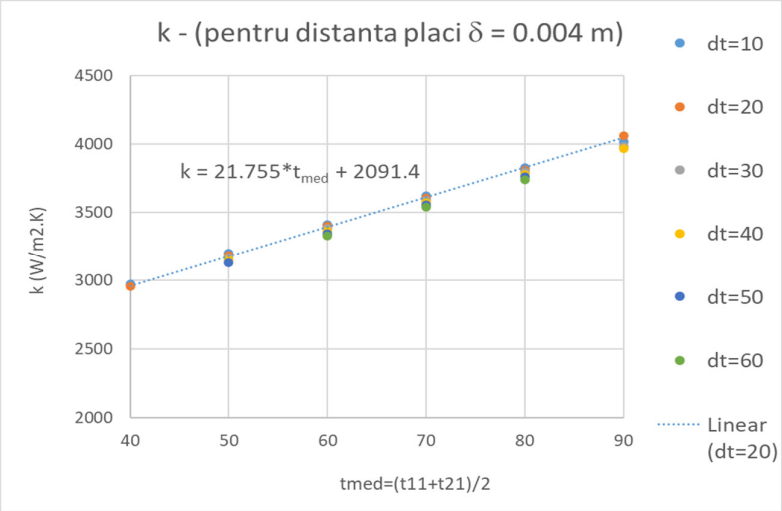

Fig. 3. The correlation for k (δ = 0.004 m)

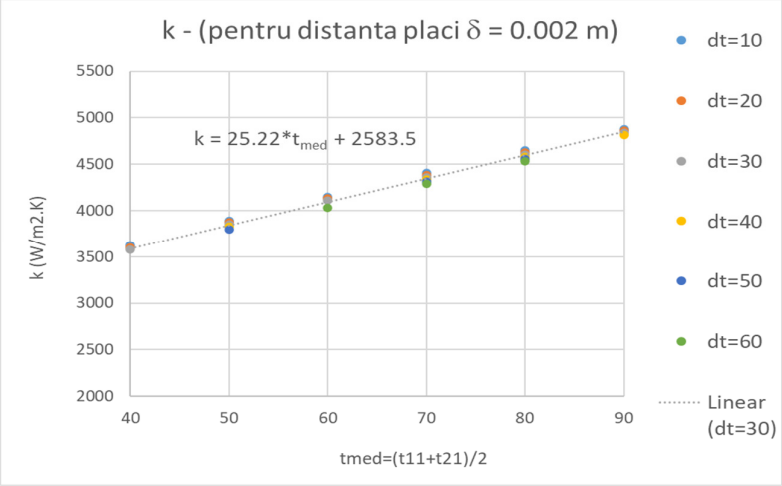

Fig. 4. The correlation for k (δ = 0.002 m)

The 3 straight lines from the figures 2, 3 and 4, placed on the same diagram, give us the opportunity to see the importance of the distance between consecutive plates.

As a conclusion, for a heat exchanger with a known distance between the plates, a straight-line equation connecting k and t_{med} can be determined, as:

$$k = m \cdot t_{med} + n \tag{12}$$

To determine the coefficients m and n, the diagram in Fig. 6 can be used. Using the expressions of coefficients m and n from fig. 6, relation (12) can be written in a more developed way:

$$k = \left(-1624.5 \cdot \delta + 28.397\right) \cdot t_{med} + \left(2969.5 \cdot e^{-78.63 \cdot \delta}\right) \tag{13}$$

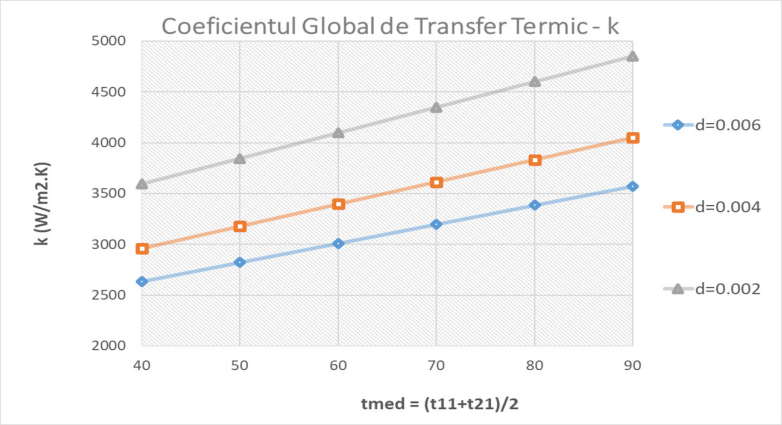

Fig. 5. The comparison of the correlations for *k*

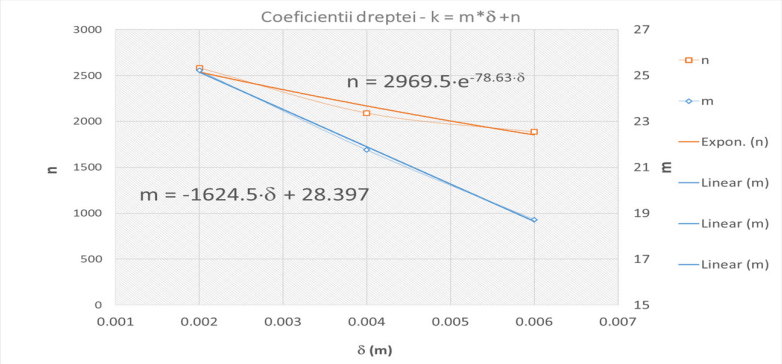

Fig. 6. The coefficients for the *k* correlation

Conclusions

The simplified procedure for determining the overall heat transfer coefficient for the analysed counter-current heat exchanger assumes establishing the distance between the consecutive plates of the heat exchanger, δ, then the coefficients *m* and *n* according to the diagram in fig. 6 and of course the average temperature t_{med}.

The presented diagrams and consequently the simplified procedure refer exclusively to the counter-current plate heat exchanger. The logical flowchart for the whole calculation procedure is presented in Figure 7.

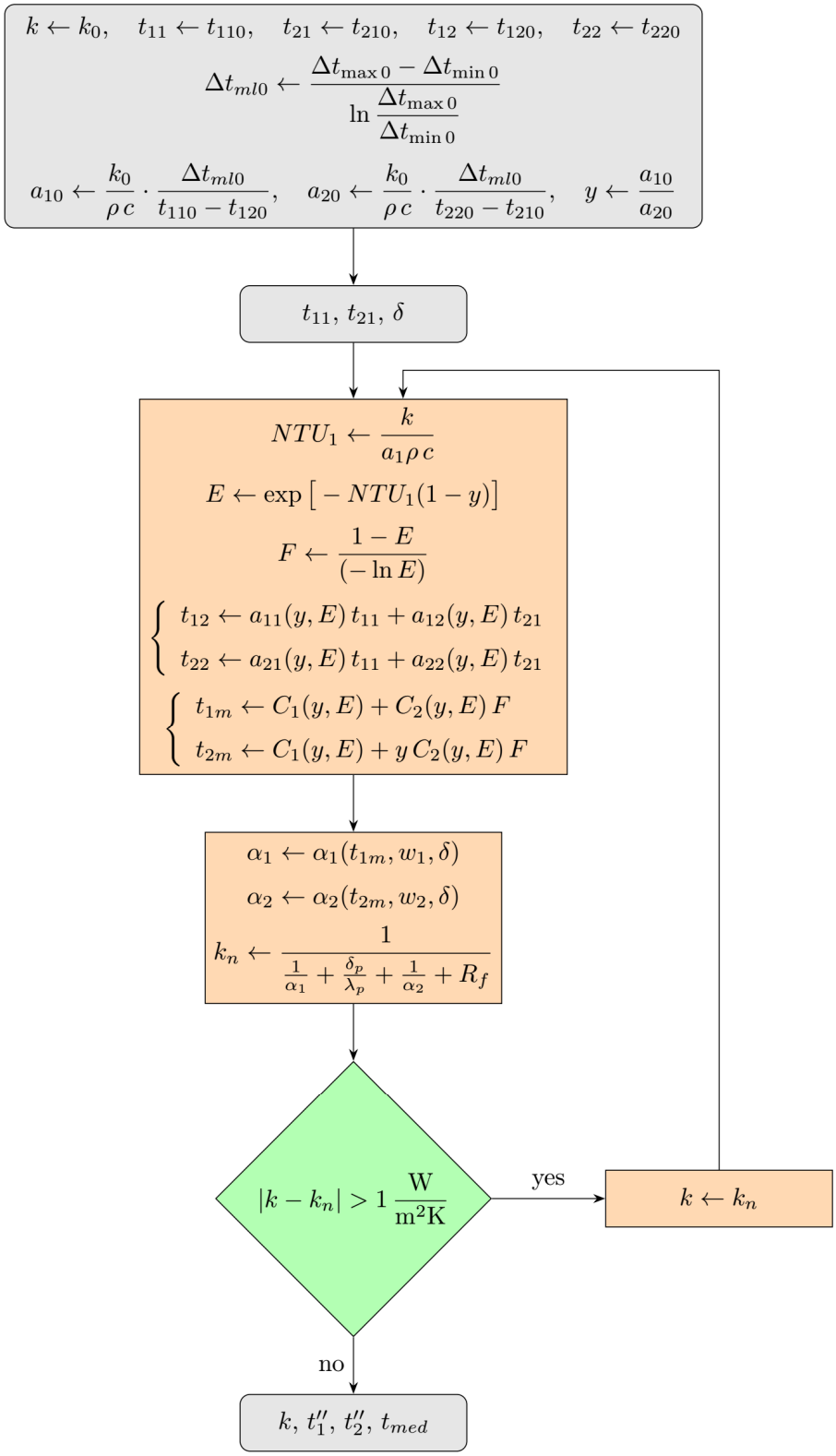

Fig. 7. The logical flowchart for the calculation procedure

Notations

t_{11} – the temperature of the primary thermal fluid at the entrance to the heat exchanger, ^oC;
t_{12} – the temperature of the primary thermal fluid at the exit from the heat exchanger, ^oC;
t_{21} – the temperature of the secondary thermal fluid at the entrance to the heat exchanger, ^oC;
t_{22} – the temperature of the secondary thermal fluid at the exit from the heat exchanger, ^oC;
t_{m1}, t_{m2} – the average temperature of the thermal fluid on the primary/secondary circuit, ^oC;
Δt_{ml} – the logarithmic mean temperature difference, K;
t_{med} – the arithmetic mean of the input temperatures of the thermal fluids, ^oC;
dt – the difference in the input temperatures of the thermal fluids, ^oC;
k – overall heat transfer coefficient of the heat exchanger, $W/m^2.K$;
α_1 – convective heat transfer coefficient for the primary fluid, $W/m^2.K$;
α_2 – convective heat transfer coefficient for the secondary fluid, $W/m^2.K$;
δ - the distance between the plates of the heat exchanger, m;
δ_p – the thickness of the stainless steel plate of the heat exchanger, m;
λ_p – the thermal conductivity of the stainless steel plate of the heat exchanger, W/m.K;
λ_f – the thermal conductivity of thermal fluids, W/m.K;
l_c – the characteristic length in the flow of thermal fluids, m;
a – the thermal diffusivity of thermal fluids, m^2/s;
ν - the kinematic viscosity of thermal fluids, m^2/s;
ρ - the density of thermal fluids, kg/m^3;
c – the specific heat of thermal fluids, J/kg.K;
w – the velocity of a thermal fluid, m/s;
G_1, G_2 – the volume flow rates of primary and secondary fluids, L/h;
a_1, a_2 - the specific volume flow rates of primary and secondary fluids, $L/(h.m^2)$;
$\rho \cdot c$ – the volumetric specific heat, 1.163 W.h/(L.K);
NTU_1 – the number of (heat) transfer units, -;
E, F – the heat transfer module and co-module, $0< E < F < 1$, -;
Nu – Nusselt number, -;
Re – Reynolds number, -;
Pr – Prandtl number, -;
0 – index for nominal values.

References

[1] H. Kumar, The Plate Heat Exchanger: Construction and Design. *1st UK National Conference of Heat Transfer*, n.86, p.1275-1286, 1984.
[2] Fábio A.S. Mota, E.P. Carvalho, Mauro A.S.S. Ravagnani, Modeling and Design of Plate Heat Exchanger, In: Md Salim Newaz Kazi (Ed.), *Heat Transfer. Studies and Applications*, IntechOpen, 2015.
[3] P. Stephan, S. Kabelac, M. Kind, D. Mewes, K. Schaber, T. Wetzel (Hrsg.), *VDI-Wärmeatlas*, *Fachlicher Träger VDI-Gesellschaft Verfahrenstechnik und Chemieingenieurwesen*, 12. Auflage, Springer Vieweg, 2019.
[4] F. Iordache, *Modelarea funcționării echipamentelor și sistemelor termice aferente clădirilor*, Editura MATRIX ROM, București, 2021.
[5] F. Băltărețu, F. Iordache, *Modelarea funcționării echipamentelor și sistemelor termice aferente clădirilor. Culegere de aplicații*, Editura MATRIX ROM, București, 2023.

Geopolymer brick composite made from building demolition materials

Compozit de cărămidă geopolimerică fabricată din materiale rezultate din demolarea clădirilor

Lucian Păunescu[1], Bogdan Valentin Păunescu[2], Enikö Volceanov[3,4]

[1]Daily Sourcing & Research SRL
95-97 Calea Grivitei, sector 1, Bucharest 010705, Romania
E-mail: lucianpaunescu16@gmai.com

[2]Consitrans SA
56 Polona street, sector 1, Bucharest 010504, Romania
E-mail: pnscbogdan@yahoo.com

[3]National University of Science and Technology "Politehnica", Faculty of Science and Materials Engineering
313 Independence Splai, sector 6, Bucharest 060042, Romania
E-mail: evolceanov@yahoo.com

[4]Metallurgical Research Institute SA
39 Mehadia street, sector 6, Bucharest 060543, Romania
E-mail: evolceanov@yahoo.com

DOI: 10.37789/rjce.2025.16.2.11

Abstract. *Unlike most manufacturing recipes of geopolymer materials containing fly ash, the current work adopted the association of clay brick and concrete resulting from building demolition together with metakaolin and blast furnace slag as materials with cementitious and pozzolanic properties suitable for substituting the extreme pollutant-Portland cement. Except for the original composition of the material mixture, the authors have adopted their own curing regime of fresh pasta at 80 °C for 24 hours, followed by traditional storage at room temperature for 7-28 days. Geopolymer brick properties were excellent through the appropriate correlation of mechanical and physical features.*

Key words: *building demolition, metakaolin, blast furnace slag, concrete waste, geopolymer brick.*

Rezumat. *Spre deosebire de majoritatea rețetelor de fabricare a materialelor geopolimerice conținând cenușă zburătoare, lucrarea curentă a adoptat asocierea cărămizii de argilă și beton rezultate din demolarea clădirilor împreună cu metacaolin și zgură de furnal, ca materiale cu proprietăți de cementare și pozzolanice adecvate pentru înlocuirea cimentului Portland extrem de poluant. Exceptând compoziția originală a amestecului material, autorii au adoptat propriul lor regim de întărire a pastei proaspete*

The article was received on 18.04.2024, accepted on 21.05.2025 and published on 22.05.2025

la 80 °C pentru 24 ore, urmat de tradiționala stocare la temperatura ambiantă pentru 7-28 zile. Proprietățile cărămizii geopolimerice au fost excelente prin corelarea adecvată a caracteristicilor mecanice și fizice.

Cuvinte cheie: demolarea clădirii, metacaolin, zgură de furnal, deșeu de beton, cărămidă geopolimerică.

1. Introduction

According to the literature [1], clay bricks were among the first man-made synthetic materials for the construction of buildings. In principle, their realization is simple, consisting of mixing clay with water. Hardening techniques have evolved over time, from facile drying in the sun heat, to thermal treatment in industrial ovens.

Clay brick is a crystalline ceramic type. Its development as a suitable material for construction was achieved through the additional use of industrial and agricultural waste. The main role of these wastes in the brick making is as a pore-supplier inside the clay body [2].

Clay bricks are manufactured by firing the raw material of clay or shale, forming a sintered porous structure [3]. Some forms of clay or shale contain organic or mineral matter, which can release gases as a result of heating, creating the adequate conditions for expanding the pelletized particles. The lightweight aggregate of expanded clay, known as LECA [4], is manufactured through this technology, the process temperature around 1200 °C being reached in a rotary kiln.

During the thermal processes at high temperatures for the production of traditional construction materials, large amounts of greenhouse gases (CO_2) are released into the atmosphere, causing major ecological problems. In these conditions, except for the need to adopt technologies with lower consumption of fossil fuel, the recycling of industrial by-products as well as the collection for the effective use of waste from usual domestic consumption, have become extremely important concerns for humanity. In the last decades, thanks to the inventions of exceptional scientific value by the French researcher J. Davidovits regarding the turn of waste rich in alumina and silica, available in the world in very large quantities, into geopolymers with physical, mechanical, chemical properties, superior to existing construction materials on the market, the opportunity was created to manufacture and test a large number of materials with new value created using the geopolymerization reaction in an activated alkaline medium [5].

Geopolymerization reaction of alumina-silicate waste in presence of alkaline activator solution is considered by specialists as a complex reaction that occurs in several stage, which can overlap. In principle, the geopolymer formation includes dissolution and hydrolysis processes, followed by condensation, which occurs in the Na_2O-Al_2O_3-SiO_2-H_2O system, sodium and silicon concentrations being decisive for the condensation process [6].

According to the literature [7-10], but also from the authors' team own experience [11-13], fly ash, metakaolin, and granulated blast furnace slag were synthesized, the effect obtained being energy savings and the reduction of geopolymer manufacturing costs. Except for the mentioned alumina-silicate materials, recycled materials from the

demolition of buildings were also used (residual concrete, residual bricks, and other components of the rubble from the demolished masonry) [14-16].

A peculiarity of preparing fly ash-based geopolymer and especially, the influence of curing at temperatures below 100 °C on its microstructure and strength was analyzed in the work [17]. It was found that the long-term precuring at ambient temperature of fresh geopolymer specimens before their introduction into the oven for hot curing for 24 hours is a beneficial process for increasing the material resistance. Class F-fly ash by-product was activated in the alkaline solution composed of Na_2SiO_3 and NaOH. J. Davidovits, the inventor of the geopolymerization process, has used except for the alumino-silicate waste, specially prepared highly reactive clay, the mixture being activated for developing the geopolymerization reaction through direct contact with the liquid alkaline activator. By comparison, the activation energy of fly ash is higher than that required in the case of granulated blast furnace slag.

Geopolymer bricks represent the latest technical innovation in the field of bricks [18] consisting of the introduction of additional cementitious materials (fly ash and granulated blast furnace slag) activated by an alkaline activator. The application of this innovative technology allowed the significant reduction of CO_2 emissions by removing the need for cement. It was experimentally found that geopolymer bricks made with fly ash require curing at a higher temperature. This curing process allows obtaining superior compression strength and lower moisture absorption. According to the paper of El-Naggar et al. [19], the manufacture of geopolymer bricks using alumina-silicate waste (clay brick waste, slaked lime waste, dealuminated kaolin, and caustic soda) offered the possibility of producing lightweight bricks (density of around 1000 $kg \cdot m^{-3}$), the compression strength still reaching 1.4 MPa.

According to [20], the use of ceramic dust waste can contribute to reducing the cost of geopolymer brick manufacturing. Durability of the same brick type produced from mine tailings significantly increased [21]. The introduction of alkali-activated industrial waste into the geopolymer brick composition can noticeably influence its physical, mechanical, and chemical properties [22].

A new original approach regarding the influence of the making process of geopolymer as well as the product itself on the environment was recently developed. According to the authors of the paper [23], the life cycle assessment of the new geopolymers based on waste from the demolition of constructions by the complete replacement of traditional Portland cement started from the adoption of precursors in the form of waste: red clay brick, hollow brick, roof tile, concrete, and glass as well as recycled concrete aggregates. The geopolymer as a result of chemical reactions between alumina-silicate oxides (alumina and silica) and the alkaline activator offers major advantages through reducing CO_2 emissions by 89 % and energy consumption by 60 % (according to authors' estimates).

Residual materials recycled from demolitions (brick waste) and by-products of the metallurgical industry (granulated blast furnace slag) were experimentally tested [24] to obtain a high-performance composite material as an alternative to concrete with similar characteristics. The results showed that the mixture of brick waste from

demolitions (with low amorphous mass) with more reactive precursors (such as the slag) can lead to performing high strength composites (compressive strength of over 60 MPa).

Several works mentioned in [23], which used fly ash, metakaolin, granulated blast furnace slag as well as sodium silicate together with sodium hydroxide as an alkaline activator for the manufacture of geopolymer, revealed the environmental implications of some geopolymeric materials (fly ash considered un-adequate for the geopolymerization reaction [25], silicates such as sodium silicate in the activator composition that should be quantitatively reduced to make the geopolymer more environmentally friendly, etc.). Of course, the results mentioned above are controversial, especially given that the respective research was not considered completed.

According to [18], class F-fly ash (with low CaO content) from the thermal power plant was the main alumina-silicate industrial by-product used for the manufacture of geopolymer brick. Also, ground granulated blast furnace as a by-product of the metallurgical industry was added together with fly ash in the starting mixture. As a fine aggregate, a type of sand available in India was chosen having the specific gravity of 2.52 $g \cdot cm^{-3}$ and particle size after sorting by sieving between 0.15-4 mm. Sodium silicate/sodium hydroxide ratio was kept at 2.5. Testing the geopolymer brick specimens, where the fly ash/slag ratio varied between 100 and 3 %, and the fine aggregate reported to the binder (fly ash and slag) was kept relatively constant at 2.64-2.71 was performed after 7 and 28 curing days. Determining results showed that the highest values of compression strength were obtained using 25 % fly ash and 75 % slag (25.2 and 51.7 MPa, respectively), water-absorbing slightly varied between 6.0-7.1 %, the lowest value corresponding to the same proportions of the binder components. The acid resistance increased with the increase of the blast furnace slag ratio, the maximum weight loss being reached for the use of only fly ash.

The rapid rate of infrastructure development in the world has led to an excessive increase in waste from demolition and construction. Storing them in landfills is unacceptable in ecological terms, so their recycling and using as a precursor material for the manufacture of geopolymers is the best method of efficient capitalization. The attempt to optimize the design of geopolymer brick from construction waste using full factorial design methodology was recently carried out by Maase and Shrivastava [26]. The loss of water by the geopolymer during the geopolymerization reaction led to an increase in the workability of the fresh mix. The properties of the geopolymer in the fresh state were affected by the silicon/aluminum, sodium/aluminum, silicon/sodium as well as solid/liquid ratios. Different conditions of the curing process were tested (40-85 °C for 5-72 hours, followed by room temperature curing). Ground brick waste (under 90 μm) as a precursor, fine sand as well as Na_2SiO_3 and NaOH solution as an alkaline activator were the materials experimentally used. The molarity of 4 M and the Na_2SiO_3/NaOH ratio of 1.5 were the main optimal parameters.

Different variants of geopolymer mixtures including waste brick powder from demolitions were prepared and tested by Fořt et al. [27]. Various compositions of alkaline activator and curing conditions were applied. The results showed that the reaction rate at early age decreases with the increase of the sodium silicate modulus and with increasing the temperature of the curing process. Compared to metakaolin-based

geopolymer, the reaction rate is slower due to the low content of the brick amorphous phase. By lowering the temperature of the curing process, the microstructural compactness gradually decreases and the specific volume of pores increases. With the increase of the sodium silicate modulus, regardless of the curing temperature value, the weight loss of the material decreases, while the dehydration of N-A-S-H and C-A-S-H gels occurs. For geopolymers cured at temperatures below 60 °C, it was found that most of the crystalline phases are similar to those of the precursor, highlighting only a partial geopolymerization, while in the case of geopolymers cured at 60-80 °C, the formation of zeolitic phases could be observed, confirming the completion of the geopolymerization process.

Recycled construction and demolition waste (CDW) was used according to Ducman et al. [28] for the manufacture of geopolymeric panels. The process involved the fine grinding of residual bricks, concrete, and mortar as well as wood chips as recycled waste. Fly ash, metakaolin, and granulated blast furnace slag had the binder role, activated by contact with the alkaline mixture consisting of potassium silicate (K_2SiO_3) and potassium hydroxide (KOH), another version of the alkaline activator predicted by J. Davidovits in his patents related to the geopolymerization of alumina-silicate waste. The results of measuring the characteristics of geopolymeric panels showed that they are suitable for cladding the building façades. Flexural strength corresponding to the panels made with brick waste, concrete, and mortar reached 5.5 MPa, while that of the panels using wood chips reached 4.3 MPa. The flexural modulus of elasticity of the two panel types had values of 2.02 and 1.38 GPa, respectively.

The work [29] proposed the synthesis of geopolymeric binders based in a very high proportion on waste provided by the building demolition. The ceramic waste constituted the alumina-silicate precursor, while the glass waste provided the silicate material necessary for the preparation of the alkaline activator. In this experiment, CDW-based geopolymers with a compression strength within the limits of 10–44 MPa were produced. The used materials contained 80–90 wt % CDW, depending on the preparation method of the activator. The paper proposed a procedure for increasing the capitalization rate of construction and demolition waste (CDW) in the geopolymer manufacturing process. Brick waste is an excellent alumina-silicate precursor. Also, window glass shards, recycled and properly processed, can be oriented towards greening the activator solution due to the high silica content.

Recently, several researchers in the field of constructions [22, 25, 29] have experimentally found that silicon and alkali contents of the alkaline activator solution seriously affects the geopolymer brick characteristics, causing the formation of additional crystalline phases such as zeolites and carbonates, which negatively influence the mechanical brick properties. Recycled glass waste from building demolition materials could effectively replace conventional activators (sodium or potassium silicate and sodium or potassium hydroxide) without affecting the level of compressive strength of the final product.

Taking into account the own previous experience of the authors' team of the current work as well as the paper conclusions mentioned above, especially in the case

of the manufacture of geopolymer brick, in this work it was decided to use high proportion-recycled waste from the rubble resulting from the building demolition (clay brick scrap and concrete scrap) as well as metakaolin and granulated blast furnace slag, all having adequate cementitious and pozzolanic properties. Fine river sand was chosen as aggregate, while the chemical activation of alumina-silicate materials specified above was carried out by adopting the traditional type of alkaline activator composed of Na_2SiO_3 and NaOH proposed by the French inventor J. Davidovits.

2. Method and materials

The geopolymer brick manufacturing method included the independent preparation in separate vessels of the liquid alkaline activator and respectively, of the mixture composed of solid materials. The liquid solution of Na_2SiO_3 (38 % concentration) thus purchased from the market had SiO_2/Na_2O molar ratio of 1.8. Commercially available NaOH solid pellets, dissolved in distilled water (molarity 10 M), were slowly introduced into the vessel containing Na_2SiO_3 under the conditions of its continuous stirring, until the Na_2SiO_3/NaOH weight ratio reached 2.5. Stirring the liquid mixture continued for about 10 hours. The liquid solution of the activator should contain 23.5 % SiO_2, 18.5 % Na_2O and 58 % water. Separately, the dry solid mixture was prepared, including metakaolin, ground granulated blast furnace slag (below 100 μm), ground clay brick scrap and ground concrete scrap (under 90 μm) as well as fine river sand (under 3.5 mm) as fine aggregate. Na_2SiO_3, until a paste was formed. The homogenized paste corresponding to each specimen was poured into a metal rectangular mould with dimensions 250 x 120 x 50 mm. For the curing process, the specimen was introduced into a drying oven at 80 °C for 24 hours. At the end of this process, the sample was removed from the mould and stored at room temperature for 7 and 28 days before determining its characteristics.

Materials used in experiment were the following.

Metakaolin is a dehydroxylated form of the clay kaolinite [30]. It is commercially available as 1-2 μm-fine particles. Its chemical composition includes: 53.0 % SiO_2, 43.8 % Al_2O_3, 1.70 % TiO_2, 0.43 % Fe_2O_3 [31].

Granulated blast furnace slag procured from ArcelorMittal Galati (Romania) ten years ago is a by-product of metallurgical industry. The molten slag was granulated by pouring into cold water pool. The grain size of granulated slag is in the range of 2-6 mm. In this experiment, the particle size was reduced below 100 μm by grinding the slag in a ball mill. The chemical composition of the slag is the following: 36.44 % SiO_2, 11.60 % Al_2O_3, 41.81 % CaO, 5.80 % MgO, 0.55 % MnO, 0.78 % Fe_2O_3, 0.35 % Na_2O, and 0.43 % K_2O [32].

Clay bricks are porous materials, their porosity influencing the low durability, high amount of water-absorbing, and firing temperature. Compressive strength of old clay bricks exhibits a wide value range between 1.5-32 MPa, up to 50 MPa [33]. The chemical composition of clay brick contains 48.7 % SiO_2, 13.7 % Al_2O_3, 10.0 % CaO, 5.7 % Fe_2O_3, 3.7 % MgO, and 2.5 % K_2O [34].

According to Jorat et al. [35], the chemical composition of concrete scrap recycled from the building demolition contains: 71.9 % SiO_2, 4.0 % Al_2O_3, 12.1 % CaO, 0.7 % MgO, 0.2 % TiO_2, 1.5 % Fe_2O_3, 0.6 % Na_2O, 0.7 % K_2O and 0.4 % SO_3. As mentioned above, particle sizes of clay brick scrap and concrete scrap used in this experiment were reduced under 90 μm as a result of their mechanical processing.

The fine river sand (below 3.5 mm) obtained after selection by sieving was utilized as fine aggregate. This product has high silica content (over 96 %) [36].

The current experiment proposed testing four manufacturing recipes of geopolymer bricks, in which the less used combination including clay brick waste and concrete scraps recovered from the building demolition was tried, without involving the most commonly used material for the production of geopolymers (fly ash). Metakaolin and granulated blast furnace slag as materials with cementitious and pozzolanic properties were preferred to the ash. The sand as a fine aggregate and the alkaline activator solution completed the material list included in the making recipe. The four experimental versions containing the dosage of the mentioned materials are shown in Table 1.

Table 1

Experimental versions of making the geopolymer brick

Material composition	Version ($kg \cdot m^{-3}$)			
	No. 1	No. 2	No. 3	No. 4
Granulated blast furnace slag	60	90	120	150
Metakaolin	250	220	190	160
Clay brick waste	450	445	440	435
Concrete waste	450	455	460	465
Sand (below 3.5 mm)	1210	1210	1210	1210
10 M NaOH	90	90	90	90
Na_2SiO_3	220	220	220	220

The investigation methods utilized in this work are known methods usually used in research activities. Archimedes' principle was used to measure the apparent density of geopolymer brick specimens. Using ASTM C642-97 standard, the apparent porosity was determined by dividing the difference between wet and dry weight by the difference between wet weight and suspended weight of the sample. Thermal conductivity was measured at room temperature using the HFM448 Lambda heat-flow-meter (SR EN 1946-3:2004). 100 kN-compression fixture Wyoming Test Fixture was used to determine the compressive strength. The flexural strength was determined using the method recommended in SR EN ISO 1412:2000, i.e. the three-point bending test. Specimen immersion under water for 24 hours (ASTM D570) allowed the measurement of water-absorbing. The microstructural aspect of specimens could be analyzed with the Biological Microscope MT5000 model, 1000 x magnification.

3. Results and discussion

Table 2 centralizes the results of the measurements performed for the physical, mechanical, and thermal characterization of geopolymer brick specimens.

Table 2

Physical, mechanical, and thermal features of geopolymer brick specimens

Characteristic	Version			
	No.1	No.2	No.3	No.4
Apparent density ($kg \cdot m^{-3}$)	2372	2389	2396	2402
Apparent porosity (%)	39.7	35.4	30.0	26.7
Heat conductivity ($W \cdot m^{-1} \cdot K^{-1}$)	0.361	0.402	0.456	0.511
Compressive strength (MPa)				
- after 7 days	18.3	20.4	22.4	24.9
- after 28 days	36.8	43.5	50.1	59.7
Flexural strength (MPa)				
- after 7 days	2.4	3.0	3.6	3.9
- after 28 days	3.9	4.8	5.9	7.1
Water-absorbing (vol. %)	6.7	7.1	6.9	6.8

The presence in increasing proportions of granulated blast furnace slag in the mixture composition significantly influenced the compressive strength of the geopolymer, both after 7 curing days (maximum 24.8 MPa) and especially after 28 days (maximum 59.7 MPa). The same conclusion is not valid in the case of flexural strength, its values being more moderate (2.4-3.9 MPa after 7 days and 3.9-7.1 after 28 days). A possible explanation would be the contribution of the amorphous mass from the clay brick waste composition.

In physical terms, the apparent density of geopolymer brick composite registered a slight increase (from 2372 $kg \cdot m^{-3}$ in experimental version 1, to 2402 $kg \cdot m^{-3}$ in version 4) due to the increase in the proportion of blast furnace slag compared to metakaolin. Also, the rather low porosity of the geopolymeric product decreased under the conditions of preparating the recipe of version 4 compared to version 1 (from 39.7 to 26.7 %).

Referring to water-absorbing, it recorded values in the range of 6.7-7.1 vol.%, considered normal [18] due to the presence of clay in the brick waste composition.

Images of the geopolymer brick specimens are shown in Fig. 1.

a b

c d

Fig. 1. Images of geopolymer brick specimens
a – specimen 1; b – specimen 2; c – specimen 3;
d – specimen 4.

The surface appearance of geopolymeric brick samples is slightly porous in the case of the first two versions (a and b) due to the physical peculiarities of clay brick waste, after which this appearance fades in the case of the last versions (c and d), that have lower proportions of clay brick in composition.

The microstructural images presented in Fig. 2 highlights the change of characteristics of the four specimens by decreasing the proportion of clay brick waste and increasing that of granulated blast furnace slag.

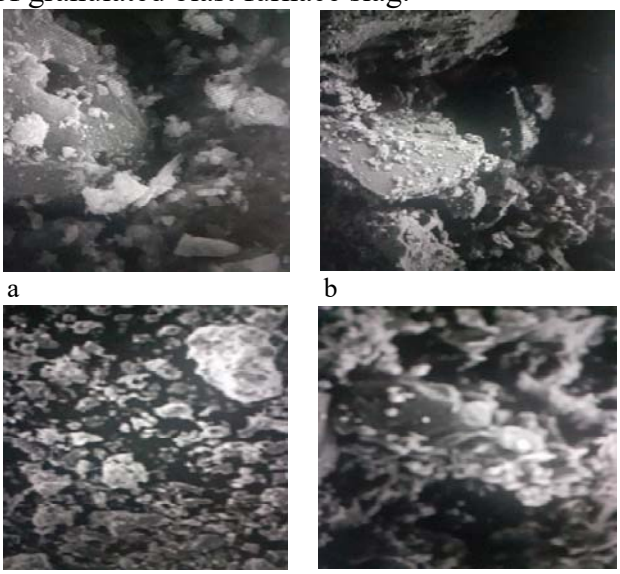

Fig. 2. Microstructural pictures of geopolymer brick specimens
a – specimen 1; b – specimen 2; c – specimen 3;
d – specimen 4.

It can be observed the reduction of spots representing the amorphous mass areas typical for clay brick as well as obtaining a higher compactness (Fig. 2d) mainly due to the blast furnace slag.

The comparative analysis of the own experimental results with other results obtained in the field of geopolymer brick and published in the literature highlighted their similarity. Although the current work completely substituted one of the most frequently

used by-products (fly ash), adopting the combination of metakaolin-granulated blast furnace slag, with cementitious and pozzolanic properties almost similar to those of ash, the performances of the final product were comparable. Also, the new method of including in the mixture for manufacturing geopolymers of the waste resulting from the building demolition (concrete and brick scraps) was adopted and applied in the recipe for the manufacture of geopolymer brick. An important role in obtaining a resistant and dense geopolymeric material is represented by the method adopted for curing the fresh material. In the conditions of a wide variety of known curing techniques, in the experiment presented in this work the authors adopted an own technique verified in several relatively similar experiments obtaining valuable results.

4. Conclusions

The objective of the current work was to test the manufacture of geopolymer brick composite without the contribution of the most frequently used material in similar processes (fly ash), replaced by metakaolin and granulated blast furnace slag as materials with cementitious and pozzolanic properties. This constituted the main element of the work originality. Building demolition waste (concrete and clay brick scraps) were also included in the mixture composition as alumina-silicate materials suitable for manufacturing the geopolymer. The curing process of the fresh material was carried out according to the authors' own method, being a secondary element of the work originality. High compressive strength values (up to 59.7 MPa after 28 days and up to 24.9 MPa after 7 days) were obtained, being almost similar to values reported in the literature. In physical terms, the geopolymer brick in the optimal version (with the highest slag proportion) had a dense and relatively compact structure, with apparent density of 2402 $kg \cdot m^{-3}$, porosity of 26.7 % and heat conductivity of 0.511 $W \cdot m^{-1} \cdot K^{-1}$. The experimentally made geopolymer brick is suitable for application in construction, being resistant, environmentally friendly, and little expensive.

References

[1] F. M. Fernandes, „Clay Bricks'', in Long-Term Performances and Durability of Masonry Structures, Woodhead Publishing Series in Civil and Structural Engineering, ISBN 978-0-08-102110-1, 2019.

[2] N. Phonphnak, P. Chindaprasirt, „Types of waste, properties, and durability of pore-forming waste-based fired masonry bricks", in Eco-Efficient Masonry Bricks and Blocks, 2015, pp. 1-10. https://doi.org/10.1016/8978-1-78242-305-8.00001-2

[3] I. Sims, J. Ferrari, „Concrete Aggregates", in Lea's Chemistry of Cement and Concrete, 5th Edition, 2019, pp. 907-1015.

[4] *** LECA Lightweight Expanded Clay, Saint Gobain, Chester, United Kingdom, 2015.

[5] J. Davidovits, M. Davidovits, N. Davidovits, „Process for Obtaining a Geopolymeric Alumino-Silicate and Products thus Obtaining", US Patent no. 5342595, August 30, 1994.

[6] P. de Silva, K. Sagoe-Crenstil, V. Sirivivatnanon, „Kinetics of Geopolymerization: Role of Al_2O_3 and SiO_2", Cement and Concrete Research, Elsevier, **vol. 37**, no. 4, pp. 512-518, 2007. https://doi.org/10.1016/j.cemconres.2007.01.003

[7] F. Kugler, J. Aumüller, W. Krcmar, U. Teipel, „Construction and Demolition Residuals as Raw Materials for the Production of Novel Geopolymer Building Materials'', Crystals, MDPI, Basel, Switzerland, M. Lach, K. Korniejenko, W-T. Lin, (acad. eds.), **vol. 12**, no. 5, 2022. https://doi.org/10.3390/cryst12050678

[8] M. Amran, S. Debbarma, T. Ozbakkaloglu, „Fly Ash-Based Eco-Friendly Geopolymers Concrete: A Critical Review of Long-Term Durability Properties", Construction and Building Materials, Elsevier, **vol. 270**, 2021. https://doi.org/10.1016/j.conbuildmat.2020.121857

[9] F. A. Shilar, S. V. Ganachari, V. B. Patil, K. S. Nisar, „Evaluation of Structural Performances of Metakaolin Based Geopolymer Concrete", Journal of Materials Research and Technology, Elsevier, **vol. 20**, pp. 3208-3228, 2022. https://doi.org/10.1016/j.jmrt.2022.08.020

[10] A. Gupta, „Investigation of the Strength of Ground Granulated Blast Furnace Slag Based Geopolymer Composite with Silica Fume", Materials Today: Proceedings, Elsevier, **vol. 44**, pp. 23-28, 2021. https://doi.org/10.1016/j.matpr.2020.06.010

[11] L. Paunescu, A. Ioana, E. Volceanov, B. V. Paunescu, „Nonconventional Ecological and Low-Energy Consumption Technique to Produce High-Strength Geopolymer Composite Based on Residual Materials as a New Type of Construction Material", Nonconventional Technologies Review, "Politehnica" Publishing, Timisoara, Romania, **vol. 27**, no. 1, pp. 32-38, 2023.

[12] B. V. Paunescu, L. Paunescu, E. Volceanov, „Porous Fly Ash-Based Geopolymer Usable as an Unconventional Construction Material", Journal of Engineering Studies and Research, "Vasile Alecsandri" University Publishing, Bacau, Romania, **vol. 29,** no. 3, pp. 57-65, 2023. https://doi.org/10.2908/jesr.v29i3.006

[13] B. V. Paunescu, L. Paunescu, E. Volceanov, „Agro-Waste Addition in the Mixture for Building Geopolymer Concrete Manufacture", Romanian Journal of Civil Engineering, Matrix Rom Publishing, Bucharest (Romania), **vol. 14**, no. 4, pp. 390-400, online ISSN: 2559-7485, 2023.

[14] L. Radina, A. Sprince, L. Pakrastins, R. Gailitis, G. Sakale, „Potential Use of Construction Waste for the Production of Geopolymers: A Review", Materials Proceedings, MDPI, K. Mráz, T. Zdeb, I. Hager (eds.), **vol. 13**, no. 1, 2023. https://doi.org/10.3390/materproc2023013002

[15] B, Figiela, K. Brudny, W-T. Lin, K. Korniejenko, „Investigation of Mechanical Properties and Microstructure of Construction- and Demolition-Waste-Based Geopolymers", Journal of Composites Science, MDPI, F. Tornabene, T. Triantafillou, (acad. eds.), **vol. 6**, 2022. https://doi.org/10.3390/jcs6070191

[16] B. V. Paunescu, A. Ioana, L. Paunescu, „Environmental Friendly Manufacturing the Geopolymer Foam from Aluminosilicate Wastes Completely Excluding the Cement", Bulletin of Polytechnic Institute of Iasi, Chemistry and Chemical Engineering Section, issue 69 (73), fascicle 1, pp. 47-56, 2023. https://doi.org/10.5281/zenodo.7767038

[17] T. Bakharev, „Geopolymeric Materials Prepared Using Class F Fly Ash and Elevated Temperature Curing", Cement and Concrete Research, Elsevier, **vol. 35**, no.6, pp. 1224-1232, 2005. https://doi.org/10.1016/j.cemconres.2004.06.031

[18] B. Lavanya, D. K. Preet, S. Suganesh, R. Indrajith, B. C. Ramesh, „Properties of Geopolymer Bricks Made with Fly Ash and GGBS", IOP Conf. Series: Materials Science and Engineering, IOP Publishing, **vol. 872**, 2020. https://doi.org/10.1088/1757-899X/872/1/0121411

[19] K. A. M. El-Naggar, S. K. Amin, S. A. El-Sherbiny, M. F. Abadir, „Preparation of Geopolymer Insulating Bricks from Waste Raw Materials", Construction and Building Materials, Elsevier, **vol. 222**, pp. 699-705, 2019.

[20] S. K. Amin, S.A. El-Sherbiny, A. A. M. A. El-Magd, A. Belal, M. F. Abadir, „Fabrication of Geopolymer Bricks Using Ceramic Dust Waste", Construction and Building Materials, Elsevier, **vol. 157**, pp. 610-620, 2017.

[21] S. Ahamari, L. Zhang, „Durability and Leaching Behavior of Mine Tailings-Based Geopolymer Bricks", Construction and Building Materials, Elsevier, **vol. 44**, pp. 743-750, 2013. https://doi.org/10.1016/j.conbuildmat.2013.03.075

[22] H. R. Gavali, A. Bras, P. Faria, R. V. Ralegaonkar, „Development of Sustainable Alkali-Activated Bricks Using Industrial Wastes", Construction and Building Materials, Elsevier, **vol. 215**, pp. 180-191, 2019. https://doi.org/10.1016/j.conbuildmat.2019.04.152

[23] N. Mir, S. A. Khan, A. Kul, O. Sahin, E. Ozcelikci, M. Sahmaran, M. Koc, „Construction and Demolition Waste-Based Self-Healing Geopolymer Composites for the Built Environment: An Environmental Profile Assessment and Optimization", Construction and Building Materials, Elsevier, **vol. 369**, 2023. https://doi.org/10.1016/j.conbuildmat.2023.130520

[24] J. Fořt, M. Mildner, M. Keppert, V. Pommer, R. Černý, „Experimental and Environmental Analysis of High-Strength Geopolymer Based on Waste Bricks and Blast Furnace Slag", Polymers, MDPI, I. Blanco (acad. ed.), **vol. 15**, no. 14, 2023. https://doi.org/10.3390/polym15143092

[25] F. Colangelo, I. Farina, C. Salzano, M. Travaglioni, M. de Pertis, R. Cioffi, A. Petrillo, „Climate Change Impact Assessment of Geopolymer Mortar", Key Engineering Materials, Elsevier, **vol. 919**, pp. 210-217, 2022.

[26] M. R. Maaze, S. Shrivastava, „Design Development of Sustainable Brick-Waste Geopolymer Brick Using Full Factorial Design Methodology", Construction and Building Materials, Elsevier, **vol. 370**, 2023. https://doi.org/10.1016/j.conbuildmat.2023.130655

[27] J. Fořt, R. Novotný, E. Vejmelková, A. Trnik, „Characterization of Geopolymers Prepared Using Powdered Brick", Journal of Materials Research and Technology, **vol. 8**, no. 6, 2019. https://doi.org/10.1016/j.jmrt.2019.10.019

[28] V. Ducman, A. Frankovič, S. Kramar, S. Tamburini, M. Natali, A. Bernardi, „Durability Assessment of Geopolymer Façade Panels Based on CDW", 4th International Conference Progress of Recycling in the Built Environment, Lisbon, Portugal, October 11-12, 2018.

[29] D. Kioupis, A. Skaropoulou, S. Tsioilis, G. Kakali, „Valorization of Brick and Glass CDWs for the Development of Geopolymers Containing More than 80 % of Wastes", Minerals, MDPI, Basel, Switzerland, **vol. 10**, no. 8, 2020. https://doi.org/10.3390/min10080672

[30] R. B. Holland, K. E. Kurtis, L. F. Kahn, „Effect of Different Concrete Materials on the Corrosion of the Embedded Reinforcing Steel", in Corrosion of Steel in Concrete Structures, 2nd Edition, Woodhead Publishing Series in Civil and Structural Engineering Book, A. Poursaee (ed.), pp. 131-147, ISBN 9780128218402, 2023.

[31] M. Lahoti, P. Narang, K-H. Tan, E-H. Yang, „Mix Design Factors and Strength Prediction of Metakaolin-Based Geopolymer", Ceramics International, Elsevier, **vol. 43**, no. 14, 2017. https://doi.org/10.1016/j.ceramint.2017.06.006

[32] L. Paunescu, B. V. Paunescu, E. Volceanov, G. Surugiu, „Geopolymer Concrete-A Suitable Nonconventional Alternative Solution for the Global Reduction of CO_2 Emissions in Manufacturing the Concrete", Nonconventional Technologies Review, "Politehnica" Publishing, Timisoara, Romania, **vol. 26**, no. 4, pp. 25-30. 2022.

[33] F. M. Fernandes, „Clay bricks", in Long-Term Performance and Durability of Masonry Structures, University of Lusiada-Norte, Vila Nova de Famalicao, Portugal, pp. 1-19, 2022. https://doi.org/10.1016/B978-0-08-102110-1.00001-7

[34] M. Šveda, R. Sokolar, B. Janik, Z. Štefunková, „Reducing CO_2 Emissions in the Production of Porous Fired Clay Bricks", Material Science, Springer Link, **vol. 23**, no. 2, 2017. https://doi.org/10.5755/j01.ms.23.2.15103

[35] E. Jorat, M. A. Aziz, A. Marto, N. Zaini, S. N. Jusoh, D. A. C. Manning, „Sequestering Atmospheric CO_2 Inorganically: A Solution for Malaysia's CO_2 Emission", Geosciences, MDPI, **vol. 8**, no. 483, pp. 1-14, 2018. https://doi.org/10.3390/geosciences8120483

[36] K. C. Bala, R. H. Khan, „Characterization of Beach/River Sand for Foundry Application", Leonardo Journal of Sciences, Academic Direct Publishing House, Cluj-Napoca, Romania, no. 23, pp. 71-83, ISSN: 1583-0233, 2013.